DISSERTATION

QUANTIFYING UBIQUITIN DYNAMICS

Submitted by

Sarah A. Bollinger

Department of Biochemistry and Molecular Biology

In partial fulfillment of the requirements

For the Degree of Doctor of Philosophy

Colorado State University

Fort Collins, Colorado

Fall 2019

Doctoral committee:

    Advisor: Robert E. Cohen

    Olve Peersen
    Tingting Yao
    Jessica Prenni
    Alan Kennan

ABSTRACT

QUANTIFYING UBIQUITIN DYNAMICS

Ubiquitin (Ub) is a small protein that is frequently attached to other proteins as a post-translational modification (PTM) to elicit a new function, cellular localization, or otherwise modulate the activity of the substrate protein. Ub addition and removal serves as a signal for proteasome degradation, regulation of cell division, gene expression, membrane and protein trafficking and signaling in a multitude of stress response mechanisms. Defects in ubiquitination or deubiquitination have been linked to cancer onset and progression, muscle dystrophies, and disorders in inflammation and immunity; these findings further highlight the critical processes regulated by Ub. Due to its high demand, cellular Ub levels are highly regulated, such that the abundance of free Ub is above a threshold enabling new ubiquitination events, a critical part of normal cell function and survival

Due to the high demand on the cellular free Ub pool to supply substrate for thousands of ubiquitination reactions, it is tightly regulated in many ways. Our knowledge of Ub homeostasis has not advanced, likely due to the lack of accurate, sensitive methods for pool quantitation that can be performed routinely. Here, a method is presented that utilizes a high affinity free Ub binding protein to quantify cellular pools of Ub after a series of treatment protocols. The methods can be performed within a day and are amenable to high throughput applications. Using these methods, the Ub pool distributions of cells under conditions such as proteasome inhibitor and heat stress were

assessed. However, this assay will only report the steady-state concentration of Ub in each pool; it provides no information about the rate of movement through them.

The rates of competing ubiquitination and deubiquitination or degradation reactions determine the steady-state level of every Ub-protein conjugate; however, measurement of the rate of Ub movement these conjugates remains a challenge. Thus, the relative contributions of conjugation and disassembly rates in cellular responses to different signals are rarely known. Moreover, even though the concentration of a particular Ub-protein conjugate may appear unchanged, the flux of Ub through that conjugate might change dramatically. To address these deficits in our understanding of ubiquitination, we have developed a method to label Ub and follow its movement through conjugation pathways that we call SILOW or Stable Isotope Labeling with ^{18}O-Water. Our method is applicable to both yeast and mammalian cells, does not perturb cellular physiology in any way and can be used with conventional proteomics methods. SILOW permits rapid changes in Ub flux to be evaluated over short times across hundreds of sites within the human cell proteome to reveal the intracellular dynamics of Ub-conjugation in specific Ub-Ub linkages of polyUb compared with Ub-protein linkages of histones.

ACKNOWLEDGEMENTS

TABLE OF CONTENTS

CHAPTER1: INTRODUCTION

Ubiquitin (Ub) is the small, highly conserved modifying protein that is conjugated to substrate proteins post-translationally to regulate protein interactions, localization, enzymatic activity and mediate degradation through the proteasome or lysosome[1,2]. Thousands of members of the proteome are reported as Ub substrates, and this highly populated "ubiquitinome" is involved, if not necessary, in most of the diverse cellular processes including membrane trafficking, gene expression, cell division, and signaling for critical responses after stress, such as DNA damage and pathogen invasion of host cells[3,4]. Ub is added to substrate proteins through a series of reactions catalyzed by an enzyme cascade. First, the activating enzyme (E1) forms a thioester with Ub in an ATP-dependent reaction, generating a reactive intermediate[5]. Next transthiolation of Ub to a conjugating enzyme (E2) occurs before Ub is finally conjugated to the target protein, either by first transferring to a ligating enzyme (E3) or by direct catalysis where E3 acts as an adaptor, bringing target and E2 in close proximity[6]. The carboxyl terminus of Ub is conjugated ε-amino group of a lysine residue within the substrate protein, forming an isopeptide bond[5]. Ub itself has 7 lysine residues; therefore, polymers of Ub (polyUb) can be built or added on substrate proteins[7,8].

As with other PTMs, ubiquitination is reversible; its removal is catalyzed by deubiquitinating enzymes (DUBs)[9]. As it is added (i.e., ubiquitination) and removed (i.e., deubiquitination), Ub is cycled through three general pools that are distinguished by the chemical status of the C-terminus[10]. Unconjugated Ub, with a C-terminal carboxyl group, is known as free Ub and includes molecules of monoubiquitin (monoUb) as well

as unanchored polyUb chains[11]. Ub C-terminally thioesterified to enzymes within the conjugation cascade are considered <u>activated,</u>[12] and upon generation of an isopeptide bond to an amino group of a substrate protein, Ub is <u>conjugated</u>[1]. A single Ub molecule moves through each pool during conjugation and is eventually removed and recycled back to the free pool when the protein substrate is degraded by the proteasome or otherwise deubiquitinated[9].

1.1 Regulation of Ub homeostasis

The maintenance of the relative amounts of Ub pools, or Ub homeostasis, is important for proper Ub metabolism and thus, cell function.[13] Ub homeostasis is sustained by a constant supply of free Ub that is neither limiting nor overabundant[14]. In mice expressing the DUB UCH-L1 mutated for loss-of-function, the free Ub pool is depleted. This phenotype resulted in gracile axonal dystrophy (*gad*), a disorder presenting sensory and motor ataxia[15]. The *gad* mice exhibited an accumulation of Ub-positive protein aggregates within the nervous system, yet no change in Ub gene expression or Ub-conjugates, implicating UCH-L1 in the stabilization of free Ub[16]. Mice deleted for Usp14 (*ax^J*) present dramatic neurological degeneration and death within 8 weeks of birth[17]. In *ax^J* mice, free and conjugated Ub were both reduced by up to 60% in synaptic regions, suggesting Usp14 plays a critical role in maintaining Ub homeostasis in the synapse. These examples demonstrate the importance of specific DUBs in neuronal Ub homeostasis, and how their misregulation can lead to aberrant neurological phenotypes.

In mice (and humans), Ub is expressed from four genetic loci, *UBA52* and *RPS27A*, Ub-ribosomal fusion genes[18], and *UBB* and *UBC*, which contain 3-4 and 9-10

tandem repeats of the Ub gene[19], respectively. Deletion of either *UBB* or *UBC* resulted in dramatic depletion of the free Ub pool[14]. Phenotypically, homozygous deletion of *UBB* resulted in degeneration of hypothalamic neurons in mice[20], and the deletion of *UBC* in MEF cells caused premature senescence and reduced proliferation[21]. As evidenced by depletion of free Ub and dramatic neurologic defects upon deletion of only one of four genes expressing Ub, gene expression is also a contributor to the tight regulation on Ub homeostasis.

Mice overexpressing neuronal Ub had elevated levels of both free and conjugated Ub and this also manifested phenotypically as reduced muscle development, retarded motor abilities and defects in certain aspects of neuronal structure[22]. Although no other attempts at Ub overexpression have been made in studies to investigate Ub homeostasis, this result demonstrates the importance of maintaining Ub levels within a tight window.

1.2 Existing methods permitting quantitation of specific Ub pools

The aforementioned examples of disrupted Ub homeostasis and resulting phenotypes demonstrate the high level of regulation and maintenance by the cell in regards to the free Ub pool; however, this field has been difficult to advance due to the lack of tools allowing for specific and quantitative measurements. Ideally, a method for Ub quantitation would distinguish between free and conjugated Ub and also resolve the (iso)peptide from thioester-linked populations. For quantitative studies, the method should be able to provide accurate Ub concentrations with precision and high sensitivity.

Over the years, several methods have been described to measure the concentration of specific Ub populations. One of the earliest methods developed allows

accurate and sensitive quantitation of free Ub within samples by conversion to [^{3}H]AMP-Ub through reactions with E1 and [^{3}H]ATP in an end-point assay[23]. This method is sensitive to picomolar amounts of Ub, but is difficult to perform and not amenable to assays with crude cell extracts because cellular ATP within the sample would alter the results. Another disadvantage is the lack of adaptability for measurements of the activated or conjugated pools.

A more common approach to quantify Ub is immunoblotting using an antibody specific for Ub[24,25]. One advantage is the ability to analyze the distribution of Ub sizes of Ub-conjugates, which are well separated from free Ub and can be quantified using standard band-quantitation techniques[26]. However, the concentration information extracted from immunoblots is generally imprecise. A further drawback to this method with respect to Ub pool analysis is the inherent difficulty in transferring free Ub onto membranes used for immunoblotting, as found by our lab (unpublished) and others[27].

More recently, mass spectrometry (MS) and the implementation of protein or peptide standard absolute quantification (PSAQ or AQUA, respectively) has considerably advanced the ability to assess Ub concentrations. One MS-based study[28] used PSAQ in conjunction with sample processing by affinity reagents that selectively bound Ub chains (e.g., UBA domain of hPlic2 protein; K_d, Ub chains = 7 μM)[29] or free Ub (BUZ domain of isopeptidase T protein; K_d, free Ub = 3 μM)[30]. This method was used to determine concentrations of total, free, mono- and even some specific linkage-types of polyUb. Though this method was quantitative, it provided no means of protection for the activated pool which may have been hydrolyzed, thus potentially inflating apparent abundance of the free pool.

4

Another MS-based study that managed to quantify all three cellular pools of Ub did

so using AQUA[31]. SDS-PAGE gel analysis of the cell lysate and in-gel digestion of the

free Ub band, under both native and denaturing conditions, was performed to quantify

the free and activated pools. Slower-migrating bands of the gel were digested to

quantify the conjugated pool. While this method achieved the goals of accuracy and

sensitivity, it required extensive sample processing with many steps, preventing its

adaptation to high-throughput or large experiments.

1.3 Tandem Ub binding domains as tools to study specific forms of Ub

Sims et al.[32] discussed the concept of linkage specific avidity as the mechanism of

for Rap80 binding to K63-linked polyUb at sites of DNA double-strand breaks. Linkage

specific avidity refers to Ub-binding domains (UBDs) fused in a manner permitting

multiple, high-affinity interactions with a single type of polyUb linkage and specificity

against other linkages and monoUb. The concept was further validated through

generation and application of a K63 polyUb binding protein called Vx3[33]. This sensor

was designed by adjusting the length of peptides connecting 3 Ub Interacting Motifs

(UIMs) to orient them for enhanced binding to the individual monomers of a K63 polyUb

chain.

The concept of avidity was also applied by a previous member of our lab, Yun-

Seok Choi who generated a suite of free Ub binding proteins[34] by fusing Ub Binding

Domans (UBDs) in tandem. For all binding proteins in this collection, the use of the IsoT

BUZ domain, which confers selectivity for free Ub,[30] is critical. Other UBDs fused to the

BUZ domain worked synergistically to increase overall affinity and specificity for Ub.

Importantly, the binding of these proteins to conjugated forms of Ub and Ub-like (Ubl)

proteins is negligible. One of these binding proteins, tUI, binds free Ub with picomolar affinity, yet remains specific against conjugated forms of Ub and Ubl even in low nanomolar and millimolar concentrations, respectively. Fluorophore conjugation at specific sites on the protein permit free Ub quantitation based on increases in fluorescence that occur upon substrate binding.

In this body of work, a series of protocols are described for sample manipulation of cell extracts, permitting accurate and sensitive Ub pool quantitation by the free Ub sensors. Initial application of these methods on proteasome inhibited and heat stressed cell samples produced measurements with low errors and in agreement with published data. Finally, other applications of these binding proteins were explored, such as free Ub enrichment from cell lysates.

1.4 Tools available to study Ub dynamics

Microscopy-based studies have successfully demonstrated Ub dynamics within specific loci or organelles. For example, cells expressing a photo-activatible version of GFP-fused Ub (PAGFP-Ub) were activated with a 405 nm laser in a nuclear region. Imaging over time then showed that PAGFP-Ub moved out of the nucleus and into other cellular compartments within 10 minutes[35]. This same system was used to assess the dynamics of cytoplasmic Ub-conjugates in untreated and heat-shocked cells. Stability of Ub-conjugates in heat-stressed cells was markedly increased in comparison to untreated cells, which is consistent with the accumulation of conjugates that accompanies heat-shock[36].

In a study by Stenoien et al.[37] using fluorescent protein fusions of Ub (i.e., YFP-Ub), ataxin-1 inclusions associated with proteotoxic stress were imaged over time after

6

photoactivation. Inclusions with low levels of YFP-Ub exhibited fast exchange with YFP-Ub in solution, while inclusions containing high YFP-Ub levels, indicative of more polyUb and aggregated protein, were comprised of slow-exchanging Ub. This result suggested that at least a fraction of Ub-conjugated to ataxia-1 or other proteins was stably contained within the inclusions, possibly due to the high degree of protein aggregation within those structures.

In yet another qualitative assessment of general Ub dynamics, within 20 minutes of proteotoxic stress, most GFP-labeled Ub moved from the nucleus to the cytoplasm, possibly as Ub-protein conjugates destined for the proteasome[38]. That study provided a direct observation of crosstalk between two Ub-dependent processes, proteasome-mediated degradation and chromatin remodeling, mediated by the regulation of Ub flux. Ub flux could regulate other processes as well, but there has been no way to look for them.

Thus far, published studies on Ub dynamics were conducted to make general observations on the movement of Ub through specific cellular compartments or bodies. By the very nature of those experiments, measurements of Ub flux at specific Ub-conjugation sites would be challenging, if not impossible.

1.5 Historical examples of ^{18}O-labeling

An ideal system for monitoring ubiquitination dynamics would provide access to kinetics of ubiquitination at specific Ub sites. Due to its mass accuracy and sensitivity, MS is well suited for measurements on specific peptide sequences within proteins, and these measurements can be multiplexed to a high degree, making measurements on thousands of sites within a single sample possible[39]. Trypsin proteolysis of ubiquitinated

proteins creates a signature peptide at the site of conjugation containing di-Gly (i.e., glycyl-glycine) from the Ub C-terminus, is an isopeptide linkage to the substrate's lysine. The di-Gly remnant yields a mass shift of 114.1 Da that can be incorporated in conventional database searches for peptide identification[40]. While MS provides access to analysis of specific Ub sites, there has been no method that allowed measurements of Ub movement through those sites. Most MS-based methods are based on quantifying the absolute or relative abundance of proteins or modifications, not their dynamics.

For measurements of Ub movement through a modification site, one intriguing idea is to exploit the chemistry of Ub addition and removal, which involves oxygen exchange at its C-terminal carboxyl group. If ^{18}O-water were in the system, ^{18}O would be exchanged into free Ub, effectively labeling it with the isotope and inducing a 2 Da shift, quantifiable by MS. As Ub moved through the population of any specific site, more ^{18}O would accumulate and could be differentiated from sites with less dynamic Ub movement, which would accumulate less ^{18}O.

The concept of ^{18}O-labeling to monitor dynamics dates back to 1952, when Mildred Cohn first proposed and used the method to probe the oxygen exchange kinetics in reactions of oxidative phosphorylation using ^{18}O-labeled phosphate[41]. Shortly after, Paul Boyer and his group harnessed the power of ^{18}O-labeling and subsequent MS analysis of metabolites. Boyer's lab made important biochemical discoveries using ^{18}O-labeling, among them was the observation of rapid oxygen (and phosphate) exchange at the mitochondria during oxidative phosphorylation, even when electron carriers were inhibited or reduced[42]. These observations hinted at some sort of high energy intermediate, and after years of study, Boyer's group demonstrated that this

"intermediate" was actually the electrochemical gradient generated by electron transport across the mitochondrial membrane during ATP synthesis[43].

As of the 1990's, ^{18}O-labeling was used to quantify relative peptide abundances through C-terminal labeling of peptides by a protease's hydrolytic event[44]. With this method, samples are proteolyzed in ^{18}O-enriched water, resulting in peptides that incorporated two atoms of [18]O in their C-terminal carboxylate and are thus shifted by +4 Da[45]. Enzyme catalyzed peptide hydrolysis is the means of the first [18]O incorporation and further interaction with the protease in cycles of binding and hydrolysis occurs until both oxygens are completely equilibrated with the solvent water[45]. Labeled samples are typically mixed at a defined ratio with an unlabeled sample before MS analysis and the relative abundance of labeled to unlabeled peptides is assessed.

The advantages of ^{18}O-labeling for peptide quantitation over other isotopic labeling methods (i.e., Stable Isotope Labeling using Amino acids in Cell culture, SILAC) include reduced cost and amenability to patient and clinically obtained samples[44]. The major drawback to ^{18}O-labeling in complex mixtures is the lack of a generalized computational tool that permits peptide identification; existing tools require considerable manual manipulation of the data[46]. Another disadvantage to ^{18}O-based peptide quantitation is the lack of complete labeling (i.e., 2 [18]O's) for some peptides, which seems generally unpredictable and varies from peptide to peptide; worse still, C-terminal peptides are not labeled at all[47].

1.6   SILOW

As with peptide bond hydrolysis by trypsin, hydrolysis of the isopeptide bond between Ub and the Lys residue of a substrate protein also is expected to incorporate a

single oxygen from the solvent water into the C-terminal carboxylate of Ub. If cells were incubated in enriched ^{18}O-water, which equilibrates across cell membranes instantly and is innocuous to cells[48], the released Ub molecule would contain ^{16}O and ^{18}O in its C-terminus. After deubiquitination, Ub is recycled back to the free pool for use in a new conjugation event[49], the product of which has a 50% chance of incorporating the ^{18}O-label. Subsequent rounds of deubiquitination and ubiquitination in ^{18}O-water would further enrich the Ub C-terminus with ^{18}O. As discussed in Section 1.5, MS analysis can be used to follow the ^{18}O-labeled Ub through conjugation and deconjugation reactions. The ^{16}O:^{18}O labeling ratio of a Ub-protein conjugation site is an indication of its relative stability, more ^{18}O indicates faster Ub exchange at the site and less ^{18}O suggests the site is more stable.

We have termed this technique SILOW or "Stable Isotopic Labeling using ^{18}O-Water". The first application of this method was to compare the relative rates of Ub exchange at conjugation sites across the proteome to shed light on the intracellular dynamics of Ub at protein Ub-conjugation sites. Prior to SILOW, quantifying these processes has not been possible..

CHAPTER 2: APPLICATIONS OF FREE UBIQUITIN SENSOR PROTEINS

Nearly all proteins in eukaryotes are affected by the essential post-translational modification (PTM) of Ub conjugation. Ubiquitination mechanisms and outcomes are heavily researched fields of study, and yet information regarding the dynamics and regulation of even free (i.e. unconjugated) Ub is scant. A major hurdle in this field has been the lack of simple and robust techniques to quantify Ub levels in cells. Here, a series of protocols are described that permit quantitation of free, protein-conjugated and thioesterified Ub by fluorescent-tagged, free Ub binding proteins in assays that are amenable to high-throughput needs. These assays were used to quantify Ub pool levels in cells after inhibiting the proteasome or activation of the heat stress response. Finally, a method for isolating free Ub from cell extracts was developed using the free Ub binding proteins.

2.1 Introduction

A former postdoctoral fellow in the lab, Yun-Seok Choi, developed a series of Ub-binding proteins with low-nanomolar Kd values and ≥1000-fold selectivity for free Ub over other forms of Ub or Ub-like proteins (Ubl) (see Appendix 1 for complete description and biochemical characterization). By conjugation to Atto532 fluorophore at specific sites, the binding proteins become free Ub sensors because significant fluorescence increases are observed upon free Ub binding. We decided to develop a series of protocols to facilitate cellular Ub pool measurements using the free Ub sensors. Deficits in the field that this assay alleviates, as well as other approaches that have been attempted for Ub pool measurement are discussed in Appendix 1.

In order to determine concentrations of non-free Ub pools, samples were divided and treated differentially to convert the conjugated and activated pools of Ub to free Ub for sensor-based measurement. Due to the extremely high affinity of the free Ub sensor, samples typically were diluted 10 to 100-fold for their Ub levels to fall within the concentration range that is linearly related to fluorescent signal. This is advantageous because it means that cell extracts can be prepared in 8 M urea to fully disrupt structural elements of extracted proteins. Ub efficiently refolds when transferred from a solution of 8 M urea to water[50]; thus cell extracts can be diluted to promote Ub refolding, while most other cellular proteins remain unstructured. The Ub pool quantitation assay was used to reveal changes in Ub pools across cell lines and in different stress conditions; these results are reported here.

Another application that exploits the high affinity and selectivity for free Ub by engineered free Ub binding proteins is their use in isolating free Ub from complex, heterogeneous samples such as cell lysates. Tethering a binding protein to a solid support, such as agarose resin, and applying a diluted solution of cell extract permits specific enrichment of free Ub. Other groups have explored similar modes of enrichment, but for Ub-conjugates by fusing UBDs that each bind regions of the Ub core acidic patch of Ub[51,52], thus enriching "pan" Ub. Those studies demonstrated significant, specific enrichment of (poly)ubiquitinated proteins. Another useful feature of those tandem-UBDs was protection against DUB hydrolysis because their high affinities outcompete the more modest affinities of endogeneous DUBs.

To our knowledge, no attempts have been made to enrich free Ub from complex samples. Perhaps because, until Yun-Seok Choi's suite of free Ub binding proteins,

there was no protein capable of binding tightly and selectively to the free form. One application of this tool is to quantitatively remove excess free Ub in polyUb synthesis reactions; thus removing contaminating free Ub without any appreciable loss of the product. Another application of this reagent is isolating cellular free Ub for analysis by gel, immunoblotting or MS.

Although not directly tested, we expect linkage-independent binding to unanchored polyUb by tUI, the highest affinity free Ub binding protein in our collection. Our hypothesis is based on the observation that the sites used for Ub-Ub linkages in polyUb (i.e., Ub's seven lysine ε-amines plus the α-amine on M1) are not obstructed when Ub is bound by the various UBDs used in tUI (Figure 1A in Appendix 1) and previous findings[53] of linkage-independent binding by UBDs of tUI. If our hypothesis holds true, unanchored polyUb chains can also be enriched by agarose-tethered tUI (agarose-tUI). Also, tUI is a demonstrated high-affinity binder of Ub phosphorylated on Ser65 (Appendix 1, Figure 1F), which has functions in mitophagy[54]; therefore, enrichment of phosphorylated forms of free Ub is another possible application for this tool.

.   In this chapter, a protocol for using agarose-conjugated free Ub binding proteins to enrich free Ub was established. The conditions for binding, washing and eluting free Ub from cell extracts were optimized to reduce non-specifically bound proteins and enrich free Ub. The established protocol was demonstrated by isolation of free Ub from HEK 293T cells prepared in denaturing conditions.

2.2 Experimental procedures

2.2.1 Preparation of enzyme-thioesterified Ub

Reactions consisting of 1 µM mouse E1, 5 µM free Ub and 20 µM E2-25K or UbcH5c (E2) were prepared in 50 mM Tris-HCl (pH 7.5), 100 mM NaCl, 1 mM TCEP (GoldBio #TCEP25), 5 mM MgCl2, 0.3 U/mL pyrophosphatase (Sigma-Aldrich #I1643) and 2 mM ATP and incubated at 25°C for 20 minutes. These reactions were quenched by adding 5 mM N-ethylmaliemide (NEM; Thermo # 23030)) and further incubating at 25°C for 10 minutes.

2.2.2 Preparation of MESNA-thioesterified Ub

Ub (1.5 mM) was incubated with 10 mM ATP, 10 mM $MgCl_2$, 100 mM sodium 2-mercaptoethanesulfonate (MESNA; Fluka #M1511), and 100 nM mouse E1 in 20 mM HEPES (pH 8.0) for 3 h at 37 °C to form Ub-MESNA thioester. The Ub-MESNA then was incubated in 300 mM aqueous hydrazine (Sigma-Aldrich #309400) for 30 minutes at 37°C to form Ub-hydrazide. The reaction product was diluted 25-fold with 50 mM ammonium acetate, adjusted to pH 4.5 (Buffer B), and purified by cation-exchange chromatography on a Mono S column (GE Healthcare, 17-0547-01). The column was washed with 20 volumes of Buffer B and eluted with a linear gradient of 0 – 1 M NaCl in the same buffer.

2.2.3 Hydrazinolysis and hydrolysis of thioesterified Ub

Working solutions of hydrazine were prepared fresh by diluting 1 part neat hydrazine with 0.63 parts neat HCl in a glass container. Hydrazinolysis was achieved by adding 10, 25 or 50 mM of the working hydrazine solution to quenched Ub~E2 at room temperature for 30 minutes. Hydrolysis of Ub~E2 was performed by incubated

quenched Ub~E2 in 200 mM β-mercaptoethanol (βME, Acros Organics #125472500) or in 50 mM dithiothreitol (DTT, Goldbio #DTT50) at 37°C for 30 minutes. Disappearance of the Ub~E2 band was assessed by SDS-PAGE and generation of Ub-hydrazide was confirmed using MALDI-TOF using a matrix of Sinapinic Acid (Millipore, D7927) in 50% acetonitrile (ACN)/0.1% trifluoroacetic acid (TFA).

2.2.4 Expression and purification of free Ub sensor proteins

See "Methods" section in Appendix 1

2.2.5 Free Ub quantitation using tIVR

A mastermix containing 0.3 nM Alexa488-Ub, 6 nM tIVR, 200 mM sodium phosphate (NaPi, pH 7.5), 50 mM NaCl, 0.75 mg/mL ovalbumin (OVA) and 1 mM TCEP was generally prepared. To aliquots of the master mix, free Ub standards were titrated and unknown samples were added. The fluorescence intensities of all samples were quantified using a HORIBA FluoroMax-4 Spectrofluorometer. Fluorescence levels of the unknowns were then compared to the fluorescence levels of samples containing free Ub standards to determine absolute concentrations.

2.2.6 Antibodies

Antibodies used in this study include: anti-Ub (clone P4G7; Covance #MMS-258R), anti-ubiquityl-Histone 2a (Lys119) (clone D27C4; Cell Signaling #8240), anti-Histone H3 (clone A3S; Millipore #04-298) and anti-FLAG (Sigma-Aldrich #F7425).

2.2.7 Cell lines, cell culturing, and cell treatments

For quantitation of Ub pools in cellular extracts, immunoblotting and gene expression levels, those details are described in the Methods section of Appendix 1. For UCH37-FLAG immunoprecipitations, inducible HEK293 FRT/TREX cells were

maintained in DMEM (Corning #15-013-CV) supplemented with 10% fetal bovine serum (FBS; Atlas #F-0500-D), 1% L-glutamine (GE #SH30034.01), 1% Penicillan/Streptamycin solution (Corning #30-001-C1). Generally, cells were induced by treatment with 1 ug/mL doxycycline for 24 hours before harvesting. Immunoprecipitations were performed using anti-FLAG resin (Millipore # A2220) and eluting with either 8 M urea or 0.1 mg/mL FLAG peptide.

2.2.8 Preparation of agarose-conjugated free Ub sensors

Sulfolink Coupling Resin (ThermoFisher #20401) and the concentrated free Ub binding protein (i.e., tISR or tUI) were equilibrated in binding buffer comprised of 50 mM Tris pH 8.0, 0.2 M NaCl and 4 mM TCEP. Conjugation occurred during a 4 hour incubation period at 4°C on while rotating end over end. The remaining protein was removed and the resin was washed with 6 resin-bed volumes of binding buffer and 2 resin-bed volumes of 1 M NaCl. Unreacted maleimide functional groups on the resin were quenched by further incubation with 50 mM L-cysteine dissolved in binding buffer for 1 hour at 4°C on while rotating end over end. Absorbance at 280 nm was measured for each supernatant and subtracted from that of the initial protein solution to quantify the amount conjugated binding protein.

2.2.9 Free Ub capture using agarose-tUI or agarose-tISR

Human cells were lysed in 8 M urea, 0.5% Sodium deoxycholate (NaDOC), 50 mM HEPES pH 8.5, 20 mM NEM, and protease inhibitor cocktail (Sigma-Aldrich #P8340) by sonication. The lysate was cleared by centrifugation at 10,000 g and then diluted at least 25-fold with binding buffer containing PBS (pH 7.4), 4 mM NEM and protease inhibitors. Agarose-tUI was equilibrated with binding buffer and then the

diluted lysate was applied for 1 hour at 4°C. The unbound portion was removed and the resin was washed with 5 resin-bed volumes of binding buffer supplemented with 0.25 M NaCl. Elution was performed by adding 50 mM citric acid (pH 2.2) at 50°C for 5 minutes and eluates were analyzed by silver staining SDS-PAGE gels using conventional methods.

2.3   Results

2.3.1   Development of an assay to quantify ubiquitin pools in human cells

Ideally, a method for Ub quantification should be able to distinguish between each of the three chemical forms of Ub: free, activated and conjugated. While a few methods have been described to measure the concentration of one or more specific Ub pools, they are cumbersome to perform and data interpretation is difficult, which limits ability to perform routine measurements or samples in high-throughput[28,31]. For quantitative studies, such a method should provide accurate, pool-specific Ub concentrations with precision and high sensitivity. Here, the development and validation of protocols for processing cellular extracts for Ub pool measurement by free Ub sensor proteins are described. Briefly, samples are divided in three and treated with Usp2cc, hydrazine (N_2H_4) or β-mercaptoethanol (βME) to release all Ub-conjugates as free Ub, convert thioester-bound Ub to Ub-N_2H_4, or release thioester-bound Ub as free Ub, respectively (Figure 2.1)

2.3.2   Conversion of Ub-thioesters to Ub-hydrazide

Protein thioesters are labile and subject to hydrolysis in basic environments[55] and when exposed to reducing agents, such as βME, are subject to intramolecular displacement, resulting in the corresponding protein-carboxylate[56]. In order to
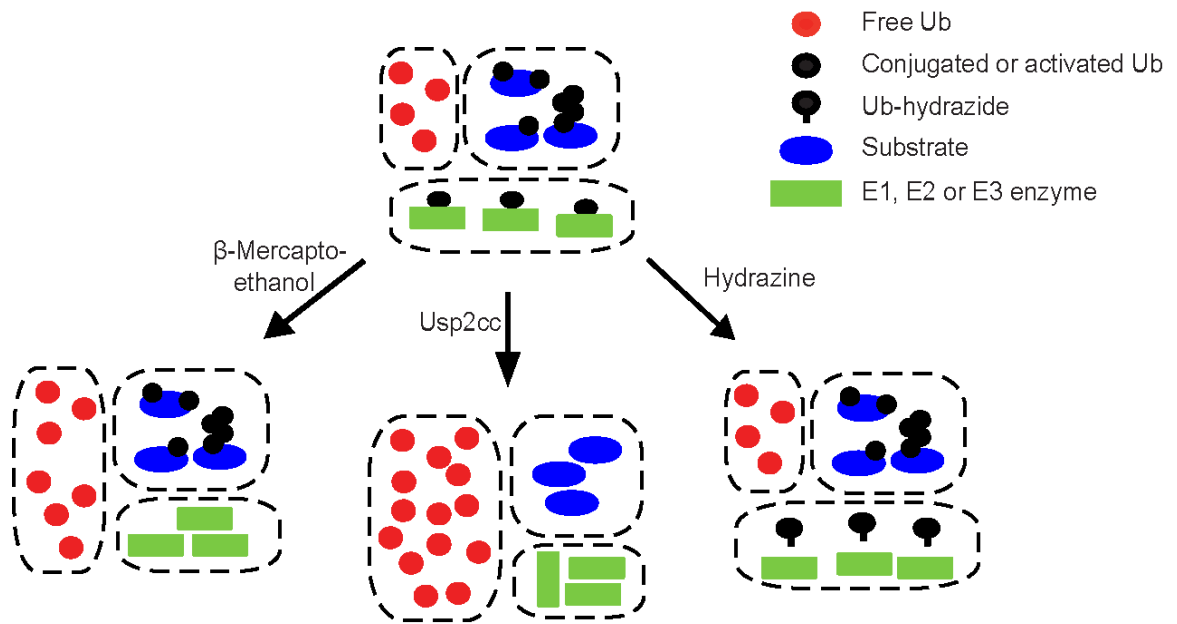
Figure 2.1 A series of protocols enables Ub pool measurements by free Ub sensors. Portions of each sample are treated with β-mercaptoethanol, Usp2cc or hydrazine and subsequently added to Atto532-tUI or related sensor to quantify Ub within the conjugated, activated and free pools.

circumvent the loss of thioesters and concurrent contamination of the free Ub pool, we decided to convert thioesters to a covalently bound adduct on the C-terminus of Ub. For this conversion, two criteria were necessary to meet: 1) the reaction should be efficient such that it is complete in a few hours and 2) the generated adduct should prevent binding of the free Ub binding protein.

First, the reaction efficiency of hydrazine was tested by prepared Ub thioesters using the conjugating enzyme E2 25K (Ub~E2 25K) and treating with increasing concentrations of hydrazine at pH 7.5 for 30 minutes at 37°C.

A sample of the reaction at each step was analyzed by SDS-PAGE (Figure 2.2A), which demonstrated that no Ub~E2 remained after hydrazine treatment. In order to demonstrate the identity of the final product, we prepared Ub-MESNA thioester and reacted it with 300 mM hydrazine at 37°C for 30 minutes and analyzed the product using MALDI-TOF MS (Figure 2.2B). This experiment demonstrated that hydrazinolysis of thioesters is complete within 30 minutes and the product of the reaction is Ub-hydrazide. Finally, it was shown that Ub-hydrazide was not recognized by the free Ub sensor proteins. This is discussed in Appendix 1.

2.3.3 *Release of ubiquitin-thioesters as free ubiquitin using βME*

The next step in Ub pool assay development was to optimize release of Ub-thioesters as free Ub (i.e., Ub with a C-terminal carboxylic acid). When treated with βME, protein thioesters are efficiently and rapidly converted to protein carboxylates, while treatment with dithiothreitol (DTT) generates a thioacid intermediate that is eventually converted to carboxylate[56]. For this reason, we decided to pursue intramolecular displacement of ubiquitin-thioesters using βME. To assess its efficiency,
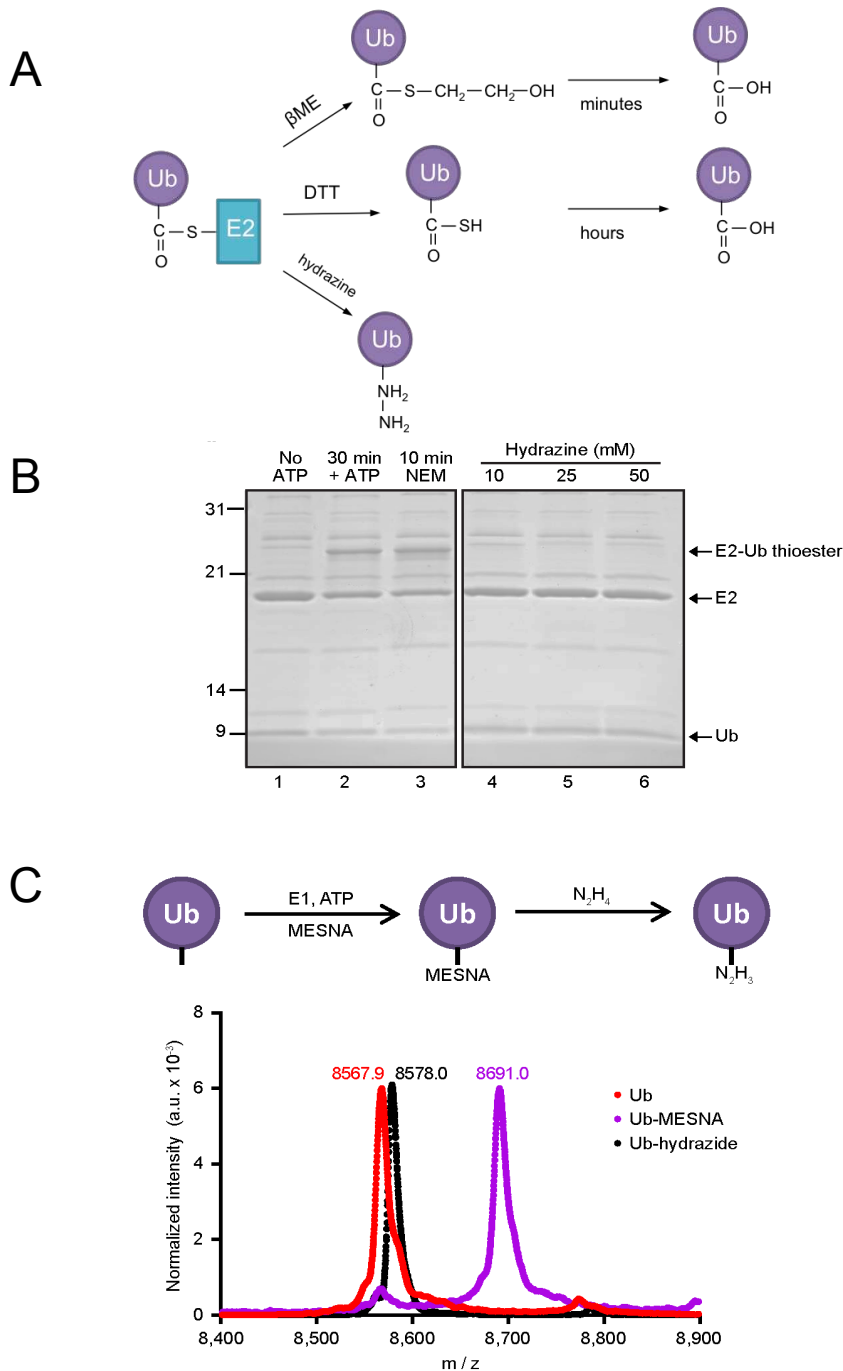
Figure 2.2 Reactions of thioester-linked Ub. A. Scheme depicting the products of Ub~E2 (or E1, E3) with βME, DTT or hydrazine. **B.** Ub was incubated with E1 and E2 (E2 25K) enzymes without (lane 1) or with (lane 2) ATP to form Ub~E2 25K thioester. After treatment with NEM (lane 3) to inactivate enzymatic activities, hydrazine was added at the concentrations indicated for 30 minutes at 37°C **C**. Upper panel shows the reaction scheme to generate Ub-hydrazide (see Methods) for Fig 1b-d titrations. Lower panel shows overlayed MALDI-TOF mass spectra of Ub and products (i.e., Ub–MESNA and Ub–hydrazide) from each step in the synthesis.

the Ub~E2 thioester adduct to the UbcH5c enzyme was prepared and treated with 200

mM βME for 30 minutes at 37°C; samples of the reaction with and, as a negate control,

without ATP were run on SDS-PAGE (Figure 2.3A). In order to validate that the free Ub-

carboxylate had been regenerated in the thioester intramolecular displacement, a tIVR

competition assay with Alexa488-Ub was used to quantify the free Ub in samples of

Ub~UbcH5c treated with DTT, βME or N_2H_4 (Figure 2.3B). This experiment

demonstrated that free Ub was most efficiently generated by treatment with 200 mM

βME for 1 hour at 37 °C, whereas when treated with DTT, hydrolysis of the Ub~thioacid

intermediate to free Ub likely takes longer.

2.3.4 *Digestion of ubiquitin-conjugates by Usp2cc*

The final treatment of cell lysates for Ub pool measurements is digestion by the

nonspecific DUB called Usp2cc. Usp2cc is the catalytic core domain of Usp2 and has

been shown to digest a wide variety of Ub-(iso)peptide bonds, regenerating free Ub

monomers[57]. This enzyme has been shown to efficiently cleave Ub in a wide range of

pH, salt and denaturing conditions[58], making it an ideal reagent to disassemble

(poly)Ub-conjugates in cell lysates.

To test the efficiency of Usp2cc digestion with cell lysate, the release of free Ub

was monitored for a cell lysate incubated with Usp2cc in real time using the tIVR

competition assay with Alexa488-Ub. Briefly, HEK 293T cells were harvested and lysed

by sonication in a buffer containing 8 M urea and protease inhibitors. Usp2cc (1:10 ratio

to total protein), tIVR and Alexa488-Ub were added to the cell extract and fluorescence

was compared to a standard curve every 15 minutes at 37°C (Figure 2.4A). This

experiment demonstrated that digestion of Ub-conjugates by Usp2cc was complete in
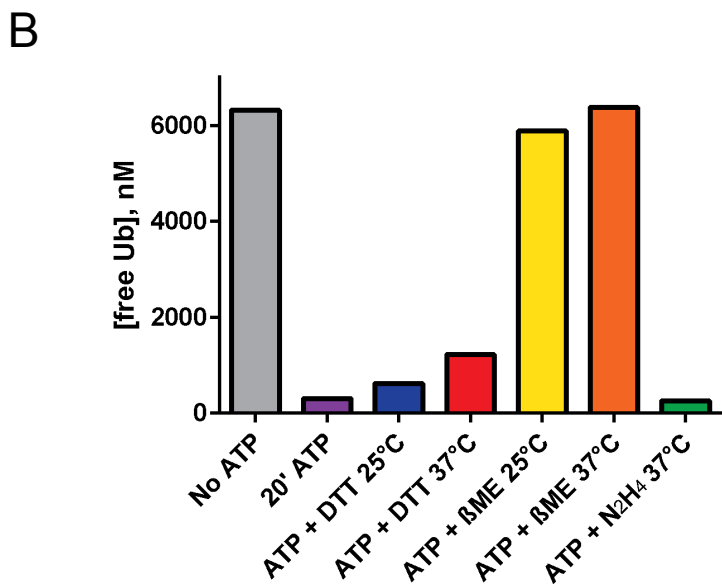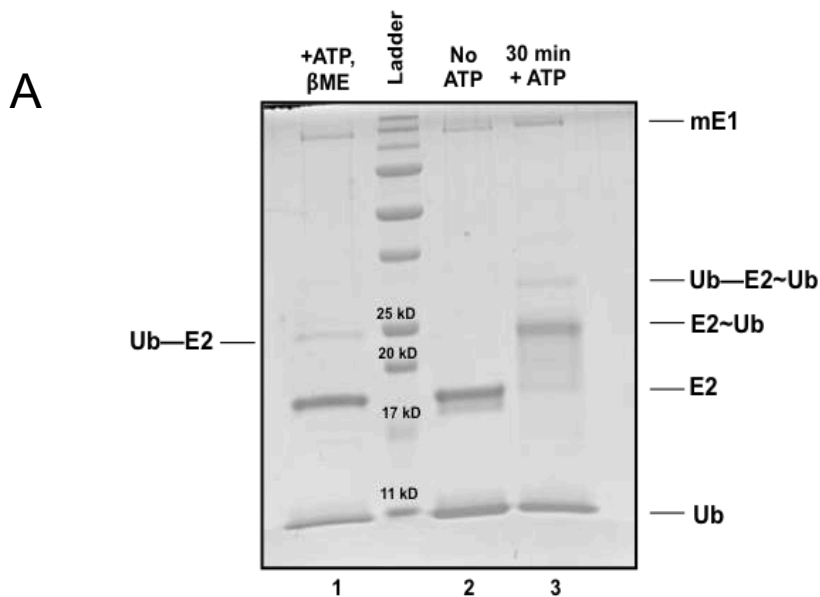
Figure 2.3 Hydrolysis of thioester-linked Ub. A. Ub was incubated with E1 and E2 (UbcH5c) enzymes without (lane 2) or with (lane 3) ATP to form Ub~UbcH5c thioester. βME was added at 200 mM for 30 minutes at 37°C. **B.** Ub~E2 25K ("20' ATP") was subjected to 50 mM DTT or 200 mM βME at 25 or 37°C or 50 mM N_2H_4 at 37°C for 1 hour. The free Ub in each reaction, measured by competition with Alexa488 for tIVR, was compared to Ub~E2 25K and "No ATP".

A
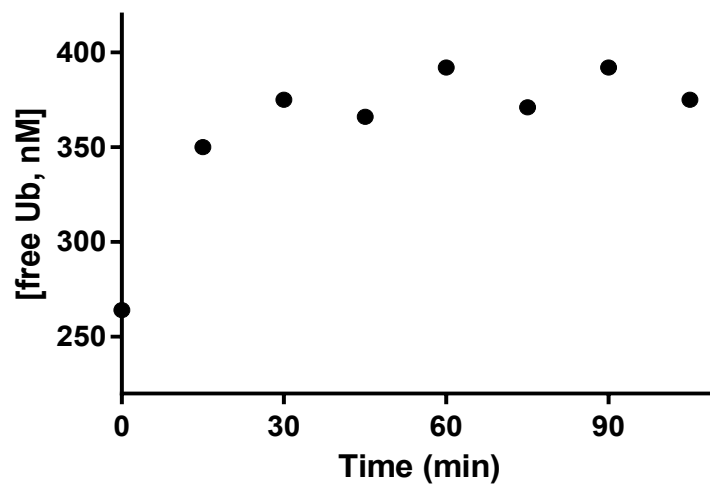
B
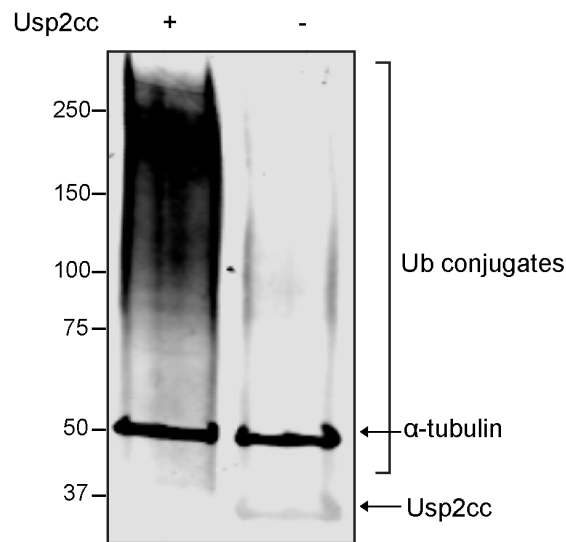
Figure 2.4 Digestion of conjugated Ub by Usp2cc. A. Real-time quantification of Ub-conjugate digestion by Usp2cc. tIVR and Alexa488-Ub were added to cell extracts with 1:10 Usp2cc and incubated at 37°C. Fluorescence measurements were taken every 15 minutes and compared to a standard curve containing tIVR, Alexa488-Ub and increasing concentrations of free Ub. **B.** SDS-PAGE and immunoblot with anti-Ub (P4G7) of cell lysate treated with Usp2cc compared to no treatment. α-tubulin was immunoblotted to use as a loading control.

60 minutes. Indeed, when HEK 293T cell lysates digested by Usp2cc for 60 minutes at 37 °C were compared to untreated lysate by western blotting against Ub, it was apparent that most conjugates were depleted (Figure 2.4B). For Ub pool measurements, 1:10 Usp2cc to protein was incubated with cell extracts for 60 minutes at 37 °C.

2.3.5   *Sensor stability under conditions used for free Ub measurements of cell lysates*

To reliably use the free Ub sensor proteins for concentration reporting, it was necessary to validate their ability to bind free Ub in each lysate treatment condition. The tIVR binding to free Ub was assessed in 350 mM urea (Figure 2.5A). Fluorescence of tIVR bound to Alexa488-Ub did not change over the 85-minute time course, indicating that the binding interaction was not perturbed by this concentration of urea.

The rationale behind this experiment is that cell extracts should be prepared in strongly denaturing conditions (i.e., 8 M urea) to eliminate protease and other enzymatic activities that otherwise would alter Ub pool levels, but that subsequent dilution in non-denaturing buffer could be done to accommodate free Ub quantitation by a sensor protein. From this experiment, it was concluded that free Ub in cell extracts prepared with 8 M urea could be accurately quantified after dilution. This type of stability test was also performed on the Alexa488-Ub bound tIVR using 40 mM βME (Figure 2.5B). Little change in fluorescence was observed in this assay and it was concluded that βME-treated samples could also be reliably quantified by tIVR.
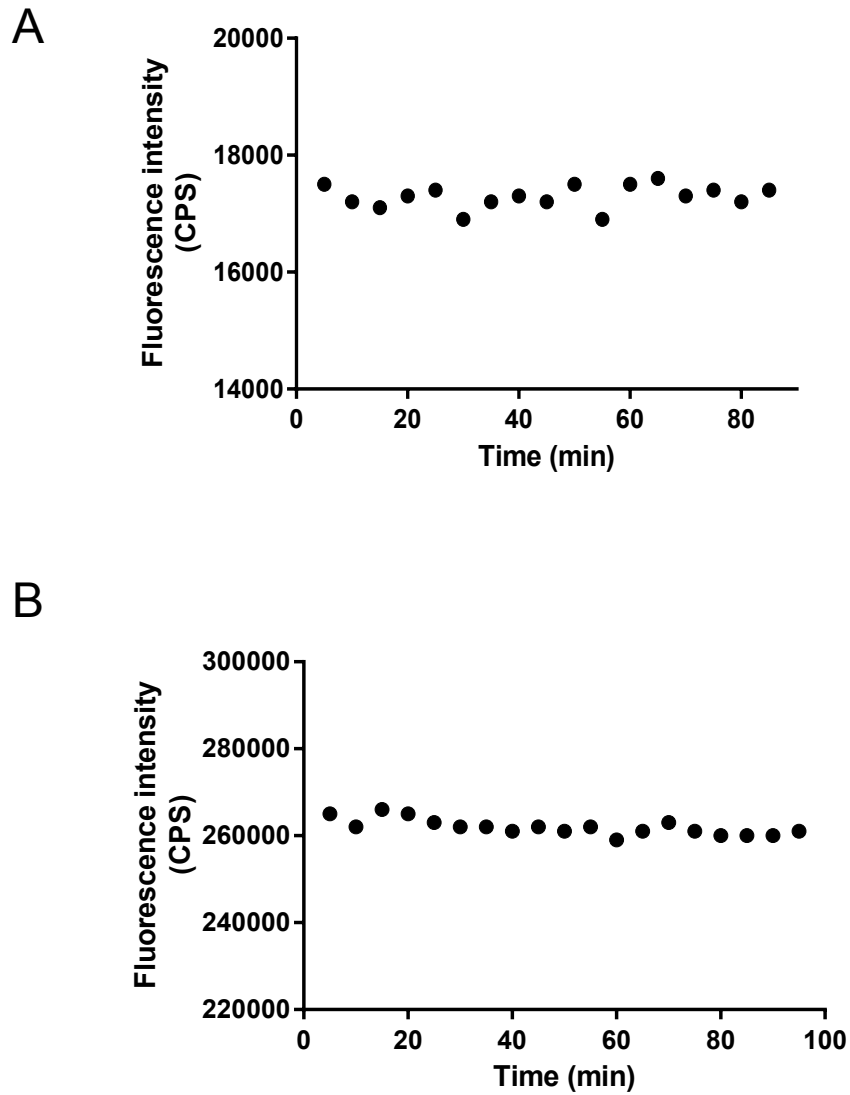
Figure 2.5 tIVR stably binds free Ub in reagents used for cellular pool measurements. Solutions containing 6 nM tIVR, 1 nM Alexa488-Ub and **A.** 350 mM urea or **B.** 40 mM βME were incubated at 25°C. Fluorescence measurements were taken every 5 minutes for 90 minutes.

*2.3.5.1	High-throughput free Ub measurements made by scanning samples in 384-well plates*

Measurements of Ub in three pools and from multiple samples requires a more high-throughput method of sample measurement than conventional fluorimeters permit, where each sample is measured individually. We decided to perform the fluorescence measurements *en masse* by pipetting samples into glass bottom 384-well plates and recording the fluorescent signal intensities with a Typhoon FLA 9500 scanner. As recommended by Gansen et al.[59], we used 384-well microplates passivated with a series of reagents including Hellmanex®, NaOH and Sigmacote™ to reduce the amount of protein absorbed to the walls of the 384-well plate, thereby increasing the accuracy of these experiments.

Competition assays using tIVR and Alexa488-Ub and unlabeled Ub were prepared in untreated and passivated 384-well plates to test whether plates needed to be treated before use in a Ub pool measurement assay (Figure 2.6). In the absence of plate treatment, almost twice as much unlabeled, free Ub was needed to compete away Alexa488-Ub when compared to the same assay performed in a passivated 384-well plate. This suggests that some free Ub or tIVR/Alexa488-Ub is absorbing onto the walls of the plate. We decided to passivate the 384-well plates before using them in all free Ub measurements (see Experimental procedures for details).

2.3.6 Sensor standard curves with free Ub

Ub can be quantified by comparing signals produced by the fluorescent sensor in unknown samples to the fluorescence generated using Ub standards. One way to do this is to start with a sub-K_d concentration of sensor and titrate Ub at concentrations
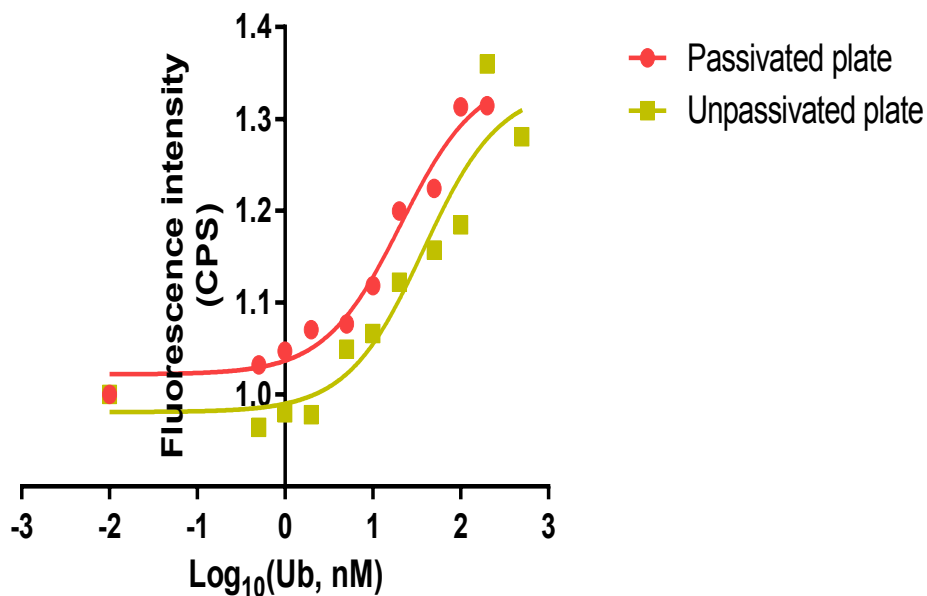
	IC$_{50}$ (nM)
passivated 384-well plate	20.9
untreated 384-well plate	37.8

Figure 2.6 384-well plate passivation is required to prevent protein adsorption. Competition assay with 6 nM tIVR, 1 nM Alexa488-Ub and increasing concentrations of unlabeled Ub were performed in 384-well plates that were untreated or treated using a passivation protocol. The curves generated by the titrations were fit using a model that assumes one binding site on tIVR.

surrounding the Kd to generate a logarithmic binding curve as in Figure 2.7A. The linear

part of the curve provides a guide to the range of Ub concentrations that are quantifiable

by the sensor under these assay conditions. This was the method of quantitation using

Atto532-tISR; generally, 6 nM Atto532-tISR was used (Figure 2.7A). Another method

that can be used to quantify free Ub is to use a concentration of sensor protein over 10-

fold above its Kd for free Ub. When free Ub is titrated, a linear signal is produced since

virtually all free Ub will be bound by the sensor (Figure 2.7B).

2.3.7   Using Atto532-tUI and related sensors to assay Ub pools in human cell lines

The assays described above were used to quantify the amounts of free, activated

and conjugated Ub in HeLa cells (Figure 2.8A). The results are in good agreement with

other reports, where free and conjugated Ub were quantified by MS and

immunoblotting[25,28,31]. The sensor assays then were used with HeLa cells after

treatment with inhibitors of the E1 Ub-activating enzyme or proteasome or heat shock

(Figure 2.8). As expected[60], the E1 inhibitor Compound 1 (C1) dramatically increased

free Ub with a concomitant loss of activated Ub and most Ub–protein conjugates (Figure

2.8A). Notably, the concentration of total Ub quantified by the sensor in C1 treated cells

was significantly lower than in the absence of inhibitor. This is possibly due to the

generation of a Compound 1 adduct on the C-terminus of free Ub that is resistant to

Usp2cc digestion and would not be recognized by the free Ub sensors[60].

Converse to E1 inhibition, proteasome inhibition by bortezomib (BTZ) promoted

accumulation of Ub conjugates that reached a maximum at 1 h and then persisted

through a 4 h treatment (Figure 2.8B). The conjugate increase was accompanied by a

modest depletion of activated Ub and a two-fold decrease in free Ub, presumably due to

A
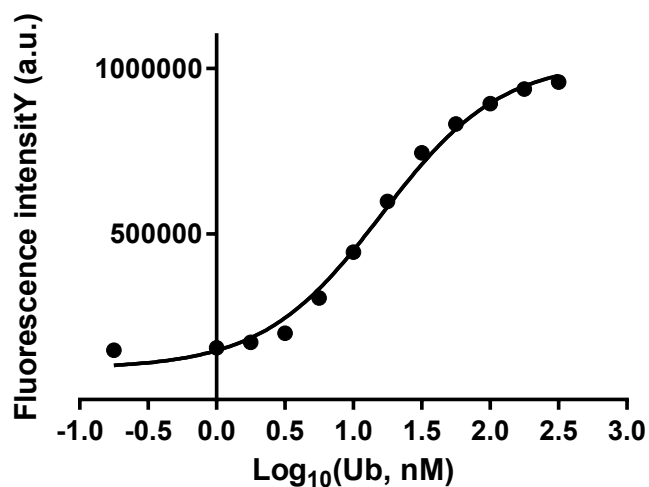
B
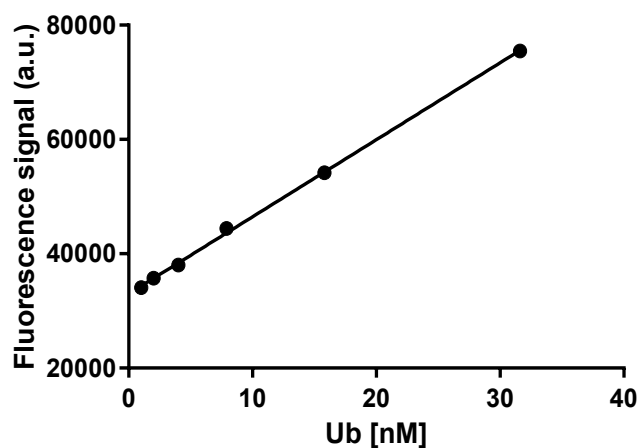
Figure 2.7 Standard curves generated by titrating free Ub to sensor proteins. Free Ub was titrated to **A.** 6 nM Atto532-tISR (below its K_d of 20 nM) or **B.** 50 nM Atto532-tUI (above its K_d of 60 pM). The curve in **A** was fit using a model that assumes one-binding site on tIVR. The curve in **B** was fit using linear regression.
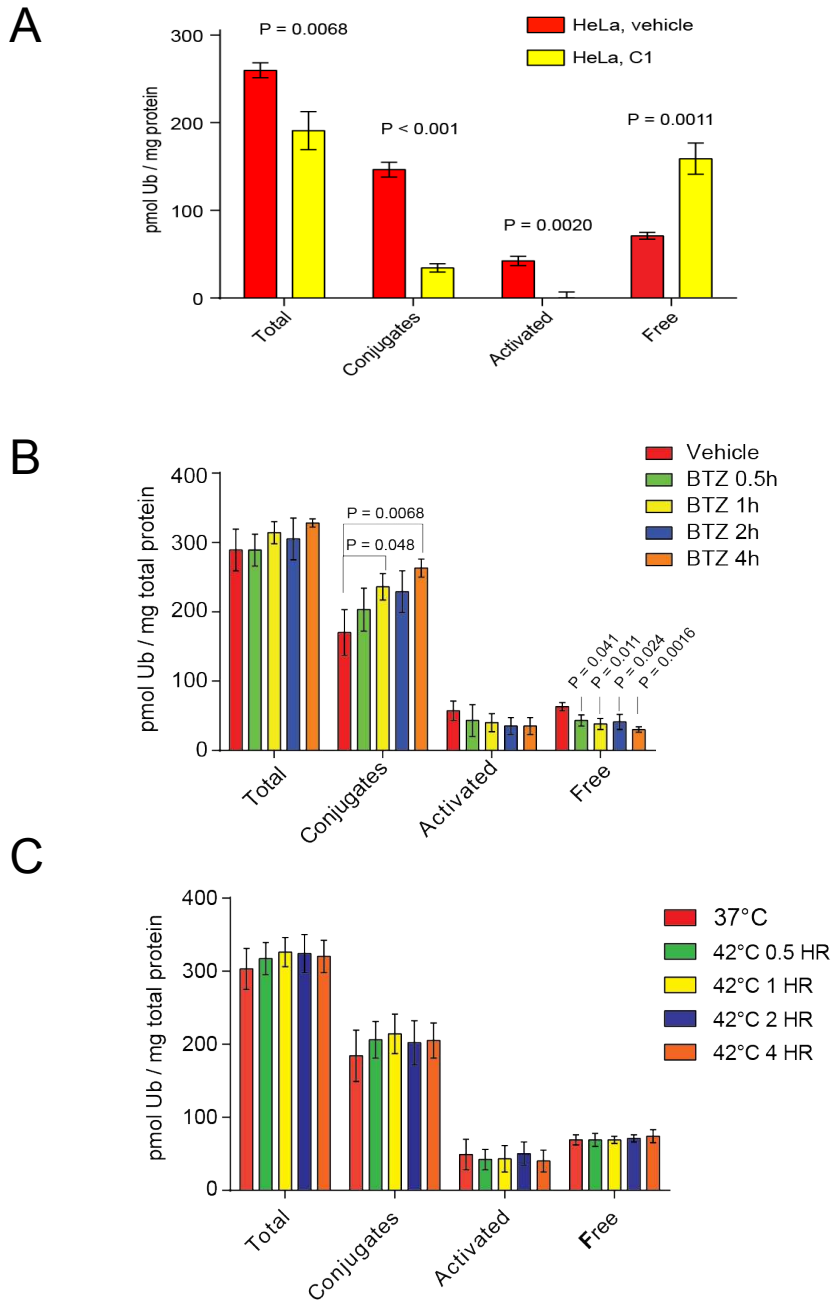
Figure 2.8 Effects of cellular stresses on Ub pools in HeLa cells.
Quantitation of Ub pools in lysates of HeLa cells after treatment with vehicle
(DMSO) or **A.** E1 inhibitor, C1, at 10 µM, **B.** proteasome inhibitor, BTZ, at 1
µM for 1-4h and **C.** heat stress at 42°C. Statistical analyses by t-test (A) and
ONE-WAY ANOVA with Bonferroni's adjustment (B,C); error bars represent ±
s.d. (n = 3).

impaired proteasome-dependent recycling of Ub from conjugates. Different from this result, heat shock at 42 °C resulted in no appreciable change in any pool. Initially, this was unexpected because Dantuma et al[38] reported that Mel JuSo cells experience a drastic increase in nuclear Ub conjugates and depletion of free Ub, as quantified by immunoblotting. Further search of the literature led to a report by Fujimoro et al.[61] that showed HeLa cells exhibit only a slight increase in conjugates upon heat shock at 42 °C, higher temperatures appreciate significant levels of Ub-conjugates.

The Ub pool assays were also used to compare the responses of HeLa and MEF cell lines to proteasome inhibition (Figure 2.9A). In both cell lines, conjugates were significantly increased, yet MEF cells maintained an unchanging level of free Ub such that the total level of cellular Ub increased, whereas HeLa cells exhibit a 50% depletion of free Ub (Figure 2.9A). Increased total Ub in MEF cells is supported by the activation of *Ubb* and *Ubc* expression in MEF cells during proteasome inhibition that was not observed in HeLa cells (Figure 2.9B). *Ubb* and *Ubc* are heat shock-inducible genes that are activated by many types of environmental stresses[62,63]. Also during cellular stress, histones are deubiquitinated *en masse*, possibly acting as a reserve to provide additional Ub when the free pool is depleted[38]. Histone 2A ubiquitinated at K119 (ubH2A) compared in proteasome-inhibited HeLa and MEF cells revealed an interesting pattern (Figure 2.9C). HeLa ubH2A was depleted to a greater extent than MEF ubH2A (~25% in HeLa versus ~50% in MEF cells).
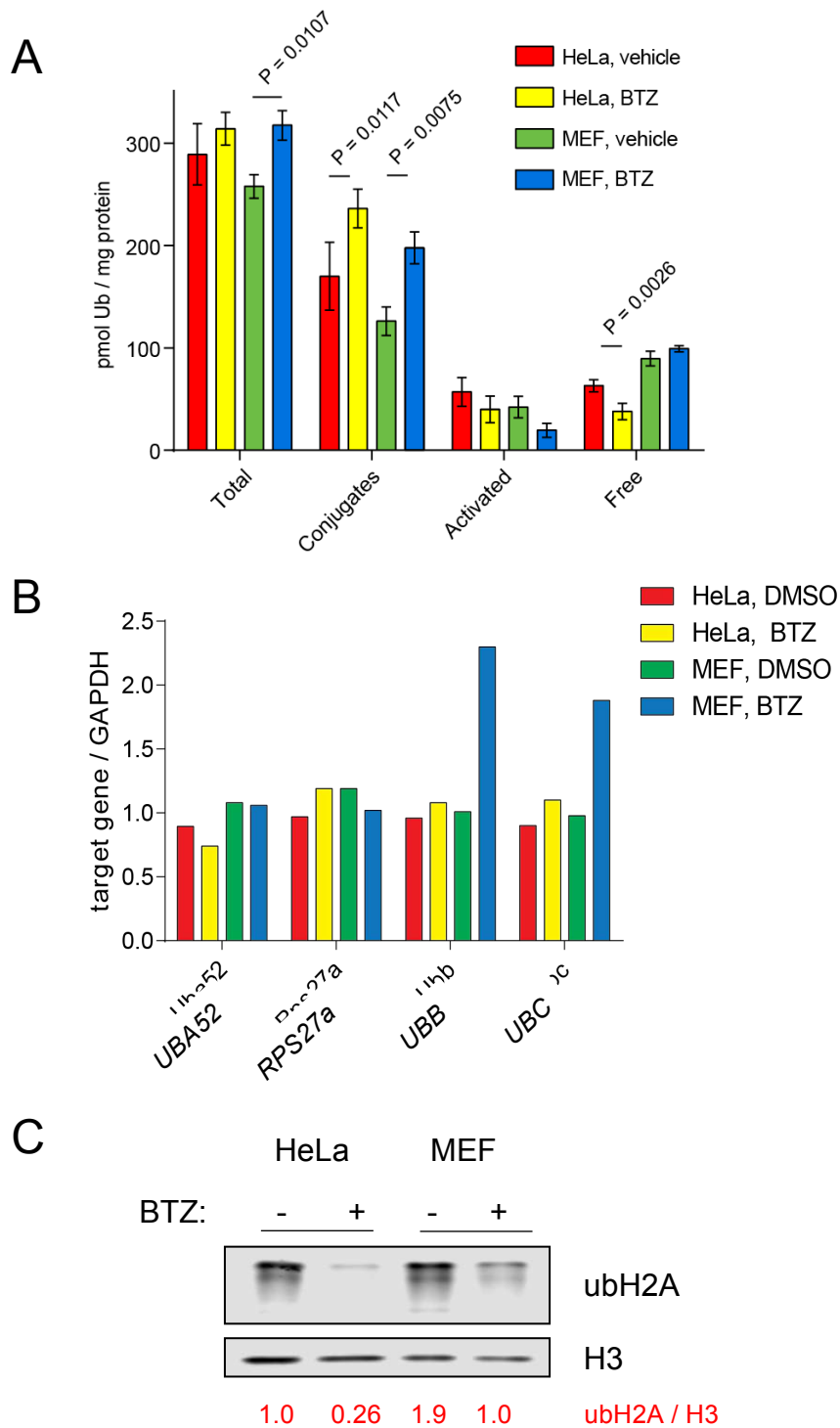
Figure 2.9 Comparison of effects of proteasome inhibition in MEF and HeLa cell lines. Comparison of **A.** Ub pools, **B.** Ub gene expression, and **C.** levels of ubH2A in indicated cell lines after vehicle or proteasome inhibition with BTZ for 1 hour. Statistical analyses by ONE-WAY ANOVA with Bonferroni's adjustment; error bars represent ± s.d. (n = 3).

2.3.8 Using Atto532-tUI to quantify Ub pools immunoprecipitated with proteasomes in Uch37 mutant cell lines

Uch37 is a DUB that is associated with the proteasome and processes unknown substrates. Proteasomes were immunoprecipiated from cells overexpressing Uch37 with the active site mutant, C88A, a non-Ub binding version, EWI (E34R, W36D and I216D), or the wild-type (WT). The Ub pools within the immunoprecipated proteins were quantified using a modified protocol with Atto532-tUI, where the Ub standards and unknown samples are all quantified in 2.5% elution buffers (8 M urea, 0.1 M MOPS pH 6.5, 20 mM NEM or 0.4 mg/mL FLAG, 0.1 M MOPS pH 6.5, 20 mM NEM,) (Figure 2.10A, B). Surprisingly, we observed over 10-fold more free Ub in the C88A cell line, as compared to WT and EWI. Conjugated and total Ub were elevated 4-fold in C88A, a reasonable outcome for proteasomes missing a DUB enzyme. These results were confirmed using SRM-MS targeted against the C-terminal peptide of free Ub as a surrogate to free Ub quantification by Atto532-tUI (Figure 2.2.9C, D).

Again, we observed significantly higher free and also conjugated (and thus total) Ub associated with C88A proteasomes as compared to WT and EWI. It was shown that K48-linked, polyUb chains are substrates of Uch37 *in vitro*[64]. If K48-linked polyUb chains on proteins destined for the proteasome are the substrate of Uch37, and it is not present, we could expect an accumulation of conjugated Ub at the proteasome. The increase in free Ub was unexpected, as it is counterintuitive that the product of deubiquitination increases in the absence of the DUB.
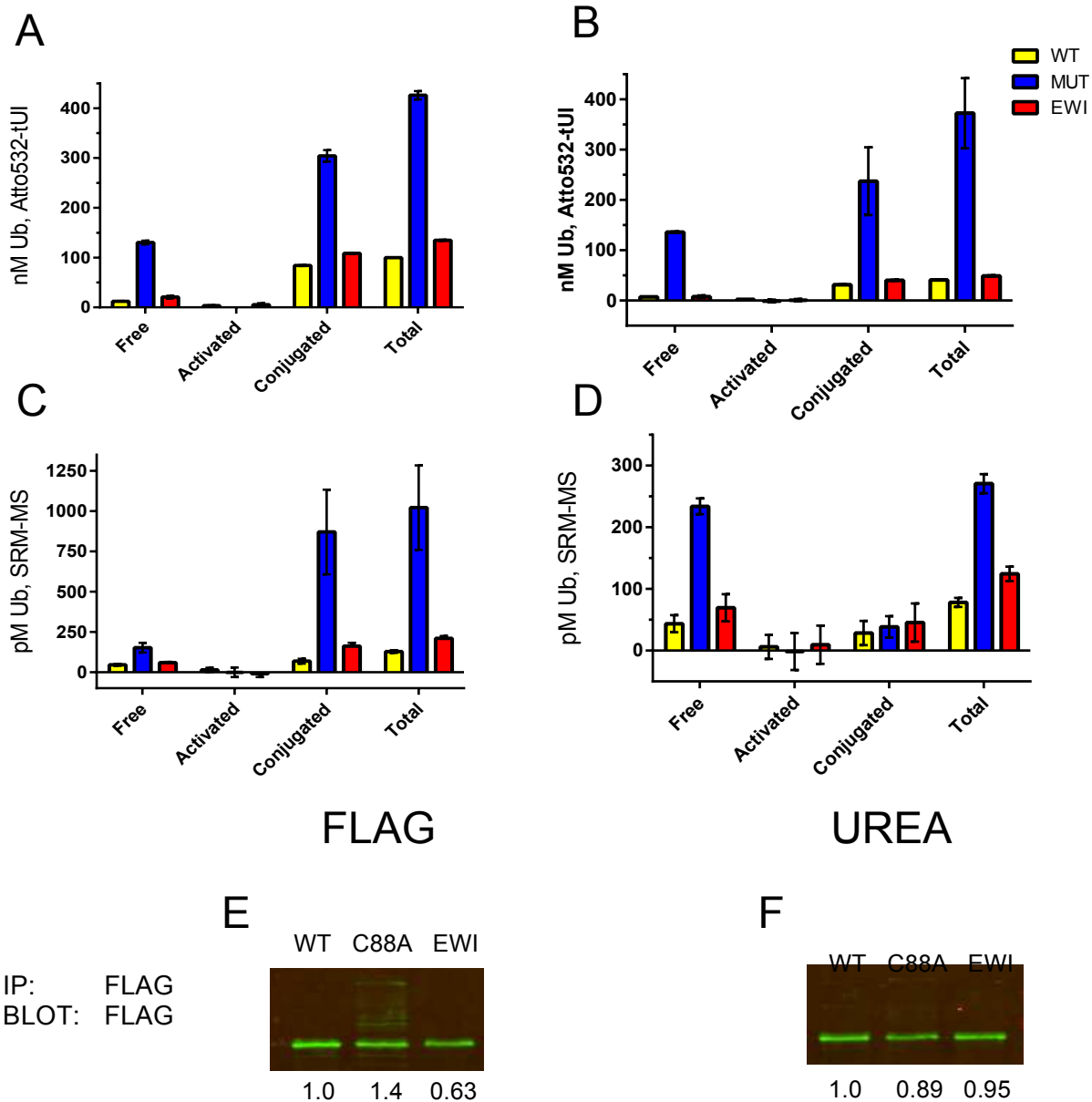
Figure 2.10 Uch37 C88A cell lines retain more free and conjugated Ub at the proteasome than WT or EWI. Cells expressing FLAG-tagged WT, C88A or EWI Uch37 were induced for 24 hours before harvesting for proteasomal IP using anti-FLAG. The amount of each Ub pool was quantified after elution with **A. C.** FLAG peptide and **B. D.** urea using **A. B.** Atto532-tUI or **C. D.** SRM-MS targeting the C-terminal peptide of LysC digested Ub. **E. F.** The Ub concentrations were normalized based on the amount of Uch37 immunoprecipitated in each condition based on western blotting with a FLAG antibody.

2.3.9 Using tUI and tISR as affinity reagents to enrich free Ub

Agarose beads derivatized with maleimide groups were used to immobilize free Ub binding proteins through Cys residues. Measuring the protein absorbance at 280 nm of input and unbound solutions provides estimation for the quantity of binding proteins conjugated to the resin. Unreacted maleimide sites were then blocked with excess L-cysteine.

In order to perform free Ub pulldowns from cellular extracts, cells need to be lysed in denaturing conditions to inactivate DUB and other protease activities. For this purpose, cell extracts used for free Ub enrichment were typically prepared in denaturing conditions (i.e., 8 M urea, 0.5% sodium deoxycholate (NaDOC), 20 mM NEM and protease inhibitors). To test the compatibility of agarose immobilized tISR (agarose-tISR) sensors with these conditions, samples of free Ub and ovalbumin (OVA) were prepared in 0.8 M urea, 0.5% NaDOC or 0.5% NaDOC and incubated with agarose-tISR. Elution was performed using SDS sample buffer (SDS SB) heated to 90 °C because this condition is extremely denaturing and is expected to elute anything that was non-covalently bound in each condition. The eluates were loaded onto SDS-PAGE gels and imaged after staining with Coomassie R250 stain. The amount of Ub eluted in each condition was compared to pull-downs in 0.2 M urea (used as a positive control), because it was previously shown that free Ub sensors stably bind free Ub in this condition (Figure 2.11A). This experiment demonstrated that free Ub is efficiently bound by agarose-tISR in up to 0.8 M urea (i.e., ten-fold dilution of cell lysates prepared in 8 M urea), but because only 50% free Ub is bound in 0.05% NaDOC, the lysates would need to be further diluted if they were prepared in 0.5% NaDOC.
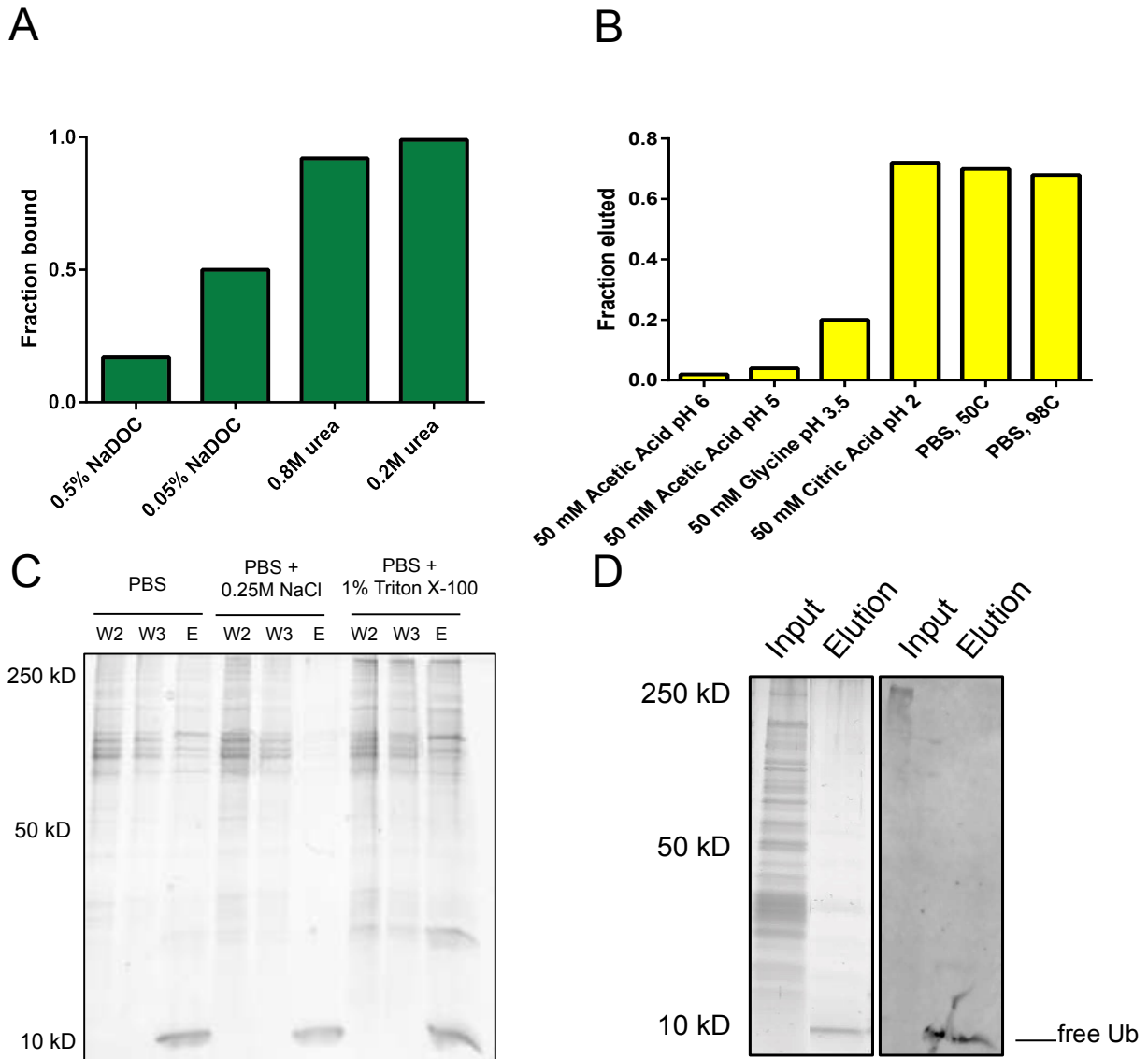
Figure 2.11 Development of immobilized sensor assays to enrich free Ub from cell lysates. Solutions of free Ub and OVA were prepared in **A.** various binding buffers or **B.** PBS before incubation with agarose-tISR and elution with **A.** SDS sample buffer or **B.** buffers of decreasing pH or at high tempertures to optimize the binding and elution conditions. **C.** Wash conditions were optimized by applying cell lysates to agarose-tISR and assessing the amount of contaminating protein in the wash and elution solutions on silver-stained SDS-PAGE. **D.** SDS-PAGE and silver staining (left) or immunoblotting using anti-Ub (P4G7) shows the levels of total protein and Ub or ubiquitinated protein in input and elution using the optimized pulldown protocol.

Next, the elution protocol was optimized to find conditions where free Ub is efficiently eluted, but buffer components should not inhibit sample processing by protease enzymes for MS analysis. To test this, a similar approach to the previous experiment was used, except free Ub with added OVA was prepared in PBS. Solutions at different pH's ranging from 2.2 to 6 as well as heating to 50°C in PBS were used as elution conditions and compared to heating in PBS at 98°C, which should completely denature the sensor and was used as a positive control (Figure 2.11B) From this experiment, it was concluded that 100 mM citric acid (pH 2) at 50°C efficiently elutes the majority of free Ub bound on agarose-tISR.

The washing step was optimized to minimize contaminating proteins in the elution product. For this test, cell extracts were prepared in denaturing lysis buffer and diluted 25-fold before addition of agarose-tISR. Wash buffers composed of 0.25M NaCl or 1% Titon X-100 in addition to PBS were tested and compared to the PBS only control. After incubating cell lysates on agarose-tISR, washes were performed and elution was achieved by adding 100 mM citric acid pH 2. A sample of each wash and elution was run on SDS-PAGE to check the ability to remove contaminating proteins. Washes with additional salt or detergent did remove more contaminating proteins than PBS alone, however, only the high salt wash resulted in a cleaner elution (Figure 2.11C).

Finally, the pulldown was performed using the optimized binding, wash and elution conditions. The input and eluate was observed on a silver-stained SDS-PAGE and by western blotting using anti-Ub (P4G7) (Figure 2.11D). These observations show that this pulldown protocol is reproducible, efficient and selective for free Ub.

2.4 Conclusions

A method to quantify free, activated and conjugated Ub in cellular extracts using high affinity, free Ub binding proteins was established and validated. This in-solution Ub pool quantitation method overcomes many difficulties faced by previous approaches. First, treatments on the cell lysate (i.e., Usp2cc, βME or N_2H_4) enables sample processing to be performed without fear of Ub~thioester hydrolysis, which would result in dilution to the activated pool and contaminate the free pool. This is an improvement from Ub-PSAQ[28], an MS-based protocol for Ub pool measurement, which makes no accommodations to protect the activated pool. Second, our sensor-based method can be performed without the use of specialized instruments like mass spectrometers; at minimum throughput, the only instrumentation this assay requires is a fluorimeter. The only other comprehensive Ub pool measurement method known to us uses SRM-MS for Ub quantitation and[31], like PSAQ, requires MS instrumentation. Also, the sensor-based Ub pool assay presented here can be performed within a day and is amenable to high throughput applications, making routine and large experiments possible.

Initial use of the in-solution Ub pool assay led to the observation that regulation of the free Ub pool is not the same in each cell type. In both HeLa and MEF cells, Ub-conjugates increase by at least 50% after BTZ treatment, but only in HeLa cells does this translate to a reduction in the pool of free Ub (Figure 2.9A). Conversely, only in MEF cells does the total amount of cellular Ub increase, and this is due to an increase in Ub gene expression by the heat shock gene *UBC* (Figure 2.9A, B). Especially for therapeutics based on proteasome inhibition, it will be important to determine what cellular factor(s) regulates the ability of cells to "sense" the depletion of free Ub and

activate gene expression.

The pool of Ub conjugated at K119 on H2A is also a hypothesized modulator of Ub homeostasis.[38] Shortly after induction of proteotoxic stress, such as heat shock or proteasome inhibition, histone monoubiquitination is depleted and thought to replenish the exhausted free Ub pool[38,65] Perhaps part of the cellular sensor is ubH2A, as it was hypothesized that a decrease in free Ub levels simply limits the availability of Ub for Rnf2, the E3 ligase responsible for ubH2A, and over time ubH2A is depleted.[66] It is well documented that ubH2A is deposited on the chromatin associated with repressed Hox genes[67,68]. Possibly, ubH2A is also playing a similar role at the chromatin associated with *UBC*, causing its activation during stress induction. Chromatin immunoprecipitation experiments could be done to test whether ubH2A occupies chromatin along *UBC*.

The in solution Ub assay was also used to quantify pools associated with Uch37, one of the Ub receptors of the 19S proteasome (Figure 2.10A-D)[69]. As expected, the inactive mutant (C88A) was associated with many more Ub-conjugates than WT or EWI. Also, C88A immunoprecitates contained free Ub levels elevated by at least 10-fold, which is surprising because free Ub is the product of reactions produced by DUBs such as Uch37. This result may be indicative of Uch37 playing a role in polyUb chain editing. Potentially, the goal of Uch37 activity is to deubiquitinate chain linkages that are poor substrates for proteasomal processing, thus allowing an associated ligase to add a different polyUb chain resulting in productive proteolysis. If this is true, it stands to reason that free Ub could accumulate in the absence of Uch37 activity because normally, that Ub would be used to make polyUb chains for proteasome processing. Further experiments to determine the true meaning of elevated free and Ub conjugates

at Uch37 depleted proteasomes are needed, but are out of the scope of this work.

Confirming the results of fluorescent sensor-based Ub pool quantitation inadvertently established a second route of Ub quantitation, employing MS. As previously mentioned, other groups have performed Ub pool measurements using MS methods[28,31], but here we combined the lysate treatments with MS-based quantitation. There are no significant advantages of the MS-based approach, but it nicely validated the results of sensor-based measurements (Figure 2.10).

Finally, a method to isolate free Ub from cellular extracts using agarose-tUI was established and used to remove virtually all other proteins (Figure 2.11D). For experiments discussed in Section 3.3.5, agarose-tUI was critical for the enrichment of free Ub from cells precipitated in 70% ethanol. Even in the midst of aggregated and unfolded proteins, eluates from agarose-tUI were mainly comprised of free Ub.

In summary, methods were developed that could enhance studies of Ub homeostasis, which is disrupted in many neurological disorders and presents as aggregates of ubiquitinated proteins or a depletion of free Ub[70–72]. Also, extracellular free Ub has been suggested as a biomarker for physical trauma; the free Ub sensor assays established here can replace less specific antibody-based assays that are typically used to quantify extracellular Ub[73].

CHAPTER 3: DEVELOPMENT AND APPLICATION OF SILOW (STABLE ISOTOPE LABELING USING ^{18}O-WATER)

Virtually all of Ub's diverse functions rely on the regulation of competing ubiquitination and deubiquitination or degradation reactions, and the rates of those reactions determine the steady-state level of every Ub-protein conjugate. However, whereas great strides have been made in methods to identify Ub conjugates and measure their concentrations, quantitation of Ub's movement through different conjugation/deconjugation pathways remains a major challenge. Thus, the relative contributions of conjugation and disassembly rates in cellular responses to different signals are rarely known. Moreover, even though the concentration of a particular Ub-protein conjugate may appear unchanged, the flux of Ub through that conjugate might change dramatically. To address these deficits in our understanding we have developed a method, SILOW, to isotopically label Ub and follow its movement through conjugation pathways by mass spectrometry. SILOW does not perturb cellular physiology, is compatible with commonly used proteomics methods for analyses of Ub-protein conjugates and can be used for both yeast and mammalian cells. Importantly, the procedure allows changes in Ub flux to be evaluated over short times. Here, SILOW was used to demonstrate the relative turnover of ubiquitination sites in proteome-wide experiments with a cultured human cell line (i.e., HEK 293T cells); the results illustrate the very rapid flux of Ub through most protein conjugates on a timescale of tens of minutes. Further, to evaluate the effects of proteasome inhibition, the relative rates of turnover for the Ub-Ub linkages in polyUb relative to Ub in Ub-histone conjugates were

41

compared in detail.

3.1 Introduction

Ub is a small modifying protein that is covalently conjugated to Lys residues of substrate proteins in an ATP-dependent reaction catalyzed by a cascade of enzymes (i.e., E1, E2 and E3)[5]. The consequences of Ub-conjugation include modulation of activity, location and binding partners, among others[7]. As with other post-translational modifications (PTMs) Ub is reversible; its removal is catalyzed by deubiquitinases (DUBs)[9]. The field of Ub biology has lacked a means to study the dynamics of cellular Ub in the regulation of processes such as protein degradation, cellular trafficking, cell cycle progression and recruitment of factors during the activation of stress responses, as with pathogen infection and DNA damage[8].

Proteomics and antibody-based techniques can be used to make quantitative measurements of steady-state Ub conjugates[3,74,75]; however, in cases where an altered Ub flux rather than a new steady-state concentration is the regulatory response, these techniques would fail to identify the change. Microscopy-based studies have successfully demonstrated Ub dynamics in specific cellular compartments or loci. Typically, a photoactivatible fluorescent protein was expressed in fusion with Ub and its rate of movement is measured after photoconversion[35]. This approach was used to compare general Ub diffusion in the nucleus and cytosol[38], assess the stability of aggregates that form post-heat stress[36] and reveal the dynamics of Ub-conjugates associated with ataxia-1 inclusions[37]. These studies were useful in understanding the nature of bulk ubiquitination within specific locations, but amending the method to assay specific Ub sites presents a challenge.

Based on the chemical mechanism that underlies Ub or polyUb removal from a protein conjugate, a single oxygen atom from water is expected to be incorporated into the free C-terminus of (poly)Ub during each removal event. If ^{18}O-water is present during the deubiquitination reaction, the free (poly)Ub will incorporate 1 atom of ^{18}O into the C-terminal carboxylate (specifically, on residue G76; see Figure 3.1A). Because this free Ub has 2 oxygen atoms in its G76 carboxylate, and only one is ^{18}O, subsequent Ub activation and conjugation results in a 50% chance of retention of the label in conjugates (Figure 3.1B). Subsequent rounds of deubiquitination and ubiquitination in ^{18}O-water will further enrich the Ub C-terminus with ^{18}O as indicated in Figure 3.1C.

We can examine the flux of Ub through various Ub-containing species over time by trypsin digestion of cellular proteins to create di-Gly-containing peptides from Ub-protein attachment sites. By determining the amounts of ^{18}O in these peptides, mass spectrometry (MS) can be used to follow the movement of ^{18}O-labeled Ub through conjugation and deconjugation reactions (Figure 3.1D). We have termed this technique *Stable Isotopic Labeling using ^{18}O-Water*, or **SILOW**. The relative ^{18}O level at the conjugation site at any time indicates relative conjugate age because conjugation sites with a slower approach to ^{18}O will have been cycled through less frequently and vice versa.

The kinetics of ^{18}O-labeling, through both deubiquitination and re-ubiquitination as well as through non-Ub related mechanisms, is critical knowledge needed to guide experimental design. Labeling kinetics for free Ub, the substrate for all Ub-protein reactions, were measured with resolution on the order of seconds to establish a minimum time frame for the ^{18}O-labeling experiments; that is, the earliest time point

A
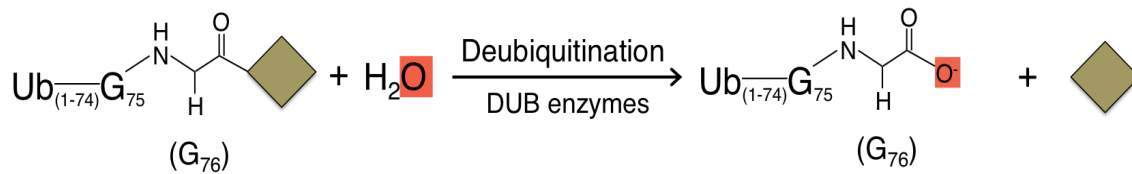
B
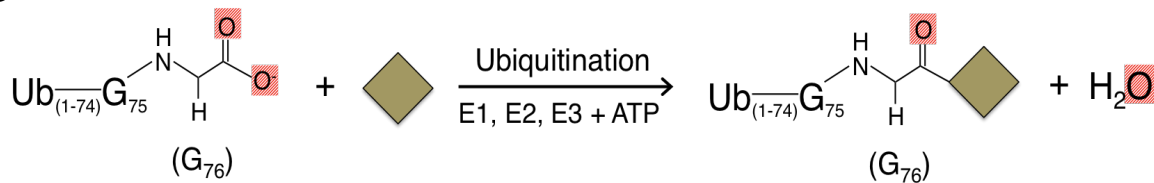
C

D
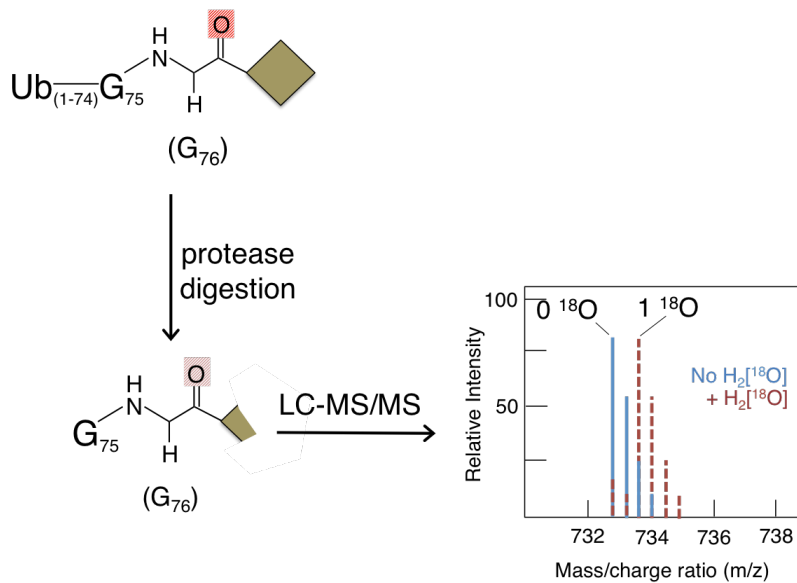
deubiquitination /	^{18}O-content	
ubiquitination cycles	free (poly) Ub	conjugated Ub
0	0	0
1	1	0.5
2	1.5	0.75
3	1.75	0.875
∞	2	1

44

Figure 3.1: Mechanism for incorporation of ^{18}O from H$_2$[^{18}O] into free and conjugate Ub. A. Removal of (Ub) ubiquitin from a Ub-protein conjugate (*brown diamond*) in the presence of H$_2$[^{18}O] incorporates an ^{18}O-atom (i.e., labeled oxygen, *red*) into the C-terminal G76 carboxylate of Ub. **B.** Chemical equivalence of the 2 oxygens in G76 of free Ub allows for scrambling of the ^{18}O position; loss of an oxygen in subsequent ubiquitination reactions leaves half of the ^{18}O (*pink*). **C.** Multiple cycles of deubiquitination and ubiquitination facilitates enrichment of ^{18}O into Ub that approaches 2 ^{18}O-atoms in free Ub and 1 ^{18}O in Ub-protein conjugates. **D.** Protease digestion of Ub-protein conjugates provides peptides of suitable size for mass analyzers to differentiate labeled (1 ^{18}O) from unlabeled (no ^{18}O atoms) Ub-proteins. The ^{18}O:^{16}O ratios for peptides corresponding to the linkage sites of specific Ub-protein conjugates will correspond directly to the relative stabilities (or "ages") of those conjugates.

needed to achieve nearly complete labeling of the free Ub pool. Conversely, the upper bound for ^{18}O-labeling was found by observing the ^{18}O-labels in the C-termini of proteins with short half-lives. In using SILOW, our goal was to perform a proteome-wide assessment of the relative ^{18}O-levels in Ub-conjugation sites, which would reflect their relative stability without any sort of cellular perturbation or alteration.

3.2 Experimental procedures

3.2.1 Yeast strains and growth conditions

Growth and manipulations of *S. cerevisiae* employed standard techniques. For yeast experiments, strain YTY690 was used. Strain YTY690, from the Yeast MATa Deletion Collection (Dharmacon #YSC1053), was generated from the parental strain BY4741 and the locus for PDR5 was replaced with the kanMX4 cassette.

3.2.2 Human cell lines and growth conditions

Growth and manipulations of HEK293T cells employed standard techniques. Cells were maintained in DMEM (Corning #15-013-CV) supplemented with 10% fetal bovine serum (FBS, Atlas #F-0500-D), 1% L-glutamine (GE #SH30034.01) and 1% Penicillin Streptomycin solution (Corning #30-001-C1).

3.2.3 Antibodies

Antibodies used in this study include: anti-Ub (clone P4G7; Covance #MMS-258R), anti-ubiquityl-Histone 2A (Lys119; clone D27C4; Cell Signaling #8240), anti-ubiquityl-Histone 2BI (Lys120; clone D11; Cell Signaling #5546S), anti-Ubiquitin, Lys63-specific (clone Apu3; Millipore #05-1308), anti-Ubiquitin, Lys48-specific (clone Apu2; Millipore #05-1307), anti-α-Tubulin (clone DM1A; Sigma-Aldrich #T9026), IRDye 680CW-conjugated goat anti-mouse (LI-COR) and IRDye 800CW-conjugated goat anti-

rabbit.

3.2.4   In vitro reactions to ^{18}O-label free Ub

Reactions containing 60 µM WT Ub or Ub with a C-terminal Asp fusion (Ub-D77),

3 µM Yuh1, 50 mM Hepes-NaOH (pH 8.0), 10 mM DL-dithiothreitol (DTT, Goldbio

#DTT50) and 50% ^{18}O-water (made from 97% O-18 enriched water, Marshall Isotopes

Ltd.) were incubated on a Thermomixer R (Eppendorf) at 22°C and 750 rpm. Samples

were quenched by addition of 5 mM N-ethylmaliemide (NEM; Thermo # 23030)

prepared in ethanol before LysC digestion, desalting and concentration as described in

Section 2.5.1.1. Preparation for analysis by MALDI-TOF mass spectrometry was by

spotting 1-2 µL of the digestion product on a 96-spot steel sample plate and mixed with

1 µL of α-cyano-4-hydroxycinnamic acid suspended in 50% acetonitrile (ACN), 0.1%

trifluoroacetic acid (TFA).

3.2.5   Rapid pulse-labeling in yeast cells

A pulse-labeling apparatus was designed as depicted in Figure 3.5A. To begin,

tubing and syringes were washed with triple-filtered deionized water and PBS (pH 7.4;

Corning #21-040-CV). For each 18O-labeled sample, a 50 mL tube was filled with 20

mL neat acetone and stored at -20°C. Also for each sample, a 15 mL round bottom

culture tube was filled with 10 mL of 95% absolute ethanol, 5% glacial acetic acid and

heated to 70°C in a thermomixer fitted with a 15 mL tube adaptor. Yeast cells were

Table 1. Parameters used with syringe pump for ^{18}O-labeling of yeast cells. The speed of the syringe pump and volume of tubing can be altered to modulate the timing of ^{18}O-labeling.

syringe pump speed (µL/min)	tubing volume (µL)	syringe volume (µL)	labeling time (s)
2000.0	65	600	0.98
990.0	65	600	2.0
502.0	65	600	3.9
245.0	65	600	8.0
470.0	250	600	16
234.5	250	600	32

grown to log phase (OD_{600}=0.4-1.0) at room temperature (24-25°C) and the equivalent of 20 OD x 1 mL of cells was centrifuged in a 50 mL at 1800 g for 3 minutes at room temperature. The supernatant medium was carefully removed by aspiration and the cells were resuspended in 700 µL of "2x Media" comprised of 0.4 g/L dextrose, 13.4 g/L yeast nitrogen base with ammonium sulfate and without amino acids (US Biological #Y2025), 0.4 g/L synthetic complete medium (Sunrise Science Products #1300-030). Concentrated cell solutions were then filtered using a 10 µm filter (pluriSelect #43-50010-50) fitted with a connector ring (pluriSelect #41-50000-50) and 10 mL syringe (BD #305462) used to generate a vacuum that pulls cells into another 50 mL tube attached to the bottom of the filter. Cells were transferred from the 50 mL tube to the tube lid, which makes the subsequent transfer to a 1.0 mL syringe (Hamilton #1001TLL) easier. This syringe was attached to the syringe pump (Chemyx Inc., Model Fusion100T) and labeling was initiated. Importantly, care was taken not to maintain cells in the concentrated state longer than 15 minutes to prevent significant alterations in metabolism due to changes in medium composition. Also, cells were not housed in syringes for time periods longer than 5 minutes to prevent changes in cellular respiration from lack of aeration. Directly after manipulation through the pulse-labeling system, cells were directed into the "quench" solution, which was 95% ethanol, 5% glacial acetic acid at 70 °C.

3.2.6 *Sample processing for analysis of ^{18}O-labeling of free Ub*

Yeast/quench/acetone mixtures were centrifuged in a 50 mL tube at 1800 g for 10 minutes at 2 °C and the supernatant removed by pipetting. The cell pellet was transferred to a 1.5 mL snap cap tube and washed with 1 mL acetone and then 1 mL 10

mM triethylammonium acetate buffer (pH 7.0; Sigma-Aldrich #90358) in acetone chilled to -20 °C. Typically, acetone was added to the cell pellet which was vortexed at high speed for 5 s and centrifuged at 10,000 g for 5 minutes at 4 °C; the supernatant was then removed. Cell pellets were dried in a Savant Speed Vac Plus SC110A at 1-2 torr for 5-10 minutes, taking care not to over-dry. Next, cells were solubilized in 70 µL lysis buffer containing 8 M urea, 1% TritonX-100, 50 mM Hepes-NaOH (pH 7.0), 2% (v/v) isoamyl alcohol, 20 mM NEM, protease inhibitors (Sigma #P8340) at 1:1000 and added to 70 mg glass beads (0.5 mm diameter; BioSpec #11079105) Solutions containing cells and glass beads were vortexed on high for 3 minutes at 4 °C a total of 3 times, with 2 minute rest periods for cooling on ice between each vortex session. Extracted cells were centrifuged 5 minutes at 10,000 g for 5 minutes at 4 °C and the soluble lysate transferred to a 1.5 mL tube. Working hydrazine•HCl solutions were freshly prepared by combining neat solutions of hydrazine and HCl to generate a solution of 6.81 M N_2H_4, 4.65 M HCl in a 2.0 mL glass tube. Lysates were treated with this hydrazine solution at a ratio of 1:10 (lysate: N_2H_4-HCl) and incubated at 37°C for 15 minutes. Hydrazine-treated lysates were diluted 25-fold with dilution buffer (DB) comprised of PBS (pH 7.4; Corning #21-040-CV), 4 mM NEM and 1:1000 protease inhibitors (Sigma #P8340). Aliquots of agarose-tUI were prepared by pre-treating with 0.05% TFA for 5 minutes at 4 °C to remove nonspecifically bound tUI or degradation products and subsequent neutralization with DB supplemented with 0.1 M Hepes-NaOH pH 7.5. The free Ub enrichment protocol described in Chapter 2 Section 2.9 was then used to isolate cellular Ub. Elution was typically performed by adding 1 resin-bed equivalent (typically 20 µL) of 5 mM 1,10 orthophenanthroline (OPA; Alfa Aesar #A14140) and incubating at 50°C for

5 minutes and a second elution was achieved by adding another 20 µL) of 0.5 mM OPA. Elutions were combined and dried at 1-2 torr for 10-15 minutes to reduce the volume below 30 µL.

3.2.6.1   LysC digestion

Proteolysis was performed by adding ProteaseMAX Surfactant (Promega #V2072) (to a final concentration of 0.05% and heating at 95°C for 5 minutes. The solution was cooled and 50 mM ammonium bicarbonate (AmBic) and 1:20 LysC (Lysyl Endoproteinase, MS grade; Wako, #125-05061) (protease:protein) were added and incubated at 37°C for 12-18 hours. Samples were acidifed by adding TFA to a final concentration of 1% just before application on C18 stage tips with 100 µL resin-bed (Agilent Technologies #A57003100) to desalt the samples. Elution from the C18 bed was by pipetting in 20 µL of 90% ACN, 0.1% TFA several times in 0.6 mL lo-bind tubes (Eppendorf #022431064) and eluates were neutralized by adding 1 µL TEAA immediately after. Finally, samples were dried at 1-2 torr for 15 minutes to remove all liquid from peptides, which were stored at -80°C until analysis by MALDI-TOF (see Section 2.4) or shipment to the Peng lab at St. Jude Children's Research Hospital.

3.2.6.2   Quantifying the contribution of Ub synthesis on ^{18}O-labeling of free Ub of yeast cells

The protocol described in Section 2.3 was used with the changes described. After cells were centrifuged, they were suspended in 2x Media supplemented with 2 mg/mL cycloheximide (CHX, Sigma-Aldrich) at 24-25 °C for a total of 5 minutes before ^{18}O-water incubation commenced.

3.2.7 Quantifying DUB-catalyzed oxygen exchange from ^{18}O-water

3.2.7.1 ATP depletion in yeast cells

The protocol described in Section 2.3 was used with the changes described. After cells were centrifuged, they were suspended in 2x Media supplemented with 2% (w/v) 2-deoxyglucose (Sigma-Aldrich #D8375) and 10 µM Antimycin A (Sigma-Aldrich #A8674) (at 24-25 °C) for a total of 15 minutes before ^{18}O-water incubation commenced.

3.2.7.2 Yeast cell free ^{18}O-labeling experiment

Yeast were grown to log phase (OD_{600}=0.4-1.0) at 25 °C and 10 OD of cells were centrifuged at 3000 g for 3 minutes. Cells were resuspended in water, transferred to a 1.5 mL tube and further centrifuged at 10,000 g for 3 minutes. The supernatant was removed and cells were resuspended in 75 µL lysis buffer comprised of 50 mM Hepes-NaOH (pH 8.0), 0.1 M NaCl, 5 mM $CaCl_2$, 0.5 U/µL Apyrase, 20 mM DTT and 1:1000 protease inhibitor cocktail (Sigma-Aldrich #P8340). Cells were lysed by vortexing on high for 2 minutes with 2 minute rest periods, a total of 4 times at 4 °C. Lysates were pre-incubated at 37 °C for 15 minutes and then 60 µL lysate was mixed with 66 µL of 97% ^{18}O-water and 2 µL of 220 ng/µL $(His)_6$-Ub for indicated times at room temperature (25°C). A final concentration of 5 mM NEM was added to quench reactions.

3.2.8 Quantifying acid-catalyzed oxygen exchange in free Ub

Free Ub was completely ^{18}O-labeled with Yuh1 as in Section 2.2. Aliquots of the labeled Ub were incubated at various pH's and temperatures overnight and then processed by LysC digestion for MALDI-TOF analysis as described in Section 2.5.1.1.

3.2.9 ^{18}O-labeling in human cells

HEK 293T cells were grown in 10 mm dishes to 80-90% confluence and transferred to a heating block equilibrated to 37°C. Conventional medium was aspirated and replaced with DMEM (Corning #50-003-P8) prepared conventionally, but supplemented with 70% ^{18}O-water. For lysis, the medium was removed and denaturing lysis buffer containing 8 M urea, 0.5% sodium deoxycholate (NaDOC), 0.1 M MOPS-NaOH (pH 6), 0.05% SDS, 15 mM NaCl, 2 mM MgCl$_2$, 0.1 mM N,N,N',N',-Tetrakis-(-2-pyridolmethyl)ethylenediamine (TPEN; Enzo ALX-450-011), 20 mM iodoacetamide (IAM; Sigma-Aldrich #I-6125), 0.3 U/μL benzonase (Novagen #70664) and 1:1000 protease inhibitor cocktail (Sigma-Aldrich #P8340) was applied on the adherent cells, which were dislodged with a rubber scraper and collected in a 2.0 mL screw cap tube and immediately frozen on dry ice. Before freezing, 10% of each sample was separated and treated with 0.3 M hydrazine-HCl for 15 minutes at 37°C for ^{18}O-labeling analysis of the free and activated Ub pools.

3.2.9.1 *Sample processing for analysis of ^{18}O-labeling of free Ub and Ub-thioesters in human cells*

Hydrazine-treated samples of cell extracts were sonicated (operating power 5, 30% duty, 8 pulses) on a Sonifier® Cell Disruptor W-350 and conventional SDS-sample loading buffer was added; these were then loaded onto freshly prepared SDS-PAGE gels (6% stacking/ 13.5% running). Gels were stained with 0.05% Coomassie Brilliant Blue R250 (Fisher #PP101-50), 25% isopropanol, 10% acetic acid for 20 seconds on high power in a microwave and 15 minutes at room temperature before destaining in 10% acetic acid under the same conditions. Bands were excised with a clean scalpel and cut into 1 mm x 1 mm pieces before they were added to a 1.5 mL tube with 50%

MeOH, 40% acetic acid and incubated at room temperature with gentle agitation for 3 hours. The MeOH/acetic acid wash was repeated twice at 50°C for 10 minutes. Finally, gel pieces were washed with neat acetone before drying in a Savant Speed Vac Plus SC110A at 1-2 torr for 5-10 minutes. The dried gel pieces were shipped on dry ice to Zhiping Wu in the Peng lab for conventional in-gel digestion[76].

3.2.10 ATP depletion in human cells

HEK 293T cells grown in conventional DMEM medium were washed with PBS twice before addition of DMEM without glucose (Sigma-Aldrich #D5030) and supplemented with 1 mM pyruvate (Sigma-Aldrich #S8636), 2 mM 2-deoxyglucose and 10 µM Antimycin A for various time points. Cell harvesting and lysis was performed as in Section 2.8 and protein content of the cell extracts was quantified using the bicinchoninic acid assay (BCA; Pierce #23225). Lysates were analyzed on 4-15% gradient SDS-PAGE gels (BioRad #456-1083) and transferred onto nitrocellulose in Towbin buffer at 270 mA for 90 minutes. Membranes were blocked in 5% milk, PBS, 0.05% Tween20 (PBS-T) for 30 minutes before overnight incubation in the primary antibody diluted in 1% milk, PBS-T. Fluorescent secondary antibodies were incubated on the membranes for 1 hour before imaging with a Licor Odyssey fluorescent scanner

3.3 Results

3.3.1 Establishing SILOW and quantifying flux through the free Ub pool

3.3.1.1 Deubiquitination promotes ^{18}O-labeling at the C-terminus of free Ub

First, the hypothesis regarding ^{18}O-incorpration through deubiquitination needed to be verified. For this, Ub with an added C-terminal Asp residue (Ub-D77) was incubated with the yeast DUB, Yuh1, for increasing periods of time in 50% ^{18}O-water
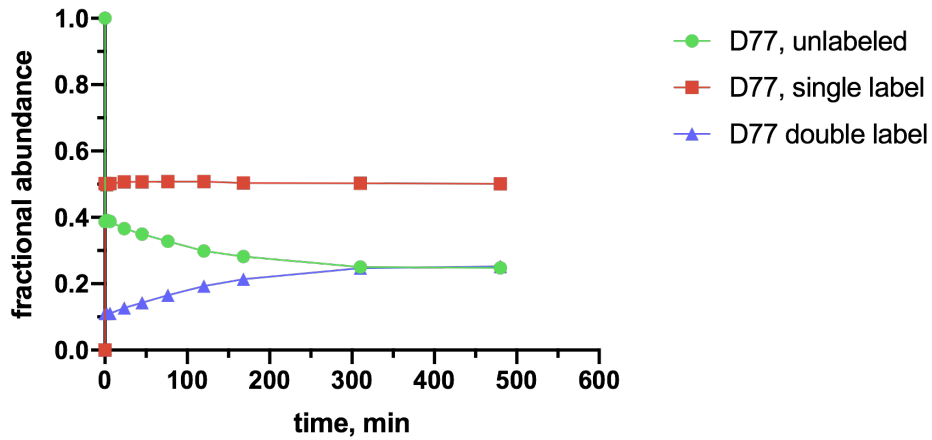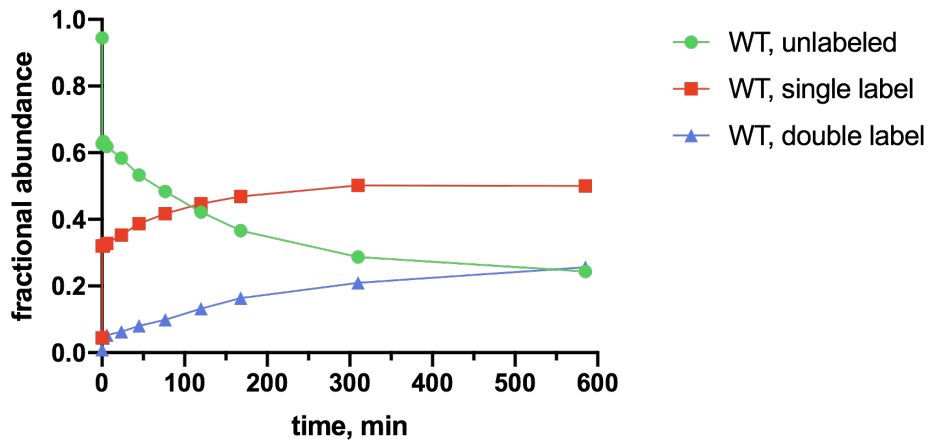
Figure 3.2: Ubiquitin is labeled with up to two ^{18}O in its C-terminus when added to Yuh1 in ^{18}O-water. A. Ub-D77 (60 µM) or **B.** WT Ub (60 µM) was added to Yuh1 (3 µM, a deubiquitinating enzyme) in 50% ^{18}O-water at room temperature. The quenched reactions were proteolyzed, analyzed by MALDI-TOF and spectra corresponding to the C-terminal peptide of Ub were used to calculate the fractional abundance of unlabeled, single and double-labeled Ub at each time point. These experiments were performed one time.

before quenching the reaction (Figure 3.2A). The samples were processed for MS analysis to obtain spectra for the Ub C-terminal peptide (i.e., amino acids 64-76, molecular weight 1450.8 Da) of Ub, which were input for the ^{18}O-labeling calculator software (discussed in Section 2.2.4) to determine the degree-of-labeling at each time point. Observing ^{18}O-label on this peptide supports the hypothesis of ^{18}O-incorporation by deubiquitination because it requires proteolysis of the 77th Asp residue by the Yuh1 DUB, thus mimicking a deubiquitination reaction.

As expected, the unlabeled fraction was depleted by over 60% and most Ub was singly labeled after Yuh1 addition. The singly labeled species remained at 50% throughout the experiment because the Ub C-terminal peptide was used as the readout and this peptide is not generated until Yuh1 removes D77. Surprisingly, the doubly-labeled species also increased over time and approached the theoretical distribution for complete labeling of the free Ub. Our expectation was that in order to observe doubly-labeled Ub, another round of ubiquitination and deubiquitination would have had to occur. There were no components in the reaction that would facilitate conjugation of the free Ub, which indicated that something other than deubiquitination facilitated the labeling. Schnölzer et al.[45] demonstrated that a second label is generated when trypsin accepts a peptide fragment as a substrate to form a covalent ester intermediate that is then hydrolyzed. An analogous mechanism likely also facilitated double labeling of free Ub in this experiment.

Next, free Ub was incubated with Yuh1 in 50% ^{18}O-water for increasing times before quenching (Figure 3.2B). In this experiment, there was no deubiquitination, yet oxygens at the Ub C-terminus were equilibrated to the ^{18}O-level in the environmental
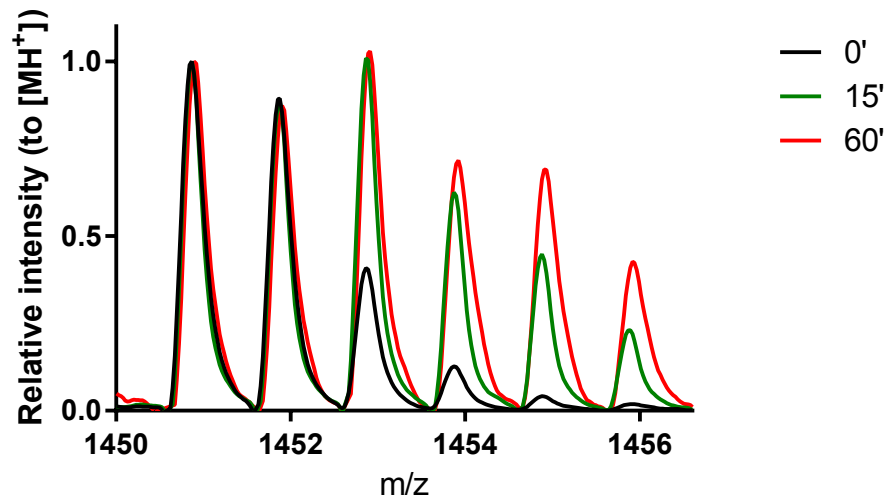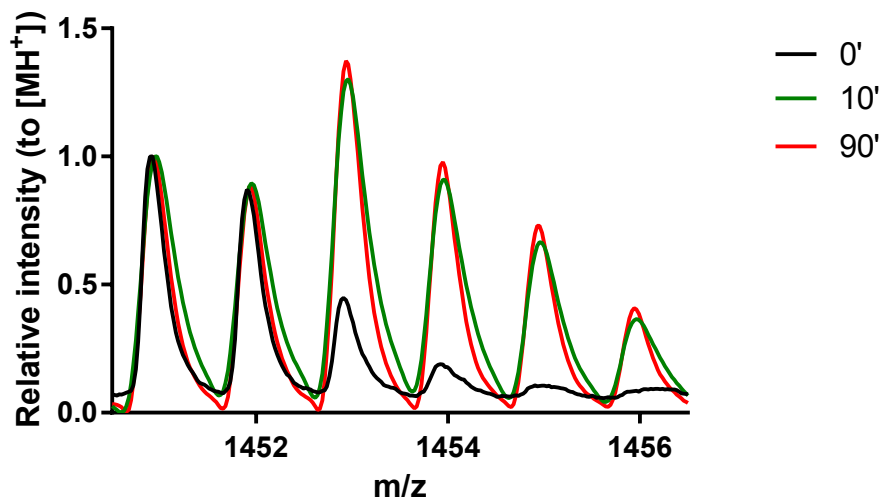
Figure 3.3: Free Ub is labeled with ^{18}O rapidly in human and yeast cells when cells are cultured with ^{18}O-water. A. HEK 293T human cells and **B.** BY4741 yeast were transferred to media supplemented with 50% ^{18}O-water before cells were quenched at the times indicated by lysis in denaturing buffer. Free Ub was enriched using agarose-tUI, digested with LysC, and analyzed by MALDI-TOF.

water, albeit at a slower rate. No ^{18}O-labeling occurred in the absence of Yuh1 (data not shown), which suggests Yuh1 mediated the oxygen exchange by forming an ester intermediate with free Ub that is hydrolyzed.

3.3.2 Pilot experiment to assess labeling time frame for ^{18}O-labeling of free Ub in human cells

After confirming that ^{18}O-labeling of Ub is possible in vitro, we used cultured human cells to validate our hypothesis in vivo. From previous work by others, the rate of ^{18}O-exchange across the cell membrane occurs within 0.1 s[48]. The exchange of ^{18}O from ^{18}O-water into the pool of free Ub needed to be assessed because free Ub is the substrate for all labeled sites of ubiquitination reactions and it is essential that the rate of labeling of the free pool should exceed the rates of labeling by other metabolic pathways or proteolysis (discussed in Section 2.2.2).

For labeling, the conventional medium used with adherent HEK293T cells was aspirated and replaced with the medium containing 50% ^{18}O-water. After 10 and 90 minutes (Figure 3.3A), cells were harvested in denaturing conditions and free Ub was enriched by application to agarose-tUI (method described in Chapter 2, Section 3.4) and then proteolyzed. The goal of this experiment was to observe mass changes in the C-terminus of Ub, so we chose LysC protease over trypsin because it generates peptides of appropriate mass for MS analysis (i.e., 1450 Da with LysC versus 133 Da with trypsin). A 2 Da shift was observed in the monoisotopic peak within the spectrum for the C-terminal peptide of Ub in the sample incubated in ^{18}O-water for 10 minutes. This result indicated that ^{18}O was being incorporated.
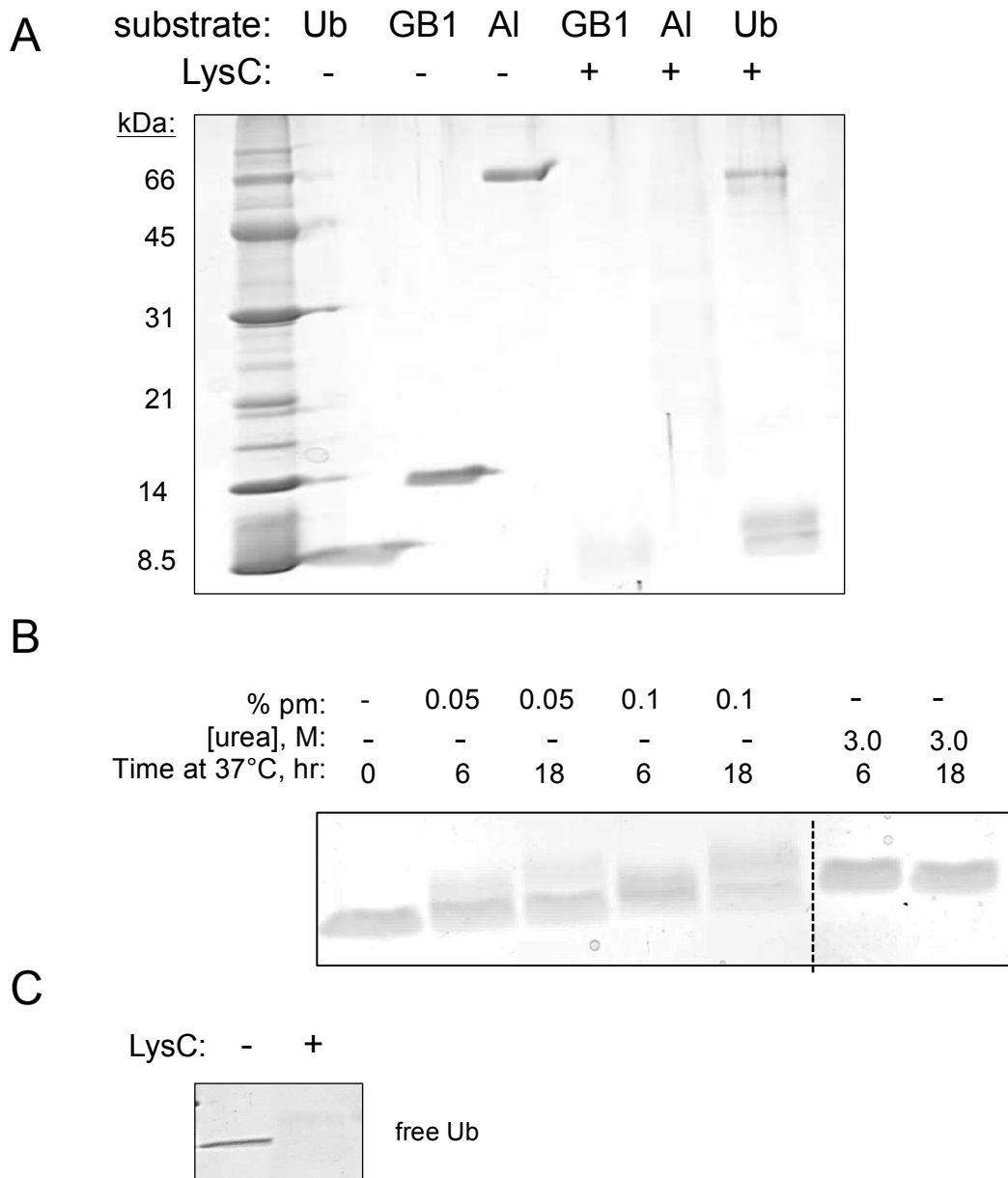
Figure 3.4: Optimization of Ub digestion by LysC protease. A. One μg of each substrate (Ub, GB1, and Albumin (Al)) were diluted in 50 mM AmBic and LysC (1:20 protein:protease) at 37°C for 12 hours. **B.** Free Ub (1 μg) was diluted in protease max (pm) or urea, 50 mM AmBic and 1:20 LysC at 37°C for indicated times. **C.** Free Ub (1 μg) was diluted in 0.05% protease max, 50 mM AmBic and heated at 95C for 5 minutes before cooling and addition of 1:20 LysC at 37°C for 12 hours. Aliquots of each reaction were analyzed on silver-stained SDS-PAGE.

The spectrum for the sample incubated in ^{18}O-water for 90 minutes was not changed further, suggesting that most labeling occurred within 10 minutes.

In parallel, yeast cells were labeled with medium containing 50% ^{18}O-water for 15 minutes (Figure 3.3B). Again, a 2 Da shift in the most abundant species was observed, indicating that ^{18}O-labeling had occurred. As in human cells, labeling did not increase past the first time point. These experiments and others with shorter ^{18}O-water incubations (data not shown) demonstrated that free Ub was labeled within minutes. From these results, we concluded the free Ub labeling reaction was likely to occur within seconds; a rapid pulse-quench system was needed to quantify the kinetics.

3.3.3 Development of a protocol to quantify free Ub ^{18}O-labeling dynamics in yeast

I decided to employ a yeast system for rapid ^{18}O-labeling because yeast have cell walls[77] and are therefore more hearty than human cells, which are only protected by a plasma membrane. In order to rapidly mix yeast cells and water, cells are pushed through a micro mixer (Dolomite #3200401) with the smallest cross-section dimensions at 50 x 125 µm. The diameters of budding yeast and human cells are 5.5 µm and 17.1 µm, respectively[78,79] Yeast cells will clear the mixer chamber more easily than human cells and, because of the cell wall, will be better protected against lysis by physical shear stress.

3.3.3.1   Protease digestion and sample processing

From previous experiments (data not shown), it was apparent that free Ub is resistant to proteolysis by proteases commonly used for MS sample processing, such as trypsin and LysC. We first ensured that LysC was active and able to digest other proteins efficiently by performing reactions in 50 mM ammonium bicarbonate (AmBic;

pH 8.0) buffer solution (Figure 3.4A). For both albumin and GB1 protein substrates, addition of LysC resulted in the disappearance of the band representing the full-length protein and appearance of a lower molecular weight smear, indicative of a heterogeneous mixture of peptide products. In the case of free Ub, LysC addition did not affect the full-length protein.

In attempts to increase the efficiency of the digestion, denaturing solutions such as urea or ProteaseMax™, a specialized detergent compatible with downstream MS applications, were added to free Ub incubations with the LysC protease (Figure 3.4B). Urea made no impact on the digestions, but increasing amounts of ProteaseMax™ detergent correlated with decreasing levels of full-length free Ub; however, the reactions were far from complete, even after 18 hours. We reasoned that free Ub was better proteolyzed in stronger denaturing conditions. To test this hypothesis, we boiled free Ub diluted in a solution containing ProteaseMax™ detergent and then cooled the solution before LysC addition (Figure 3.4C). In that reaction, the free Ub was fully digested, as shown by the complete disappearance of the full-length band representing free Ub. From this series of optimization experiments, an efficient protocol for free Ub digestion by LysC was developed, this was crucial to the analysis of ^{18}O-labeling in free Ub.

3.3.3.2   *Rapid pulse-labeling of yeast cells*

We devised a pulse-labeling system (Figure 3.4A) that begins with two syringes controlled by a syringe pump that expels liquid at a precise rate through narrow tubing to a microchip mixer. The mixer rapidly and efficiently mixes concentrated yeast cells in rich medium and ^{18}O-water, which are carried by more tubing to a quench solution comprised of 95% EtOH and 5% acetic acid at 70 °C. The protocol for pulse-labeling

A

thermomixer housing quench solution

$$\text{Reaction time} = \frac{\text{Tube volume}}{\text{Flow rate}}$$

syringe

micromixer chip
Internal volume = 4.67 uL

B

- unlabeled
- single label
- double label

fractional abundance

Time (sec)
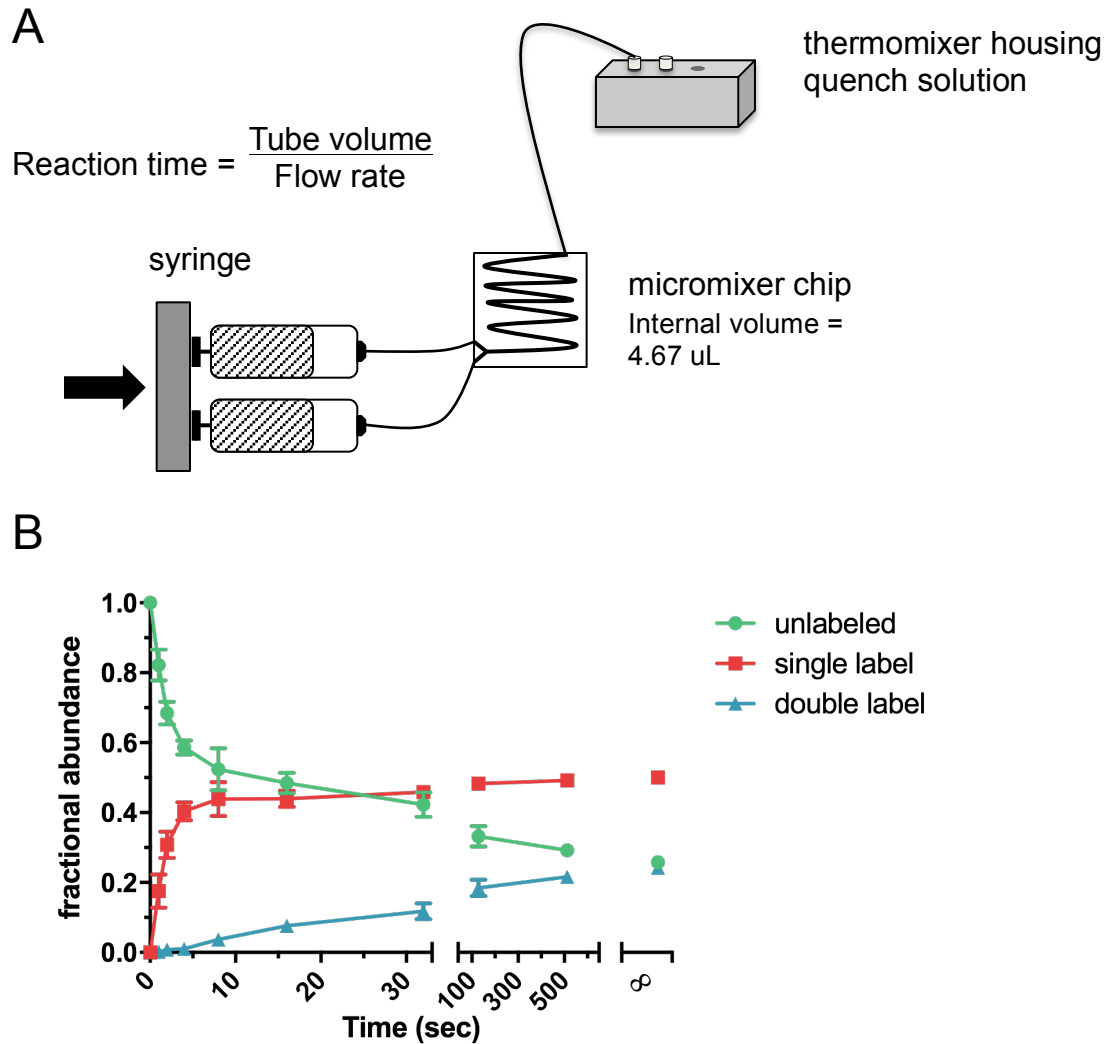
Figure 3.5 Free Ub is labeled in seconds when yeast cells are pulse-labeled with ^{18}O-water supplemented media. A. Schematic representation of apparatus used for rapid pulse-labeling of yeast cells. A syringe pump controls the movement of two matched syringes, one containing concentrated cells, the other containing enriched ^{18}O-water. As cells and water move from the syringes, they are transferred to a micro mixer which rapidly and efficiently mixes the two solutions. After mixing, the solution is carried to quench, which is 95% ethanol, 5% acetic acid at 70°C. **B.** 18O-labeling kinetics of free Ub in yeast grown at 25°C when pulsed in 48.5% ^{18}O-water. Cells were pulse-labeled and lysed for free Ub enrichment, LysC digestion and LC-MS/MS. Ub C-terminal peptide spectra were input to the ^{18}O-calculator software to determine labeling distributions at each time point. For each time point, n=3; average and standard deviations are plotted.

yeast cells with the microchip mixer was utilized to pulse-label cells for up to 32 seconds; manual manipulation of the samples was performed to label yeast for longer than 1 minute. Typically, 1 mL of 20 optical density units (OD) per mL of yeast cells were centrifuged and resuspended in rich medium containing two-fold synthetic complete yeast nutrients, yeast nitrogen base and glucose. The concentrated yeast cells were strained using a 20 μm filter and loaded into one of the two matched syringes to be controlled by the syringe pump, the other of which was loaded with highly enriched (>95%) ^{18}O-water. Both the rate of the syringe pump and the length of the tubing delivering cells from the micromixer to the quench solution were used to modulate changes in the duration of ^{18}O-labeling. Cells were precipitated in the quench solution for 2 minutes before the entire mixture was poured into 1 volume equivalent of acetone at -20°C.

3.3.4 Quantifying free Ub flux

The optimized protocol for rapid pulse labeling of yeast cells was used to implement sub-minute incubations with medium containing 48.5% ^{18}O-water (Figure 3.5B). Yeast cells were solubilized in denaturing lysis buffer and proteins were extracted by bead beating the cells (details described in Section 2.5.1). The lysates were diluted and applied to agarose-tUI to isolate free Ub, which was proteolyzed by LysC using the optimized protocol described in Section 2.1.4.1. Finally, the resulting peptides were analyzed by LC-MS/MS. In 10 seconds, the singly-labeled Ub (i.e., 1 ^{16}O, 1 ^{18}O) plateaued and the doubly-labeled species began to accumulate. After several minutes of incubation in ^{18}O-enriched medium, the labeling of free Ub was approaching the theoretical endpoint for the system (i.e., unlabeled:singly:doubly = 0.26:0.5:0.24). This

experiment demonstrated that flux through the free pool is extremely fast and raised the possibility that free Ub was labeled in part by mechanism(s) not related to Ub hydrolysis from sites of conjugation. These additional mechanisms for the ^{18}O-incorporation into free Ub are discussed below.

3.3.4.1 *Quantifying the contribution to ^{18}O-labeling by Ub synthesis*

Ub is synthesized as a fusion protein with additional copies of Ub or C-terminally fused ribosomal proteins[18,63] that needs to be processed by a deubiquitinating enzyme to release mature monomeric Ub[80] (Figure 3.6A). To probe the extent that this phenomenon contributes to ^{18}O-labeling of free Ub, yeast cells were pre-treated with cycloheximide (CHX) before SILOW was performed. An experiment reported by Gerashchenko and colleagues[81] demonstrated that rapid shutdown of yeast translation occurs in minutes when cycloheximide concentrations on the order of several milligrams per milliliter are applied to cells. Yeast were treated with 2 mg/mL CHX for 5 minutes before exposure to ^{18}O-water using the rapid pulse-labeling protocol (Figure 3.6B) The initial velocity of free Ub labeling after CHX treatment was similar to the untreated cells, indicating that Ub synthesis does not significantly contribute to the free Ub ^{18}O-labeling kinetics.

3.3.4.2 *Estimating the contribution to ^{18}O-labeling by DUB-catalyzed oxygen exchange*

Another route for ^{18}O-incorporation at the C-terminus of free Ub that does not require Ub hydrolysis from a substrate protein is DUB-catalyzed oxygen exchange (Figure 3.6A). From experiments such as those presented in Figure 3.2B, we know that high concentrations of DUBs (i.e., 3 µM) *in vitro* can associate with free Ub and catalyze
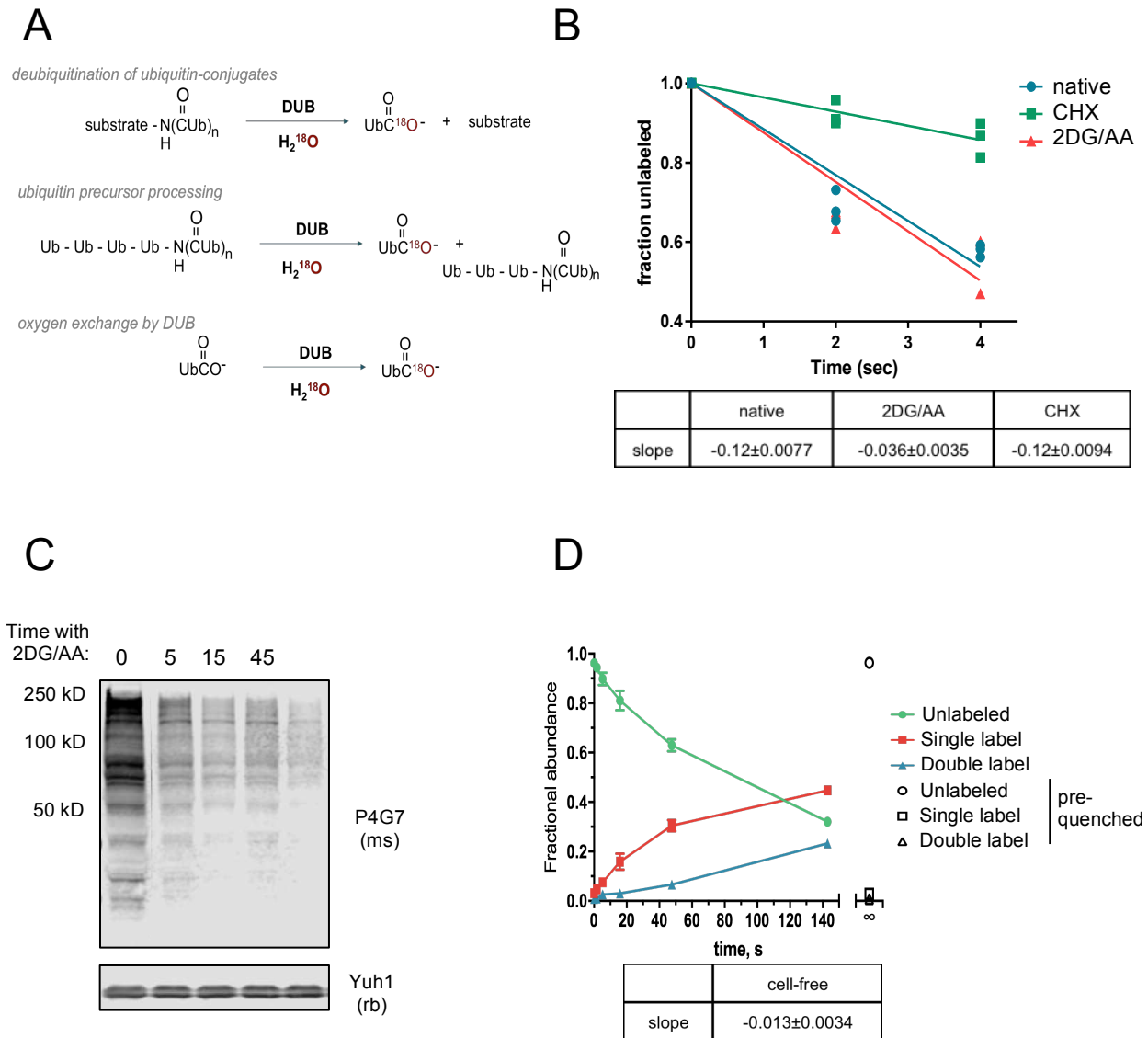
Figure 3.6 Quantifying the contributions to Ub-labeling by Ub synthesis and DUB-catalyzed oxygen exchange. A. Oxygen can be exchanged at the C-terminus of Ub through deubiquitination of Ub-conjugates, Ub-precursor processing and though DUB catalysis. **B.** Initial velocities of free Ub ^{18}O-labeling through in yeast cells pre-treated with 2% (w/v) 2-deoxyglucose, 10 µM antimycin A, "2DG/AA" or 2 mg/mL cycloheximide, "CHX" or without pretreatment, "native". **C.** Yeast treated with 2DG/AA were analyzed by western blotting for Ub-conjugates (anti-Ub, clone P4G7) and normalized against Yuh1 as a loading control. **D.** His$_6$-Ub was spiked into an ATP depleted, cell-free system to assess the efficiency of DUB catalyzed oxygen exchange. Enriched His$_6$-Ub was digested and analyzed by MALDI-TOF. The spectrum from Ub C-terminal peptide were used to calculate the labeling distribution at each time point. For each time point, n=3; average and standard deviations are plotted.

oxygen exchange at the C-terminal carboxylic acid. We took two different approaches to assess whether DUB-catalyzed oxygen exchange occurs *in vivo*; for each, conditions needed to be established where new Ub conjugation events are inhibited yet DUBs remained active.

In the first experimental system, cells were pre-treated with 2-deoxyglucose and antimycin A to decrease cellular levels of ATP, thus inhibiting new ubiquitination events. After 5 minutes of treatment with these conditions, the cellular Ub conjugates had decreased by about 70% as compared to the extracts from untreated cells (Figure 3.6C). From 5 to 45 minutes of ATP depletion, the abundance of Ub conjugates did not change significantly, suggesting that the bulk of deubiquitination had occurred primarily during the first few minutes of treatment. Therefore, ATP depletion was performed for 15 minutes prior to ^{18}O-labeling; then, SILOW reactions less than 10 s were to assess the rate of ^{18}O incorporation into free Ub (Figure 3.6B). Even in the ATP-depleted cells, ^{18}O-labeled Ub was still produced, albeit at a 3.3-fold slower rate than labeling in the absence of treatment. From this experiment, we can conclude that the *upper* limit of ^{18}O-labeling contributed by DUB-catalyzed oxygen exchange into free Ub is about 30%. In order to make this conclusion, we must assume that no new conjugation or deconjugation events occurred during the SILOW reaction times. We also assume that, subsequent to the 15 min ATP-depletion period, intracellular Ub thioesters are negligible and that their hydrolysis does not contribute significantly to ^{18}O-labeling of free Ub.

I also took a cell-free approach to quantifying the contribution of DUB-catalyzed oxygen exchange on free Ub ^{18}O-labeling (Figure 3.6D). Yeast extracts were prepared

in non-denaturing conditions in a buffer supplemented with apyrase, an enzyme that catalyzes the hydrolysis of ATP and ADP, to inhibit new Ub activation and conjugation. His-tagged free Ub ($(His)_6$-Ub) and 50% ^{18}O-water were spiked into the extracts at various times before quenching. $(His)_6$-Ub was recovered from the extracts using Ni-NTA agarose resin and digested using LysC before analysis by MALDI-TOF. The rate of ^{18}O-labeling of $(His)_6$-Ub in this cell-free experiment was 9-times slower than the Ub-labeling rate observed when yeast cells were pulse-labeled with ^{18}O-water. Because ubiquitination was inhibited and an exogenous version of free Ub was spiked in, ^{18}O-labeling due to residual deconjugation activity or thioester hydrolysis is unlikely; therefore, direct DUB-catalyzed oxygen exchange appears responsible. However, this rate represents only a lower bound of the contribution by DUB-catalyzed exchange because we must assume that all cellular DUBs were extracted and remained fully active in the cell-free system, which was diluted by over 60-fold from the intact cell state; this assumption has not been tested. Nonetheless, from these two experiments we can conclude that the contribution of DUB-catalyzed oxygen exchange on the labeling kinetics of free Ub most likely is between 10 and 30%.

3.3.5 *Quantifying and optimizing protocols to prevent back-exchange in free Ub*

The first time ^{18}O-labeling was performed in yeast, doubly-labeled free Ub did not accumulate as the unlabeled species was depleted over time (Figure 3.7A). Instead, the singly-labeled Ub plateaued without any appreciable accumulation of doubly-labeled Ub. Niles et al.[82] demonstrated that peptidic carboxyl groups can be completely exchanged with oxygen from the solvent water in a couple of days if incubated in 1% TFA. We suspected that oxygen exchange was occurring in the C-terminal carboxyl
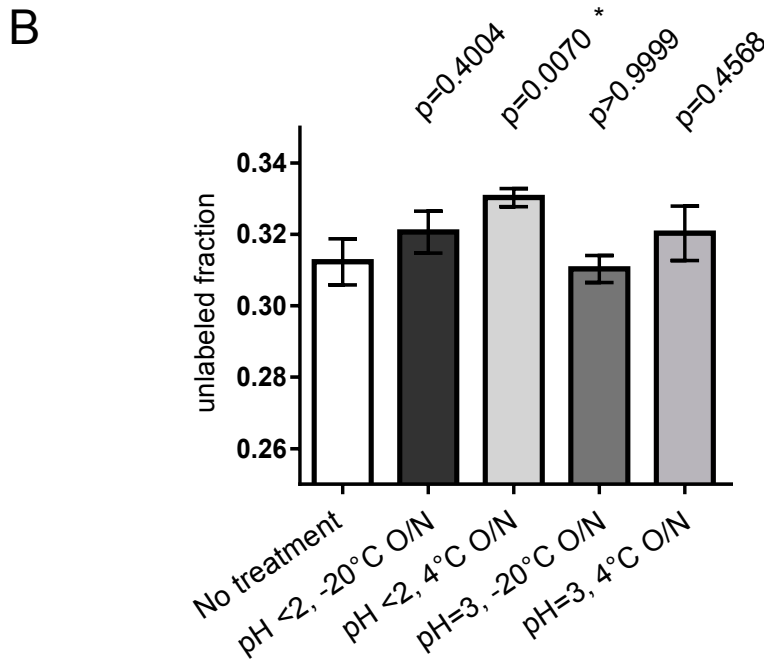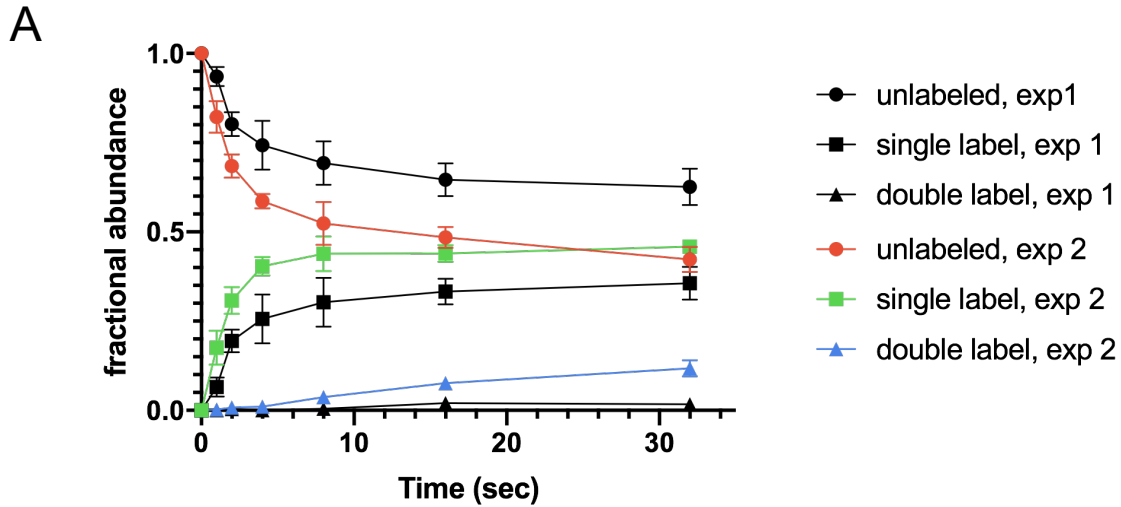
Figure 3.7: Acid catalyzed back-exchange of ^{18}O at the C-terminus of ubiquitin in different conditions A. Comparing the labeling kinetics of free Ub in samples that experienced acid-catalyzed oxygen exchange, "exp 1", and in samples using optimized protocols to minimize time in low-pH and high temperatures, "exp 2". **B.** Ub was labeled with ^{18}O-water and then subjected to different conditions overnight (O/N) in order to quantify the extent of acid-catalyzed back exchange at different pH and temperatures that any given sample may experience during sample preparation. Ub samples were digested by LysC, analyzed by MALDI-TOF and the spectrum from C-terminal Ub peptide was used to calculate the unlabeled fraction in each sample. For all experiments, n=3; avrages and standard deviations are plotted. P-values were determined by one-way ANOVA using Bonferonni's correction.

group of free Ub during the steps in the sample preparation where the material was acidified. To address this concern, ^{18}O-labeled free Ub was prepared in a Yuh1-catalyzed reaction (see Figure 3.1) and then subjected to a variety of temperature and pH conditions representative of different stages of sample preparation. The most significant loss of ^{18}O from the ^{18}O-labeled Ub occurred when the sample was left at 4 °C overnight at pH 1 (i.e., 1% TFA). We found that the acid-catalyzed back-exchange problem is circumvented by simply neutralizing the sample pH and freezing the samples as soon as possible; thus, for subsequent analyses we adopted the "optimized protocol" used in Figure 3.7A.

3.3.6 *Proteome-wide comparison of relative Ub flux through conjugation sites*

The ultimate goal for SILOW was observation and comparison of the movement of ^{18}O-labeled free Ub into specific sites of ubiquitination across a cell's proteome. With the knowledge that free Ub is ^{18}O-labeled in seconds, we can be confident that the ^{18}O-labels found in sites of conjugation are due to cycles of deubiquitination and ubiquitination.

3.3.7 *Determining the dynamic range of ^{18}O-labeling in Ub-conjugation sites*

Before attempting to analyze the entire proteome, more information was needed regarding the time frame of conjugate labeling; therefore, the kinetics of some abundant ubiquitination sites were quantified in a pilot experiment. For this, HEK 293T cells were pulsed with ^{18}O-water in the culture medium before application of a denaturing lysis buffer to quickly quench DUB and other protease activities. The soluble cell lysate was trypsinized and analyzed by LC-MS/MS and the resulting mass spectra were converted to values representing the degree of labeling for the conjugation site (Figure 3.8) using
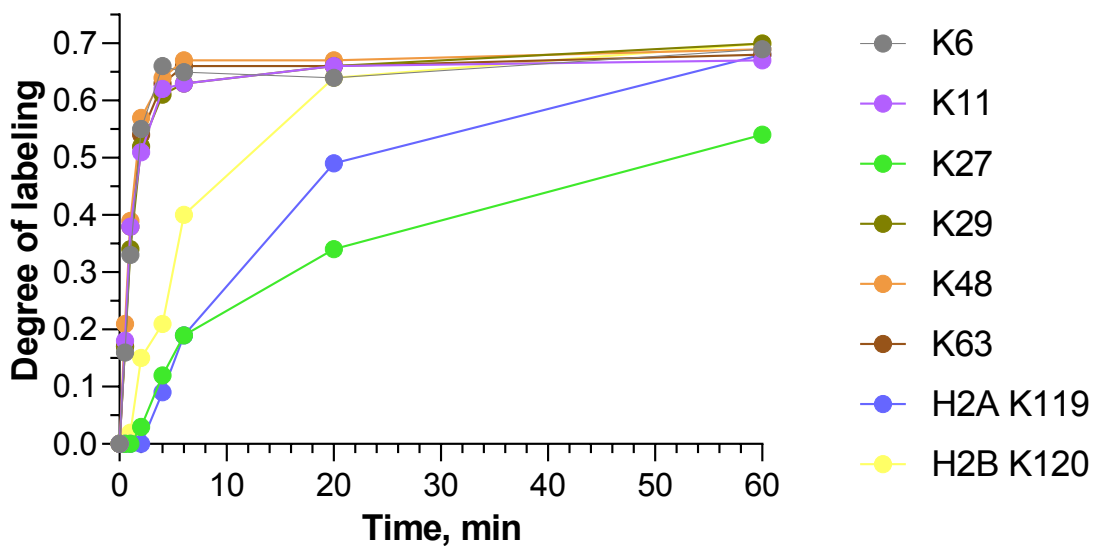
Figure 3.8: Ubiquitin conjugates are ^{18}O-labeled within minutes when human cells are exposed to ^{18}O-water HEK293T cells were treated with 70% ^{18}O-water over time before cells were harvested in denaturing lysis buffer, trypsinized and analyzed by LC-MS/MS. The degree of labeling calculated based on the resulting spectrum of each peptide. For each time point, n=1.

[18]O-quantification software developed in collaboration with Junmin Peng's lab (discussed in Section 2.2.4). With the exception of K27-linked Ub, all Ub-Ub linkage types were saturated with the ^{18}O-label after 6 minutes, which means that these linkages are completely turned over within that time frame. The high level of instability exhibited by the Ub-Ub linkages was unexpected, but even more surprising was the stark difference in dynamics exhibited by K27-linked Ub, which was never fully saturated with the label, even after an hour. The rates of labeling for ubH2B and ubH2A were slower than for bulk polyUb linkages, but complete labeling was eventually achieved by the end of the one-hour labeling experiment. From this experiment, the time frame for proteome-wide labeling, 1 to 9 minutes, was selected because all ubiquitination sites examined were actively labeled within that range.

3.3.8 *[18]O incorporation is not significant in the C-termini of high-turnover proteins*

For SILOW to be a useful method for quantifying Ub dynamics in live cells, we needed to demonstrate that the rate of labeling for free Ub and Ub conjugates surpassed the rate of ^{18}O-labeling by other, non-Ub related mechanisms. In the cell, oxygens from ^{18}O-water can be incorporated into proteins by several routes; these include C-terminal labeling upon release of nascent polypeptides from the ribosome, proteolytic processing, protein synthesis with amino acids that had incorporated [18]O biosynthetically or from protein recycling, and deamidation reactions. To address this, we searched for [18]O enrichment in C-terminal peptides of proteins known to undergo rapid turnover (Figure 3.9). Our rationale was that proteins that are rapidly made and turned over are most likely to incorporate biosynthetic and recycled amino acids, so by making observations on peptides of these proteins the chances of observing [18]O-

enrichement from these routes are increased. Also, proteins that have short half-lives are more likely to be synthesized during the short labeling periods required by SILOW.

In a paper by Yen and colleagues[83] most genes within the HEK 293T human call genome was expressed from a plasmid fluorescent-based reporter system. Fluorescence levels were quantified over time to determine the relative stability of each translation product (i.e., relative half-life). Their measurements were used to generate a Protein Stability Index (PSI) where each protein was rated based on its stability in the assay. Lower PSI values were indicative of low stability (i.e., high turnover) whereas higher values represented proteins that more resistant to degradation (i.e. low turnover).

In our experiment HEK293T cells were pulsed with ^{18}O-water-containing medium for 6 and 20 minutes and processed similarly to the experiment described in Section 2.2.1. Spectra from C-terminal peptides of low PSI proteins were identified by manual inspection and the degree of ^{18}O-labeling was calculated using ^{18}O-calculator software (discussed in Section 2.2.4). Of the 6 C-terminal peptides corresponding to low-PSI proteins, only CHMP5 was significantly ^{18}O-labeled after 20 minutes incubation with 70% ^{18}O-water. Interestingly, CHMP5 has a higher PSI (i.e. longer half-life) than most of the other proteins identified in this experiment, which is inconsistent with the hypothesis that rapid turnover would lead to more C-terminal labeling from the higher proportion of new translation products.

The ^{18}O-labeling and analysis of specific sites of ubiquitination (Figure 3.8) provided the dynamic range for deubiquitination/ubiquitination specific labeling, 1 to 9 minutes. Here, the lack of significant labeling in C-terminal peptides from high-turnover proteins at 6 and 20 minutes provides us with confidence for this time frame that

labeling is not due to protein synthesis using amino acids or by ribosomal processing at the protein C-terminus.

3.3.9 Peptide identification in high-throughput analysis of ^{18}O-labeled proteome

In traditional MS experiments, peptides are identified by algorithms like Mascot or Sequest that assign a peptide sequence to each spectrum by comparing the empirical spectra against theoretically predicted spectra of peptides within a database[84,85,86]. Even when a sample is labeled for experiments such as SILAC, the labeling is complete and algorithms can easily accommodate the expected mass changes[87]. Also with SILAC, mass changes are large enough that the unlabeled peptide spectrum is distinct from the singly and doubly-labeled peptide spectra[87] (Figure 3.10A). With SILOW, analysis requires that labeling not go to completion because the different degrees of labeling indicate the relative flux through the sites of ubiquitination. Further complicating data analysis, the mass change induced by the label is not big enough to allow complete separation of the labeled and unlabeled peptide spectra, which results in a mixed spectrum (Figure 3.10B). These complications made computational proteome-wide peptide identification a challenge. Ji-Hoon Cho, in the lab of Junmin Peng, initially attempted to modify peptide identification algorithms to accommodate 2 Da mass shifts in the MS^2 spectra of ^{18}O-labeled peptides. This attempt ultimately failed because the 2 Da mass windows permitted an unacceptable number of false-positives.
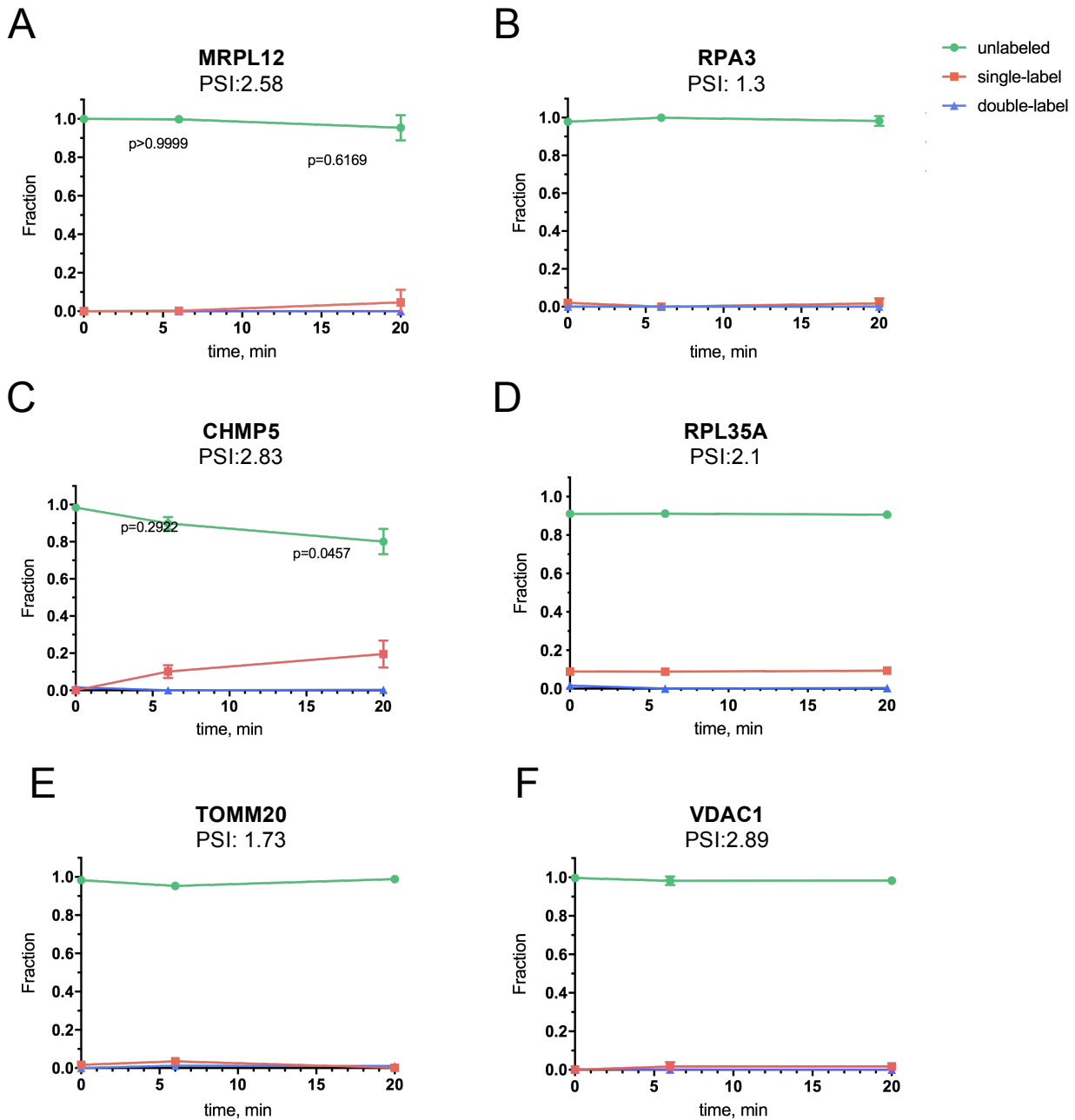
Figure 3.9: C-terminal peptides of unstable proteins do not incorporate significant amounts of ^{18}O during the short labeling periods C-terminal peptides of proteins with high turnover rates were manually identified in the proteomes of cells incubated with media containing 70% ^{18}O-water and assessed for occurrence of ^{18}O-labeling. Relative protein turnover rates were referenced from Yen et al, where turnover is reported on a protein stability index with: PSI~1.3 for short, PSI~3.5 for medium PSI~5,5 for long and PSI~6.5 for extra-long half-life. For each time point, n=2; averages and standard deviations are

In an alternative approach, Ji-Hoon generated an in-house library based on features defined in the unlabeled sample. For this, the mass spectra of the large-scale unlabeled sample were queried against the Uniprot human proteindatabase for peptide identification using the Sequest algorithm. Identified peptides were recorded along with features such as m/z and chromatography retention time to generate the library. The mass spectra from a labeled sample there were aligned to the library for feature matching to identify peptides.

3.3.10 Quantifying ^{18}O-degree of labeling

Again, we collaborated with Ji-Hoon Cho of Junmin Peng's lab, to generate a script capable of estimating the degree of ^{18}O-labeling for any given peptide sequence. The premise of the estimation method is that each experimental spectrum is a mixture of the fully labeled and unlabeled spectra. This script requires the abundances of the first six isotopic species from the spectral envelope; the first two isotopes, monoisotopic (M) and M+1 peaks, will only come from natural isotope abundances of the unlabeled species. To determine the degree-of-labeling, the proportion of unlabeled peptide, α, is calculated using the abundances of the M and M+1 peaks, relative to the other 4 peaks within the isotopic envelope. The labeled portion is calculated by subtracting α from 1. Software validation was achieved by computing the degree-of-labeling for free Ub after incubation with Yuh1 in 50% ^{18}O-water to equilibrium (as in Figure 3.2A).

3.3.11 Proteome-wide assessment of Ub flux through conjugation sites

Finally, all steps of the SILOW analysis were ready to assess ^{18}O-labeling in Ub sites across a human cell proteome (Figure 3.11A). HEK293T cells were incubated in
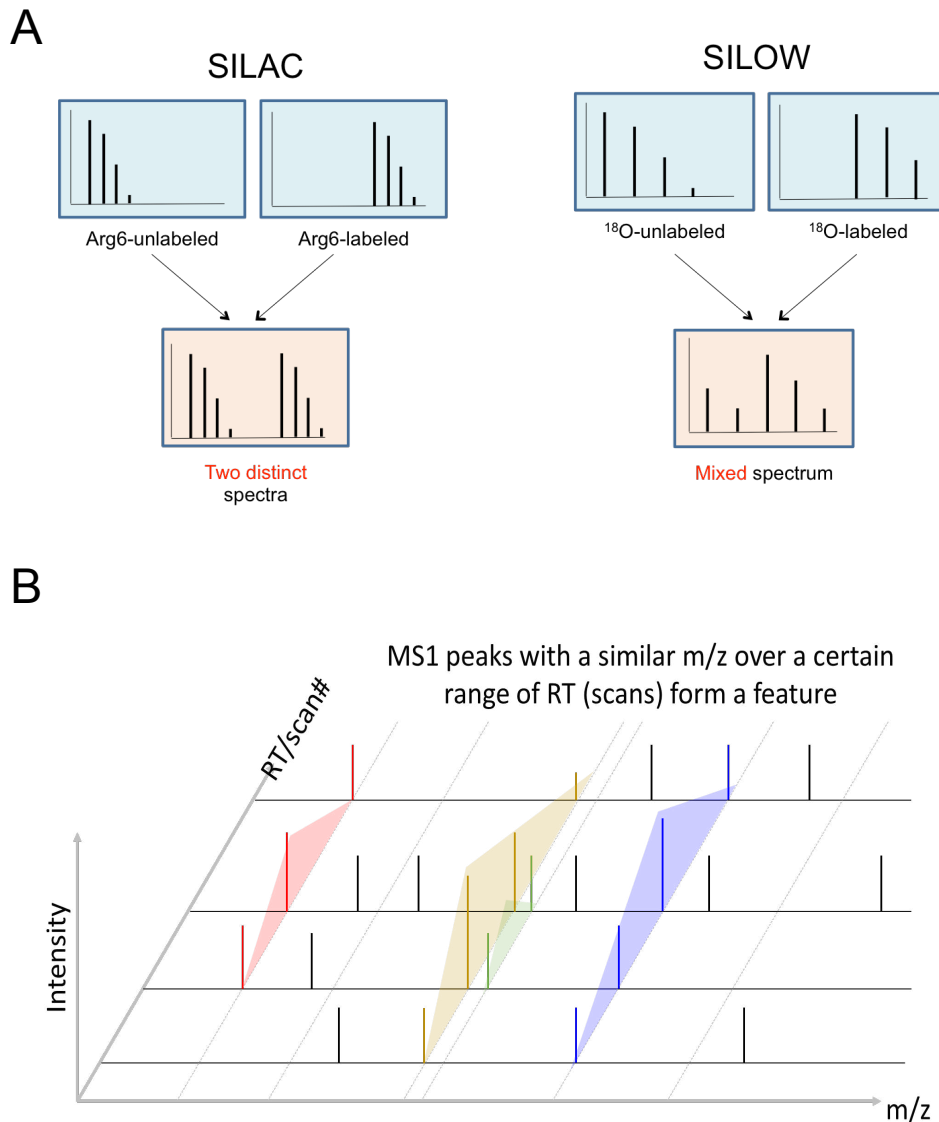
Figure 3.10: Achieving peptide identification when SILOW is implemented.
A. Schematic illustration demonstrating the challenge to peptide identification when samples are ^{18}O-labeled. SILAC requires complete isotopic labeling using an isotope of at least 6 Da, resulting in two distinct spectra. SILOW requires incomplete labeling and the only induces a 2 Da mass change, resulting in a single, heterogeneous spectrum. **B.** Schematic representation of feature-based peptide identification. Peptides are identified by aligning their isotopic envelopes and retention times to a library built using an unlabeled proteome.

medium containing 70% ^{18}O-water for 1, 3 and 9 minutes, and each time point was

repeated for a total of two biological replicates. Cells were lysed in denaturing buffer to

quench labeling and the samples were shipped on dry ice to Zhiping Wu in the Peng

lab, who performed trypsinolysis, immunoprecipitation with an anti-K-ε-GG sites

antibody to enrich for peptides from Ub-conjugation sites and LC-MS/MS for proteome-

wide analysis of ^{18}O-labeling at those sites[3,88].

On average, 3700 peptides were identified per sample, but only 723 peptides

were identified from each time point and in both replicates. This 723-peptide dataset

was further filtered based on agreement of the ^{18}O-enrichment between the two

biological replicates. This step was deemed important in order to provide more

confidence in the peptide identification, which depended on feature alignment rather

than by stringent database searching. Biological replicates were compared and filtered

out if more than one time point showed ≥ 100% deviation among the replicates.

Application of this filter removed an additional 57, leaving 666 peptides. These

remaining peptides, and their corresponding ^{18}O-enrichment levels over the time series

were organized into groups using k-means clustering[89] in which the total number of

clusters were allowed to vary 2 to 10 (Figure 3.11B).

The clustering analysis resulted in 8 groups of peptides, each with a slightly

different pattern of ^{18}O-labeling kinetics. No single cluster was over or

underrepresented, with 8 to 18% of the total residing in each. The most stable sites of

ubiquitination are represented in Cluster #3, where little to no labeling is seen

throughout the 9-minute experiment. On the other end of the spectrum, ubiquitination

sites within Cluster #4 are almost completely labeled within 1 minute,
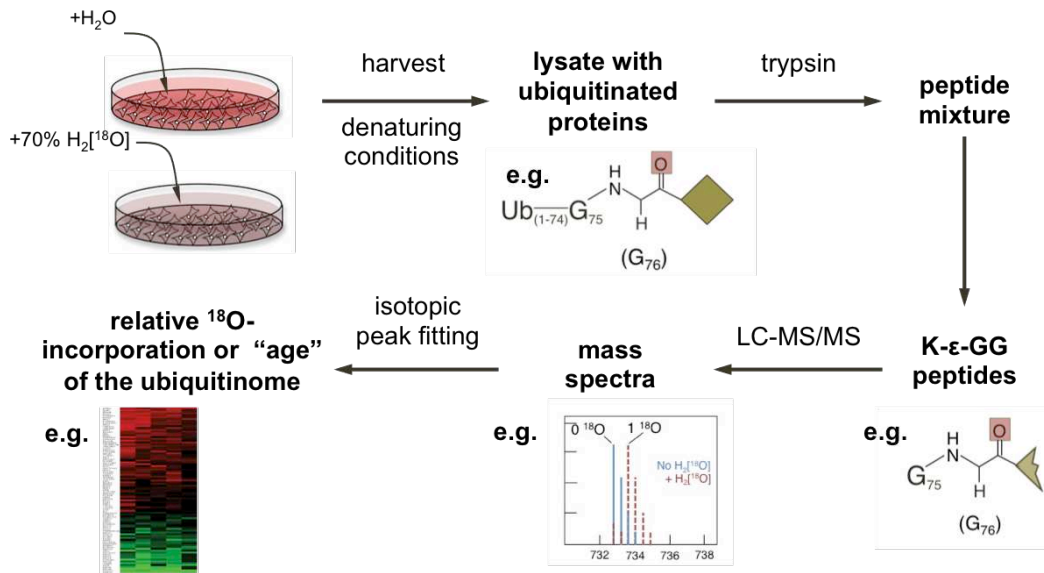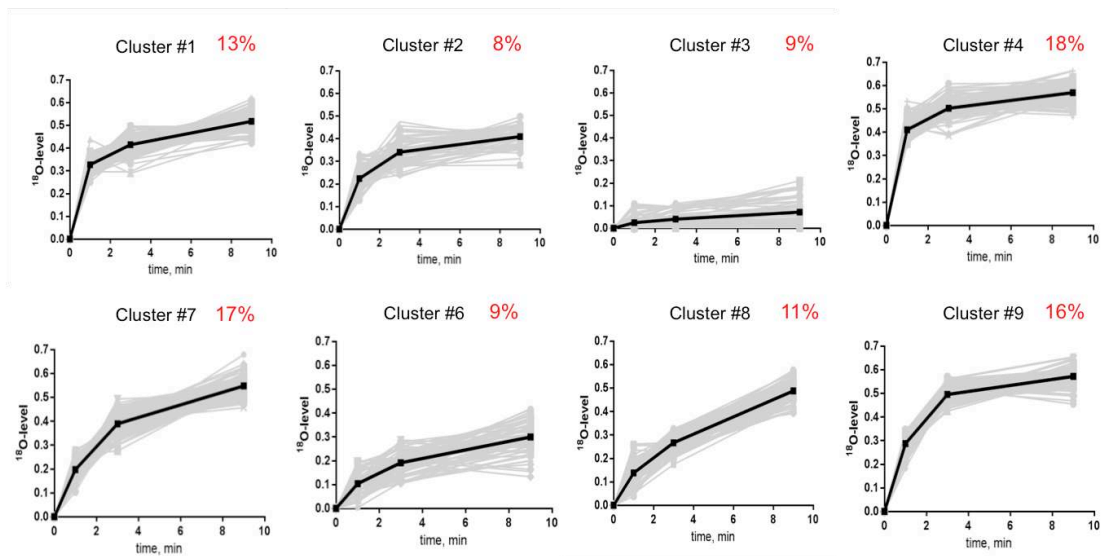
Figure 3.11: A platform for ^{18}O-labeling and automated analysis was developed and used to demonstrate ubiquitination dynamics across the proteome A. Diagram of the experimental workflow for proteome-wide ubiquitin flux measurements in human cells. Conventional media was replaced with media supplemented with 70% ^{18}O-water for 1, 3 and 9 minutes. Cells are harvested in denaturing conditions, digested with trypsin and enriched with the K-GG antibody before analysis with LC-MS/MS and peptide identification/peak fitting to determine the ^{18}O-level at each ubiquitination site. **B.** K-means clustering analysis of times series for 666 Ub sites allowing k to float between 2 and 10. The cluster average is plotted in black against the individual time series in grey.

demonstrating their very rapid turnover. Other peptides, such as in Clusters #1, #8 and #9, seem to have multiple populations. For example, Cluster #1 has a population that turns over rapidly, comparable to cluster #4, as demonstrated by the initial steepness in the curve at 1 minute. Cluster #1 peptides also have a stable subset of the population, which is reflected in the more gradual increase in ^{18}O-labeling at minutes 3 and 9. This apparent biphasic labeling kinetics could be due to heterogeneity in patterns of nearby modifications, protein localization or binding partners associated with the protein. The DAVID bioinformatics software program[90,91] was used to look for pathways enriched among the different clusters, but using the current data, there is no obvious correlation between a particular kinetic pattern and a metabolic pathway or signaling pathway.

3.3.12 ^{18}O-labeling of free Ub and Ub-hydrazide in human cells

A small fraction of each human cell lysate was treated with hydrazine to replace thioesters with hydrazide adducts that are less susceptible to hydrolysis (as discussed in Chapter 2 Section 3.1.1 and Appendix 1). Those fractions were loaded onto SDS-PAGE gels and the 8 kDa band was excised, processed for in-gel proteolysis by LysC and subsequently analyzed by LC-MS/MS to check ^{18}O-labeling of free (Figure 3.12A) and hydrazide (i.e. thioesterified, Figure 3.12B) Ub. In yeast, the majority of free Ub labeling occured within 30 seconds, although there may be a more stable pool of conjugates that turned-over from 1 to 8 minutes (Figure 3.5B). Similar kinetics were observed for free Ub labeling in HEK293T cells, where most labeling occurred within the first minute, but a fraction of Ub was labeled over the course of the next 8 minutes (Figure 3.12A). By the end of 9 minutes, the labeling distribution approached complete labeling, as theoretically predicted.

A qualitative analysis of the labeling kinetics of Ub-hydrazide showed similarity to that of free Ub in that most of the labeling occurred within the first minute; however, labeling did not progress after the first minute (Figure 3.12B). Instead, no additional labeling occurs after Ub-hydrazide is about 80% labeled, suggesting that around 20% of the cellular activated (i.e., thioesterified) Ub was stable during the 9-minute labeling period, while the other 80% was turned-over, either by hydrolysis or by Ub-protein conjugation, in less than a minute. These observations (and those for free Ub) are based on manual inspection of ^{18}O-incorporation curves and will be used in fitting analyses to determine rates and the fraction of each population (i.e. slow versus fast exchanging).

3.3.13 Validating the results of SILOW

The results of the SILOW analyses indicate that Ub flux through the majority of ubiquitination sites is rapid, with half-lives of most of nearly 700 sites on the order of minutes. To obtain independent support for this result, we examined cells under conditions that would block new ubiquitination events without affecting deubiquitination. First, HEK 293T cells were incubated with Compound 1 (C1), an inhibitor of the Ub activating enzyme (i.e., E1)[60]. After increasing incubation periods with C1, cells were harvested and extracts were analyzed by immunoblotting against conjugated Ub (Figure 3.13A). In this experiment, the apparent half-life of bulk ubiquitination is on the order of dozens of minutes, significantly slower than what was found by SILOW. Since C1 works by competing with ATP for binding to the E1 enzyme[60], we reasoned that the IC50 could be different in cells, depending on cellular ATP levels.
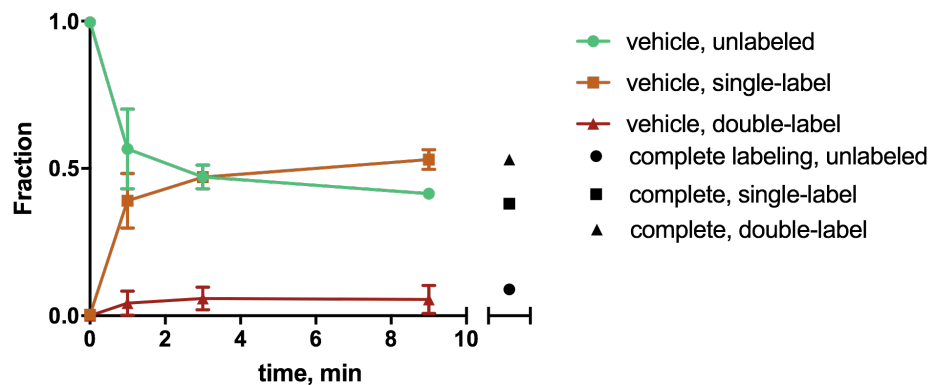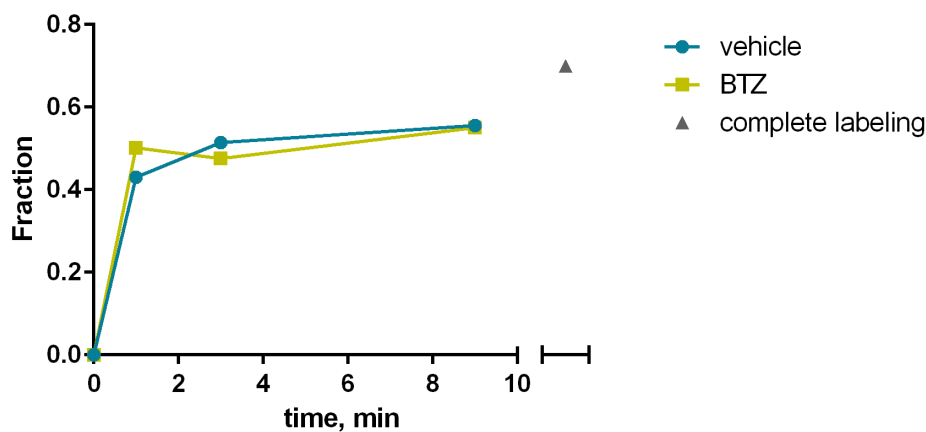
Figure 3.12: Kinetics of free and activated Ub ^{18}O-labeling in human cells A. HEK293T extracts were treated with hydrazine in order to convert labile ubiquitin-thioesters into stable ubiquitin-hydrazide. LC-MS/MS was used to quantify the ^{18}O-content in ubiquitin C-terminal peptides that are modified by hydrazine to establish the labeling kinetics of **A.** free Ub and **B.** Ub-hydrazide (i.e. Ub-thioesters). For each time point, n=2; averages and standard deviations are plotted.

Also, the kinetics of C1 diffusion into the cell are unknown and could be rate-limiting. Both these factors may contribute to the time difference in this experiment and SILOW.

Instead of trying to optimize the concentration of E1 inhibitor and attempting to estimate the diffusion kinetics, rapid ATP depletion was used as another approach to halt Ub activation by E1. ATP was reduced in cells by replacing conventional medium with that lacking glucose and supplemented with 2-deoxyglucose and antimycin A, as demonstrated by Feldenberg and collegues[92] (Figure 3.13C). With this treatment, over 60% of the cellular polyUb was depleted in 15 minutes. These results are more similar to the results quantified by SILOW, where most ubiquitination sites were completely ^{18}O-labeled (and thus turned over) within 9 minutes (Figure 3.11B).

Site-specific antibodies were used to check the levels of K48 and K63 linked Ub, as well as ubiquitination at K119 of Histone 2A (H2A) and K120 of Histone 2B (H2B) (Figure 3.14A). The bands corresponding to the specific antibody signals were quantified and the depletion of specific ubiquitination sites conjugates (i.e. deubiquitination) was compared to the ^{18}O-labeling kinetics (i.e. deubiquitination and re-ubiqitination) (Figure 3.14B). From this analysis, it was apparent that the measured half-times are not equivalent in both experiments. Differences and assumptions in the two experiments can account for this. First, SILOW measurements were taken when the cells were at steady state, yet this was not the case for the cells after inducing ATP depletion where massive metabolic changes are underway[93]. Second, in the condition of ATP depletion, we assume that no new ubiquitination events occur. This could easily
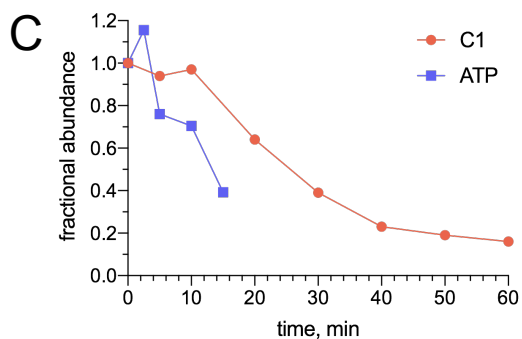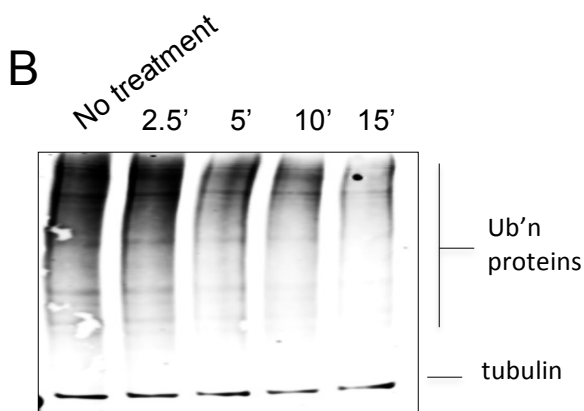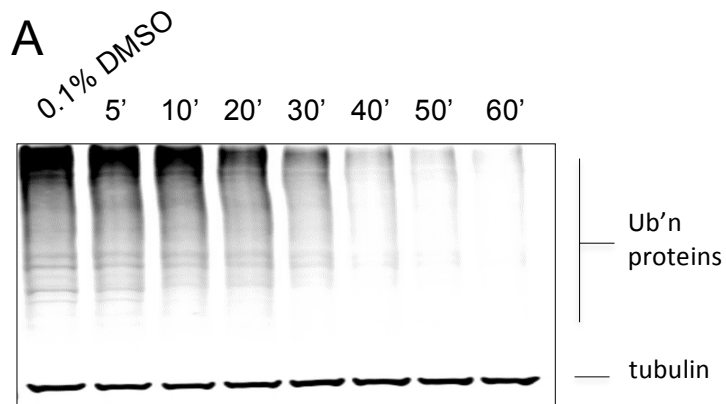
Figure 3.13: Optimizing conditions to validate SILOW results A. HEK293T cells were treated with E1 inhibitor over time and cell extracts were analyzed by immunoblotting with against Ub (P4G7) and tubulin as a loading control for **B.** normalized qunatification. **C.** HEK293T cells were treated with media lacking glucose and supplemented with 10 mM 2-deoxygluocse, 10 μM antimycin A over time and cell extracts were analyzed as in **A**, **B**.

be tested by measuring ^{18}O-content in very rapidly exchanging ubiquitination sites after initiating ATP depletion, but as yet, this has not been done. The final assumption is that DUBs are as active post-ATP depletion as before treatment commenced. For example, the binding of certain thioesterified E2's stimulates hydrolysis of K48-linked polyUb by the OTUB1 DUB[94]. In ATP-depleted cells, thioesterified E2's will be rapidly depleted (Figure 3.12B) and thus, DUBs activated in this manner are expected to lose activity during the experiment.

3.3.14 Examples of site-specific ^{18}O-labeling illustrate differences Ub flux at different sites within the same protein

Manual analysis of the proteome-wide SILOW results led to the observation that different ubiquitination sites on the same protein can undergo different rates of ubiquitination/deubiquitination cycling (Figure 3.15). For example, histone 1 (H1) is comprised of almost 30% lysine residues[95] and our analysis identified Ub attachments to 7 of those lysines with ^{18}O-labeling kinetics that ranged from slow to medium and to very fast (Figure 3.15A). Adjacent H1 residues K63 and K64 exhibit nearly identical labeling patterns, which may be explained by their similar tertiary environments recruiting the same regulatory elements. The Ub flux is similar at K75, which is 11 residues C-terminal to K63/K64. On the other hand, K97 and K106, separated by only 8 residues exhibit very different kinetics, where K97 is nearing complete labeling in minutes, yet K106 never surpassed 50% labeling.

In H1, the ubiquitination sites were spread throughout the protein and the relative rates of Ub flux among them had a broad range of speeds. Next, the labeling dynamics of ubiquitination on the C-terminal tails of histone 2A (H2A) variants were assessed
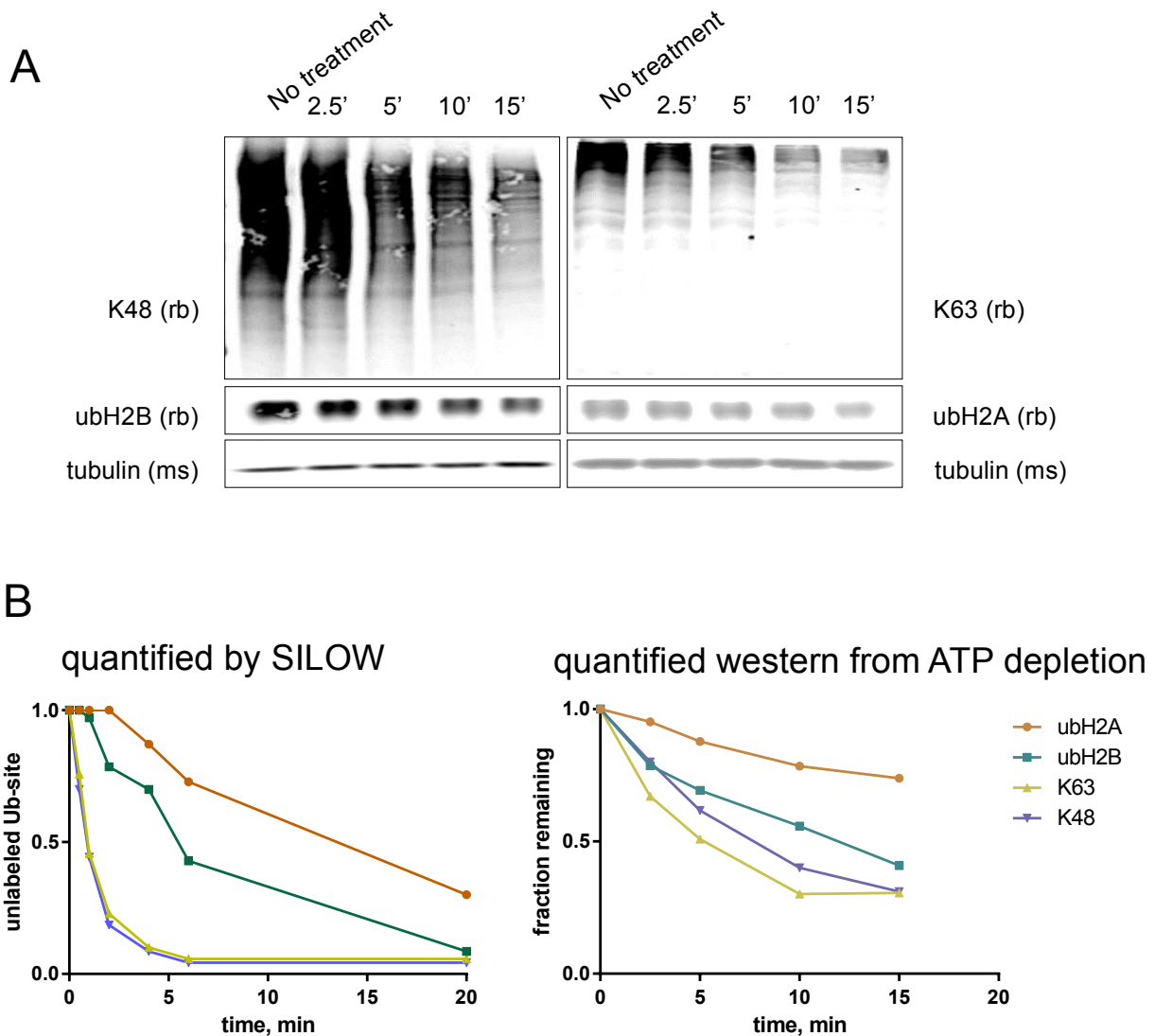
Figure 3.14: ATP depletion and site-specific Ub quantitation validates trends identified by SILOW. A. HEK293T cells were treated with media lacking glucose and supplemented with 10 mM 2-deoxygluocse, 10 µM antimycin A over time and cell extracts were analyzed by Ub site-specific antibodies including K48 (Apu2), K63 (Apu3), ubH2A (), ubH2B () and tubulin, used as a loading control for **B.** normalized quantitation and comparison to the initial velocities of labeling measured by SILOW

(Figure 3.16B). One of two major sites of H2A ubiquitination, K118[96], showed the

slowest dynamics.. Interestingly, K119 on H2A variant X (H2A.X) displays significantly

higher degrees of labeling at earlier time points, indicating that flux through K119 of

variant X is faster than on the canonical H2A. The functions of ubiquitination on both

K125 of H2A.Z and K127 on H2A.X are currently unknown[97,98]. It is clear, however, that

ubH2A.X conjugated on K127 is far less abundant than ubH2A conjugated on K119[97];

this may indicate that, for at least some sites, the abundance of Ub-conjugation on

specific histone sites may correlate inversely with the Ub flux through them. However,

this is clearly not the case for Ub-Ub linkages within polyUb. Whereas K27 linkages are

only 0.5% of the total yet exhibit the slowest kinetics, flux through K11 and K48 Ub-Ub

is very rapid and these linkages account for 15% and 37% in rat brains tissue,

respectively.

From this assortment of histone-Ub dynamics, we can conclude that the kinetics

of ubiquitination at different sites within the same protein can range from being nearly

equal to drastically different. Modulation of specific ligase or deubiquitinase activities in

conjunction with SILOW will be a powerful combination to gain mechanistic insight on

the regulation of these histone and other ubiquitination sites.

3.3.15 Effect of proteasome inhibition on dynamics of specific ubiquitination sites

In parallel to the study of Ub dynamics in untreated cultures, HEK 293T cells

were pre-treated with a proteasome inhibitor for 1 hour before ^{18}O-labeling and

sampling after 1, 3 and 9 minutes (Figure 3.16A). The same processing procedures
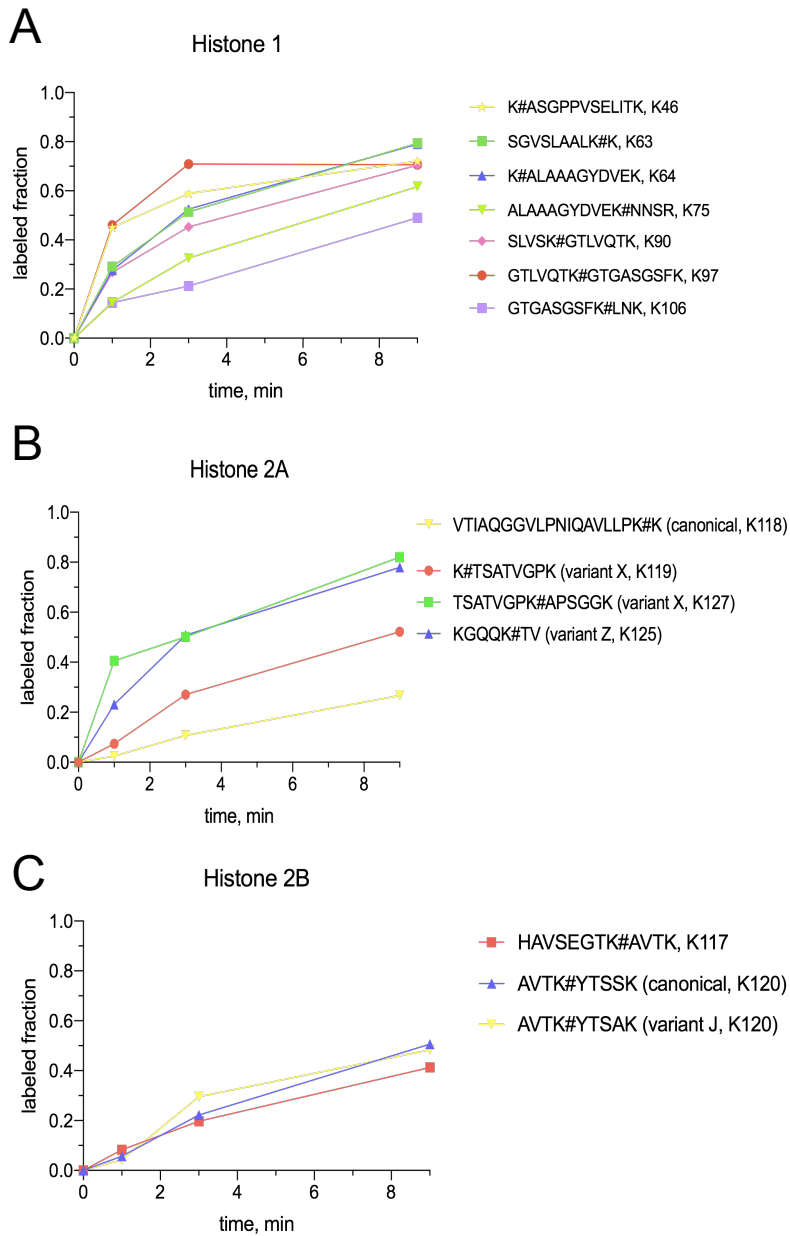
Figure 3.15: Intraprotein ¹⁸O-labeling dynamics can be both homogeneous or heterogeneous. Specific Ub sites on **A.** Histone 1 **B.** Histone 2A and **C.** Histone 2B were extracted from the large proteomics data set and plotted together. For each time point, n=1.

described in Section 2.2.5 were used, resulting in another ~10,000 peptides that were then pared down to a list of peptides observed in every time point and with less than 100% deviation in ^{18}O content between biological replicates in 2 of the 3 time points. The final list contains 236 peptides, but the focus was on a subset of conjugation sites selected based on their interesting dynamic patterns (Figure 3.16B).

With the exception of K63, all polyUb linkages were more stable upon proteasome inhibition. This result is supported by the observations of Xu et al.[99], who reported that all Ub linkage types except K63 increase by 2 to 8-fold in abundance during proteasomal inhibition. If the efficiencies of enzymatic activities that maintain these sites are not changed during proteasome inhibition, it stands to reason that the abundance of these linkages increases significantly, the rate of Ub movement through them will be reduced.

Interestingly, ^{18}O-labeling at ubiquitination sites K119 of H2A and K120 of H2B did not change when the proteasome was inhibited. Kaiser et al[28] and Dantuma et al[38] both demonstrated that histone-associated monoubiquitination is reduced by over 70% when the proteasome is inhibited. If the reduction at these sites is due to a reduction in the rate of ubiquitination, then the sites would have lower levels of ^{18}O. No difference in ^{18}O-labeling at sites between native and proteasome-inhibited states suggests that the decrease in abundance is due an increased rate of deubiquitination.

Conversely, Dantuma et al.[38] monitored PAGFP-Ub mobility during proteotoxic stress and observed no difference in nuclear diffusion of PAGFP-Ub compared to untreated cells. Their conclusion was that no change in the rate of deubiquitination occurs during proteotoxic stress. One major difference in their experiment and ours, is
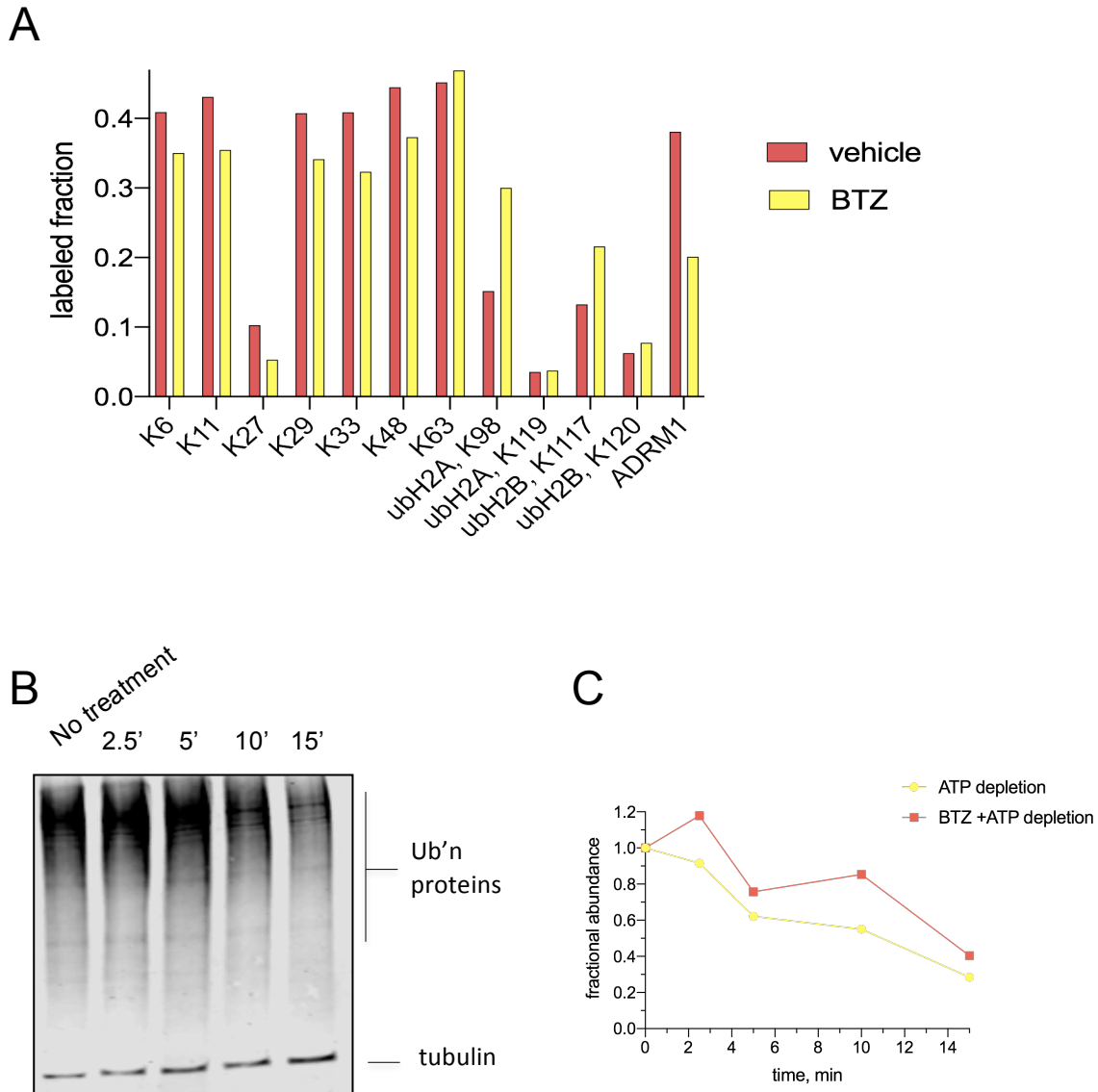
Figure 3.16: ^{18}O-labeling kinetics in cells treated with proteasome inhibitor. A. Timeline for treatment of HEK293T cells with protesome inhibitor, BTZ, and SILOW. For each time point, n=1.**B.** Cells were treated as indicated in **A** and processed for proteome-wide LC/MS-MS analysis and subsequent peak fitting to calculate degree of labeling after 1 minute incubation with ^{18}O-water (values are normalized against the amount of ^{18}O in the system). **C.** HEK293T cells were pre-treated 10 μM BTZ for 1 hour before treatment with media lacking glucose and supplemented with 10 mM 2-deoxygluocse, 10 μM antimycin A over time and cell extracts were analyzed antibodies with against Ub (P4G7) and tubulin as a loading control for **D.** normalized qunatification.

the ability to monitor dynamics in real-time immediately after stress induction using microscopy, whereas SILOW was performed after one hour of proteotoxic stress. ADRM1, also known as Rpn13, is a substrate receptor and DUB docking site on the proteasome that is reportedly polyubiquitinated and can itself become a substrate of the proteasome[100].The degree of ^{18}O-labeling on ADRM1 is significantly reduced when the proteasome is inhibited, perhaps because more ubiquitinated ADRM1 had accumulated.

3.4   Conclusions

Isotopic labels have enhanced proteomics studies by permitting relative and absolute quantitation, and now SILOW-MS allows observations on dynamics through sites of ubiquitination. SILOW is performed by incubating cells in medium containing ^{18}O-water which equilibrates across cell membranes within ~ 0.1 s and, as with other stable isotope-labeling methods, the presence of the ^{18}O is not expected to cause any perturbations of normal physiological processes[48,101]. This experimental aspect makes SILOW less perturbing than microscopy-based measurements of Ub dynamics, which generally required overexpression of fluorescent protein-fused Ub. Among other phenotypic differences induced by Ub overexpression in neurons Ub-conjugates were upregulated[22], suggesting that Ub homeostasis was misregulated.

Importantly, the timing of labeling in Ub-conjugates was demonstrated to be well resolved from other, non-Ub related modes of labeling. Free Ub was labeled within seconds and Ub-conjugates were labeled on the order of minutes, while labeling by other modes was rarely observed, even after 20 minutes. For many sites of Ub-conjugation, labeling was complete in minutes, and since the rate of labeling is directly

related to half-life of the modification, our results suggest a large fraction of the Ub system is highly dynamic and rapidly changing.

For all polyUb linkages the labeling kinetics were largely similar, with the exception of K27, whose dynamics were slower than many sites identified in our SILOW experiment. Casteñeda et al.[102] reported resistance of K27-linked polyUb against linkage non-specific DUBs USP2, USP5, and Ubp6. NMR analysis revealed K27 is least solvent exposed of all lysine residues in Ub and the G75 and G76 residues of the distal Ub in K27-Ub_2 are more ordered than in other Ub_2 chains. These characteristics likely make the K27 linkage less accessible and more structured than all other polyUb chains. In cells, those observations could be translated to inefficient disassembly, which would also explain the slow labeling kinetics of K27-Ub_2 measured by SILOW.

Our confidence in the results generated by SILOW was heightened by validation of the kinetic patterns of select Ub sites upon cellular depletion of ATP. Also, SILOW performed in cells pre-treated with proteasome inhibitor presented kinetic patterns consistent with results published in other studies. All polyUb linkages, except K63, were less dynamic, by 15-50%, in proteasome inhibitor pre-treated cells. This is consistent with the report by Xu et al.[74] in which all polyUb chains increased in abundance, from 2 to 8-fold, when proteasomes are inhibited. In this study, K27-linked polyUb increased only 2-fold, while most other linkages were elevated by at least 4-fold. Conversely, SILOW demonstrated K27-linkage dynamics decrease most out of all polyUb linkages, perhaps merely reflecting the structural challenges in processing this chain type.

A limitation of SILOW-MS is our current ability to identify peptides from complex samples in high-throughput. Performance by the feature alignment-based approach

hampered our ability to thoroughly survey the dynamics of Ub-conjugation sites across the proteome. Although 10-12,000 Ub sites were identified in the ^{18}O-unlabeled sample using traditional methods (i.e., using the Sequest algorithm to search the human Uniprot database), only 3-4,000 Ub sites were identified in each sample using feature alignment-based detection. In hindsight, an additional biological replicate would have prevented some of the further reduction to ~700 peptides due to missing time points. For future SILOW studies, it will be worthwhile to improve the current peptide identification method or move to an approach based on supplementing current algorithms like Sequest to accommodate mass shifts induced by ^{18}O-labeling. Due to the present state of SILOW data processing, we recommend enriching site(s) of interest or directly targeting specific sites using parallel reaction monitoring MS (PRM-MS), which has high enough resolution to quantify ^{18}O-labeled peptides.

In the future, we plan to fit the ^{18}O-level kinetics to a model that describes the half-life of peptide-specific ^{18}O-labeling. Using the model, we can obtain kinetic parameters for: 1. the fraction of labeled peptide at the end of the time series and 2. the apparent half-life of labeling. Using these parameters, I hope to be able to classify the labeling kinetics exhibited by cellular ubiquitination sites in a more rigorous way than by k-means clustering. The model fittings will provide confidence intervals for each of the two kinetic parameters rendered, thus permitting statistical analyses.

In conclusion, SILOW-MS methods were established, validated and used to demonstrate relative dynamics of ubiquitination across the proteome. The ability to quantify intracellular Ub kinetics will enhance the field's accessibility on the largely unappreciated dynamic nature of the system.

CHAPTER 4: DISCUSSION

4.1 Accessible measurements on Ub pools will deepen our understanding of Ub homeostasis

4.1.1 The effect of proteasome inhibition on Ub pools

In addition to the breadth of phenotypic evidence exhibited by mice and neurons in cell culture suggesting that cellular Ub levels must be maintained within a tight window, Ub pool and gene expression quantitation on proteasome inhibited MEF cells also highlighted strict cellular regulation. In the face of Ub depletion due to proteasome inhibition, MEF cells were somehow able to sense the change in cellular Ub levels and activate Ub gene expression, thus recovering the loss all within two hours. Conversely, the free Ub of HeLa cells was drastically reduced, likely due to the lack of Ub gene activation. In the absence of a robust and accessible method to routinely quantify the free Ub pool, many in the field have assumed that a vast increase in Ub conjugates is associated with a concomitant depletion of free Ub, as with HeLa cells. Currently, there are at least 3 FDA-approved proteasome inhibitors being used to treat multiple myeloma and mantle cell myeloma and many clinical trials underway to test efficacy of proteasome inhibitors in treating solid tumours[103]. Obviously, the proteasome inhibitor is more efficacious at disrupting Ub homeostasis in some cell types than in others, and these differences can now be defined with the pool quantitation method.

4.1.2 Understanding the relationship between free Ub levels, Ub-bound histones and Ub gene expression

An outstanding question in the field of Ub homeostasis regards the nature of the

relationship between the free Ub pool and histone-conjugated Ub. Which comes first, depletion in free Ub or in histone-bound Ub? and is one event causal over the other? Dantuma et al[38]. demonstrated that nuclear Ub (presumably histone-bound) begins to diminish within 15 minutes of proteasome inhibition, about the same time cytoplasmic Ub starts accumulating (presumably polyUb), yet we still don't know the dynamics of free Ub. A detailed analysis of free Ub depletion in MEF cells over early time points of proteasome inhibition may reveal a brief period where free Ub levels dip. Free Ub levels in HeLa cells were decreased by half in 30 minutes (Figure 2.8B), which indicates depletion begins early in the treatment.

To test causality, the ubH2A ligase, Rnf2, could be inhibited and the levels of free Ub monitored through Ub pool quantitation. Although there is no easy way to reduce Ub levels in human cells, methods and cell lines were recently developed that permit efficient and reversible Ub overexpression[104]. In a study using the Huntington's Disease mouse crossed with a *Ubc* heterozygous mouse, a positive correlation between total cellular Ub and ubH2A was observed[66]. We may find the reason is simply substrate availability for Rnf2, where elevated levels of free Ub enhance the rate of catalysis.

4.2   *The dynamics of cellular Ub chain editing may be unveiled by SILOW*

Signal transduction by post-translational modification (PTMs) is usually recognized as a change in PTM levels in response to some cellular cue. To our knowledge, there are no published reports of signals being transduced by changes to PTM flux. Importantly, this novel concept can now be tested using SILOW for pulse-labeling Ub to test a specific example of correlation between Ub flux and cellular outcome.

4.2.1 Stress-induced changes in polyUb linked to substrates of the PQC response

Under heat stress WT yeast cells accumulated K63-linked polyUb within 10 minutes, but by 45 minutes, this accumulation was resolved without recovery at a lower temperature (Figure 4.1). In contrast, if Ubp2 or Ubp3 is deleted in cells (i.e. *ubp2Δ or ubp3Δ*), K63-linked Ub polymers persist throughout the heat treatment. Obviously, Ubp2 and Ubp3 facilitate flux through K63 polyUb during heat-stress, but there has been no method to test this directly prior to the establishment of SILOW.

Hul5 and Rsp5 are two Ub ligases implicated in protein quality control (PQC) in yeast cells under heat stress[105,106]. The accumulation of polyUb was partially abrogated in cells expressing a temperature sensitive mutant of RSP5 (i.e., *rsp5-1*) or in a HUL5 deletion strain (i.e., *hul5Δ*). But only in the double mutant background (i.e., *rsp5-1, hul5Δ*) were polyUb conjugates completely eliminated, indicating either that each ligase has its own subset of substrates or the crosstalk of both ligase activities is needed to fully process clients of PQC[106].

Both Hul5 and Rsp5 preferentially synthesize K63 polymers[105,107] of Ub so the finding that K48-linked polyUb was impaired in heat-stressed *rsp5-1* cells was surprising. Conversely, *hul5Δ* cells had decreased heat-stress induced K63-linked polyUb, but no effect was observed on K48-linkages[106]. Also, in a subsequent study, Fang et al.[108] reported the involvement of Ubp2 and Ubp3 in modulating K63 polyUb levels during heat stress. If either DUB was deleted, a dramatic accumulation of K63-linked polyUb was observed (Figure 4.1).

These results suggest the modifications on substrates of the PQC are dynamic and subject to regulation by the flux of Ub through them. Using SILOW, the
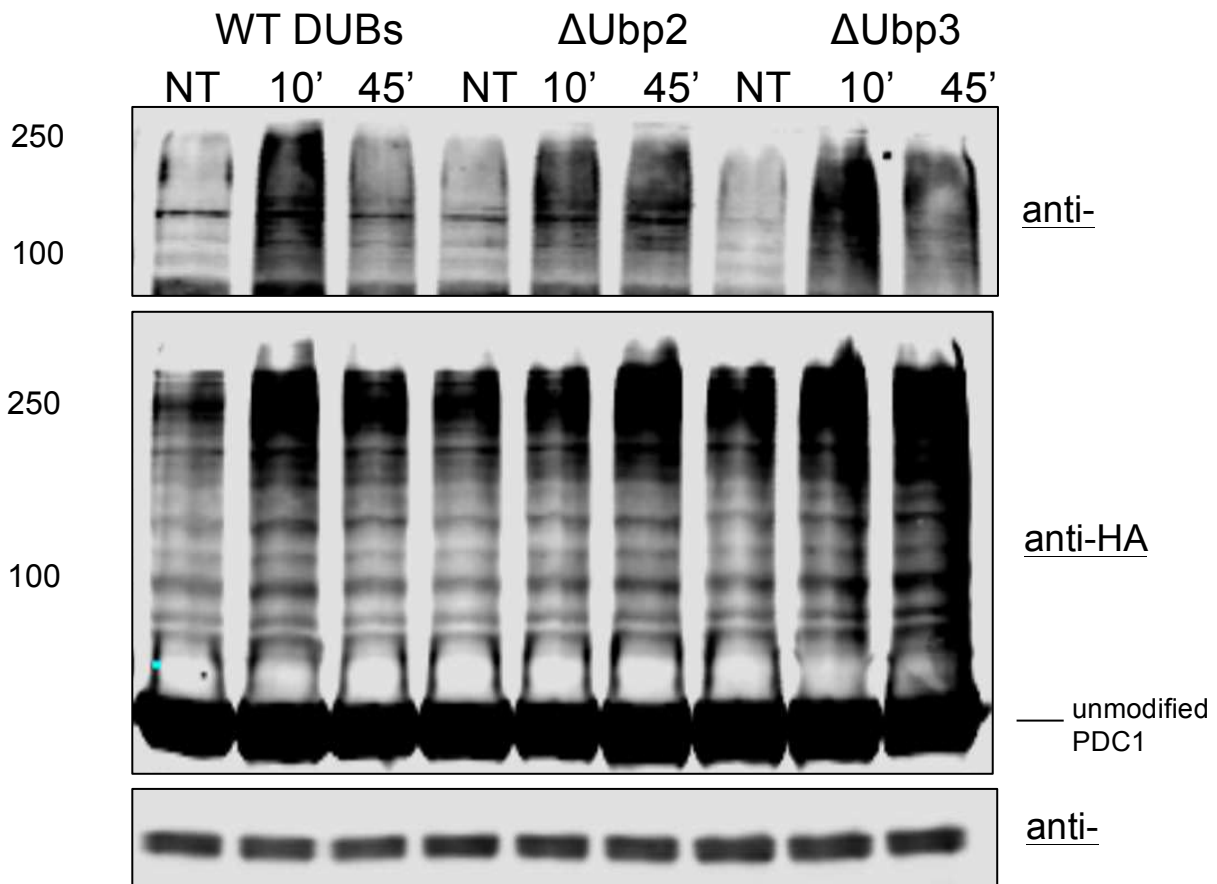
Figure 4.1: Yeast cells undergo a rapid burst of K63 polyubiquitination during heat stress that is regulated by Ubp2, Ubp3 Yeast cells expressing PDC1-HA(3) and either WT or deleted for Ubp2 or Ubp3 were grown to log phase were treated heat stress at 45°C for various times and cell extracts were blotted with a K63-polyUb specific antibody, anti-HA and Yuh1 as a loading control.

contributions by specific ligases and DUBs on the dynamics of polyUb, for example during heat stress, can be defined.

4.2.2 Using SILOW to reveal polyUb dynamics during heat stress

Fang et al.[106] compared SILAC experiments in untreated WT, heat-stressed WT and *rsp5-1* cells to compile a list of proteins that were ubiquitinated upon induction of heat shock in an Rsp5-dependent manner. In the same study, three model proteins, Pdc1, Cdc19 and Sup45, were selected for in depth study by expressing HA-tagged versions of the proteins and performing additional experiments. Thibault Mayor was kind enough to gift us with these strains, which have subsequently been genetically altered for deletion of UBP2 or UBP3 or installment of temperature sensitive RSP5. HUL5 deletion in HA-tagged target strains would also be wise, as we could also reveal its involvement in polyUb chain creation on model PQC substrate proteins.

For SILOW, the labeling status of the Ub site must be within the window of $^{16}O/^{18}O$ ratios that linearly correlate with time. We have no information regarding the labeling kinetics for any Ub conjugation sites in yeast, but the oxygens in free Ub are equilibrated with ^{18}O-water in media within 30 seconds; as a starting place, 1-minute pulses with ^{18}O-water will be used. An example of a labeling experiment would include pulsing cells prior to, 10 minutes after and 45 minutes after induction of heat stress.

Ideally, ^{18}O-levels would be assessed in the proximal Ub site (i.e., between model protein and the first Ub moiety) as well as any distal Ub sites (i.e., polyUb linkages). As discussed in Chapter 3 Section 4, a limitation of SILOW is the inability to identify ^{18}O-labeled peptides at low abundance. To increase chances of faithfully observing model proteins and the polyUb covalently associated with them,

immunoprecipitation with the HA antibody will be performed and enriched fractions processed for MS.

4.2.3 Expectations for SILOW quantification of polyUb dynamics during heat stress

We may see different rates of ^{18}O-labeling in native cells as compared to heat stressed cells at 10 or 45 minutes, but more informative will be the rate comparisons across strains (i.e. WT versus *ubp2Δ* or *ubp3Δ).* In a ligase or DUB deletion background, less ^{18}O-label at any Ub site will be indicative of participation in promoting Ub flux through the site. Further testing would be needed to determine whether the enzyme works to directly influence flux, as in ubiquitination or deubiquitination, or indirectly through promoting action of another ligase or DUB.

4.2.4 PolyUb editing at the proteasome

Another study that inferred polyUb dynamics based on steady-state measurements over time focused on activities of the many factors associated with the proteasome. The polyUb chain elongation by Hul5 was directly opposed by deubiquitination by Ubp6 for proteins at the proteasome destined for degradation. One possibility is the continual extension of the substrate polyUb by Hul5, to increase affinity to the proteasome. Another attractive explanation for this interplay is maintenance of the net length of the polyUb chain by Hul5 in the face of Ubp6 activity. Measurements of flux through the K48 polyUb linkages associated with the proteasome in yeast strains deleted for Hul5 or Ubp6 could finally shed light on which scenario actually occurs.

4.3   SILOW broadens horizons of the Ub field

The network of Ub-dependent signaling comprises hundreds if not thousands of proteins, many connected through positive or negative feedbackloops[10]. As with gene

regulation, understanding the organization and regulation of this complex network will require a systems biology approach[109]. Until now, key parameters needed to define a model describing Ub regulation even at a rudimentary level, such as the rate of Ub movement through the free, activated and conjugate pools, were unattainable. Using the Ub pool assay in conjunction with SILOW, the absolute concentrations and rates of Ub flux in each pool can be measured to define the parameters of an initial model to describe Ub homeostasis. Once a model is defined, cellular perturbations such as inhibited ubiquitination or Ub synthesis can be instituted and the parameters re-measured to refine the initial model.

Another dimension that would be required to fully refine the model describing cellular Ub homeostasis is the level of Ub gene expression. As discussed in Chapter 2 Section 4, it is clear that Ub synthesis plays an integral role in maintaining free Ub levels within a tight window. For each cellular perturbation instituted, the expression level for each of the 4 genes expressing Ub should also be quantified.

4.4 Extensions of SILOW

Because SILOW works by harnessing naturally occurring chemistries to perform cellular labeling of Ub, other PTMs with similar addition and removal chemistry can also be studied by ^{18}O-labeling.

4.4.1 Phosphorylation

Phosphorylation is another abundant PTM within the cell that is well studied, with many tools available to facilitate rigorous studies on the abundance or where or when the modification is added[110]. Incubating cells with media supplemented with radiolabeled ^{32}P-orthophosphate is a similar approach to studying the flux of phosphate

through metabolic pathways; however, the data is difficult to interpret because cellular uptake of orthophosphate is on the order of hours. Also, working with radiolabeled material requires additional safety, regulatory and disposal precautions making these experiments labor intensive.

Using SILOW to quantify movement of phosphate through cellular pathways has several advantages over ^{32}P-labeling. As discussed in Chapter 3, ^{18}O-water equilibrates across cellular membranes instantly, which facilitates measurements on unstable, dynamic reactions like PTMs. The ^{18}O isotope used for labeling with SILOW is innocuous and thus requires no extra, protective steps, making it poised to provide detailed observations to quantify intracellular phosphorylation dynamics. The increased number of terminal oxygens on phosphate as compared to Ub (i.e., 4 versus 2) will provide more sensitive flux measurements, but may require more time to fully equilibrate with ^{18}O in solution since labeling occurs by passage through reaction cycle.

4.4.2 Ub-like proteins

There are more than 15 eukaryotic proteins that make up the Ub-like (Ubl) family of proteins, with Nedd8, Sumo and ISG15 being the most studied[112]. The C-terminal remnant left by trypsinization of Nedd8 and ISG15 is also di-Gly, complicating data analysis. However, several studies have demonstrated methods for specific enrichment on neddylated or ISG15-ylated proteins[3,113], and these tools would also facilitate the study of 18O-labeling in those Ubls.

BIBLIOGRAPHY

1. Komander, D. & Rape, M. The ubiquitin code. *Annu. Rev. Biochem.* **81**, 203–29 (2012).

2. Mukhopadhyay, D. & Riezman, H. Proteasome-Independent Functions of Ubiquitin in Endocytosis and Signaling. *Science (80-.).* **315**, 201–205 (2007).

3. Kim, W. *et al.* Systematic and quantitative assessment of the ubiquitin-modified proteome. *Mol. Cell* **44**, 325–40 (2011).

4. Aguilar, R. C. & Wendland, B. Ubiquitin: Not just for proteasomes anymore. *Curr. Opin. Cell Biol.* **15**, 184–190 (2003).

5. Pickart, C. M. Mechanisms nderlying biquitination. *Annu. Rev. Biochem.* **70**, 503–533 (2001).

6. Hochstrasser, M. Lingering mysteries of ubiquitin-chain assembly. *Cell* **124**, 27–34 (2006).

7. Komander, D. The emerging complexity of protein ubiquitination. *Biochem. Soc. Trans.* **37**, 937–953 (2009).

8. Komander, D. & Rape, M. The ubiquitin code. *Annu. Rev. Biochem.* **81**, 203–29 (2012).

9. Reyes-Turcu, F. E., Ventii, K. H. & Wilkinson, K. D. Regulation and Cellular Roles of Ubiquitin-Specific Deubiquitinating Enzymes. *Annu. Rev. Biochem.* **78**, 363–397 (2009).

10. Clague, M. J., Heride, C. & Urbe, S. The demographics of the ubiquitin system. **25**, (2015).

11. Strachan, J. *et al.* Insights into the molecular composition of endogenous unanchored polyubiquitin chains. *J. Proteome Res.* **11**, 1969–1980 (2012).

12. Stewart, M. D., Ritterhoff, T., Klevit, R. E. & Brzovic, P. S. E2 enzymes: More than just middle men. *Cell Res.* **26**, 423–440 (2016).

13. Kimura, Y. & Tanaka, K. Regulatory mechanisms involved in the control of ubiquitin homeostasis. *J. Biochem.* **147**, 793–798 (2010).

14. Park, C. W. & Ryu, K. Y. Cellular ubiquitin pool dynamics and homeostasis. *BMB Rep.* **47**, 475–482 (2014).

15. Saigoh, K. *et al.* Intragenic deletion in the gene encoding ubiquitin carboxy-terminal hydrolase in gad mice. *Nat. Genet.* **23**, 47–51 (1999).

16. Osaka, H. *et al.* Ubiquitin carboxy-terminal hydrolase L1 binds to and stabilizes monoubiquitin in neuron. *Hum. Mol. Genet.* **12**, 1945–1958 (2003).

17. Anderson, C. *et al.* Loss of Usp14 results in reduced levels of ubiquitin in ataxia mice. *J. Neurochem.* **95**, 724–731 (2005).

18. Finley, D., Bartel, B. & Varshavsky, A. The tails of ubiquitin precursors are ribosomal proteins whose fusion to ubiquitin facilitates ribosome biogenesis. *Lett. to Nat.* **338**, 394–400 (1989).

19. Wiborg, O. *et al.* The human ubiquitin multigene family: some genes contain multiple directly repeated ubiquitin coding sequences. *EMBO J.* **4**, 755–759 (1985).

20. Park, C. W., Ryu, H. W. & Ryu, K. Y. Locus coeruleus neurons are resistant to dysfunction and degeneration by maintaining free ubiquitin levels although total ubiquitin levels decrease upon disruption of polyubiquitin gene Ubb. *Biochem.*

Biophys. Res. Commun. **418**, 541–546 (2012).

21. Ryu, K. Y. *et al.* The mouse polyubiquitin gene UbC is essential for fetal liver development, cell-cycle progression and stress tolerance. *EMBO J.* **26**, 2693–2706 (2007).

22. Hallengren, J., Chen, P. C. & Wilson, S. M. Neuronal Ubiquitin Homeostasis. *Cell Biochem. Biophys.* **67**, 67–73 (2013).

23. Rose, I. A. & Warms, J. V. A specific endpoint assay for ubiquitin. *Proc. Natl. Acad. Sci. U. S. A.* **84**, 1477–81 (1987).

24. Haas, A. L. & Bright, P. M. The immunochemical detection and quantitation of intracellular ubiquitin-protein conjugates. *J. Biol. Chem.* **260**, 12464–12473 (1985).

25. Oh, C., Yoon, J. H., Park, S. & Yoo, Y. J. Simultaneous quantification of total and conjugated ubiquitin levels in a single immunoblot. *Anal. Biochem.* **443**, 153–155 (2013).

26. McDonough, A. A., Veiras, L. C., Minas, J. N. & Ralph, D. L. Considerations when quantitating protein abundance by immunoblot. *Am. J. Physiol. - Cell Physiol.* **308**, C426–C433 (2015).

27. Patterson, C. & Cyr, D. M. *Ubiquitin-Proteasome Protocols*. *Methods in molecular biology (Clifton, N.J.)* **301**, (2005).

28. Kaiser, S. E. *et al.* Protein standard absolute quantification (PSAQ) method for the measurement of cellular ubiquitin pools. *Nat. Methods* **8**, 691–6 (2011).

29. Hurley, J. H., Lee, S. & Prag, G. Ubiquitin-binding domains. *Biochem. J.* **399**, 361–372 (2006).

30. Reyes-Turcu, F. E. *et al.* The Ubiquitin Binding Domain ZnF UBP Recognizes the C-Terminal Diglycine Motif of Unanchored Ubiquitin. *Cell* **124**, 1197–1208 (2006).

31. Yang, X. *et al.* Absolute Quantification of E1, Ubiquitin-Like Proteins and Nedd8-MLN4924 Adduct by Mass Spectrometry. *Cell Biochem. Biophys.* **67**, 139–147 (2013).

32. Sims, J. J. & Cohen, R. E. Linkage-Specific Avidity Defines the Lysine 63-Linked Polyubiquitin-Binding Preference of Rap80. *Mol. Cell* **33**, 775–783 (2009).

33. Sims, J. J. *et al.* Polyubiquitin-sensor proteins reveal localization and linkage- type dependence of cellular ubiquitin signaling. *Physiol. Behav.* **9**, 303–309 (2012).

34. Choi, Y.-S. *et al.* High-affinity free ubiquitin sensors for quantifying ubiquitin homeostasis and deubiquitination. *Nat. Methods* **16**, 771–777 (2019).

35. Salomons, F. A., Ács, K. & Dantuma, N. P. Illuminating the ubiquitin / proteasome system. **6**, 0–6 (2010).

36. Salomons, F. A. *et al.* Selective Accumulation of Aggregation-Prone Proteasome Substrates in Response to Proteotoxic Stress. *Mol. Cell. Biol.* **29**, 1774–1785 (2009).

37. Stenoien, D. L., Mielke, M. & Mancini, M. A. Intranuclear ataxin1 inclusions contain both fast- and slow-exchanging components. *Nat. Cell Biol.* **4**, 806–810 (2002).

38. Dantuma, N. P., Groothuis, T. A. M., Salomons, F. A. & Neefjes, J. A dynamic ubiquitin equilibrium couples proteasomal activity to chromatin remodeling. *J. Cell Biol.* **173**, 19–26 (2006).

39. Bantscheff, M., Schirle, M., Sweetman, G., Rick, J. & Kuster, B. Quantitative mass

spectrometry in proteomics: A critical review. *Anal. Bioanal. Chem.* **389**, 1017–1031 (2007).

40. Peng, J. *et al.* A proteomics approach to understanding protein ubiquitination. *Nat. Biotechnol.* **21**, 921–926 (2003).

41. Cohn, M. A study of oxidative phosphorylation with 18O-labeled inorganic phosphate. *J. Biol. Chem.* **201**, 735–750 (1952).

42. Boyer, P. D., Falcone, A. B. & Harrisoon, W. H. Reversal and Mechanism of Oxidative Phophorylation. *Nature* **174**, 401–403 (1954).

43. Boyer, P. D. A research journey with ATP synthase. *J. Biol. Chem.* **277**, 39045–39061 (2002).

44. Chahrour, O., Cobice, D. & Malone, J. Stable isotope labelling methods in mass spectrometry-based quantitative proteomics. *J. Pharm. Biomed. Anal.* **113**, 2–20 (2015).

45. Schnolzer, M., Jednejewski, P. & Lehmann, W. D. Protease-catalyzed incorporation of 18O into peptide fragments and its application for protein sequencing by electrospray and matrix assisted laser desorption/ionization mass spectrometry. *Electrophoresis* **17**, 945–953 (1996).

46. Miyagi, M. & Rao, K. C. S. Proteolytic 18O-labeling strategies for quantitative proteomics. *Mass Spectrom. Rev.* **26**, 121–136 (2007).

47. Ong, S. E. & Mann, M. Mass Spectrometry–Based Proteomics Turns Quantitative. *Nat. Chem. Biol.* **1**, 252–262 (2005).

48. Ibata, K., Takimoto, S., Morisaku, T., Miyawaki, A. & Yasui, M. Analysis of aquaporin-mediated diffusional water permeability by coherent anti-stokes Raman

scattering microscopy. *Biophys. J.* **101**, 2277–83 (2011).

49.   Leggett, D. S. *et al.* Multiple associated proteins regulate proteasome structure and function. *Mol. Cell* **10**, 495–507 (2002).

50.   Candotti, M., Esteban-Martín, S., Salvatella, X. & Orozco, M. Toward an atomistic description of the urea-denatured state of proteins. *Proc. Natl. Acad. Sci. U. S. A.* **110**, 5933–5938 (2013).

51.   Hjerpe, R. *et al.* Efficient protection and isolation of ubiquitylated proteins using tandem ubiquitin-binding entities. *EMBO Rep.* **10**, 1250–1258 (2009).

52.   Wilson, M. D., Saponaro, M., Leidl, M. A. & Svejstrup, J. Q. MultiDsk: A Ubiquitin-Specific Affinity Resin. *PLoS One* **7**, (2012).

53.   Zhang, D., Raasi, S. & Fushman, D. Affinity makes the difference: nonselective interaction of the UBA domain of Ubiquilin-1 with monomeric ubiquitin and polyubiquitin chains. *J. Mol. Biol.* **337**, (2008).

54.   Koyano, F. *et al.* Ubiquitin is phosphorylated by PINK1 to activate parkin. *Nature* **510**, 162–166 (2014).

55.   Bracher, P. J., Snyder, P. W., Bohall, B. R. & Whitesides, G. M. The Relative Rates of Thiol-Thioester Exchange and Hydrolysis for Alkyl and Aryl Thioalkanoates in Water. *Orig. Life Evol. Biosph.* **41**, 399–412 (2011).

56.   Gates, Z. P., Stephan, J. R., Lee, D. J. & Kent, S. B. H. Rapid formal hydrolysis of peptide- α thioesters. *Chem. Commun.* **49**, 786–788 (2013).

57.   Catanzariti, A.-M., Soboleva, T. A., Jans, D. A., Board, P. G. & Baker, R. T. An efficient system for high-level expression and easy purification of authentic recombinant proteins. *Protein Sci.* **13**, 1331–1339 (2004).

58. Shahnawaz, M., Thapa, A. & Park, I. S. Stable activity of a deubiquitylating enzyme (Usp2-cc) in the presence of high concentrations of urea and its application to purify aggregation-prone peptides. *Biochem. Biophys. Res. Commun.* **359**, 801–805 (2007).

59. Gansen, A., Hieb, A. R., Böhm, V., Tóth, K. & Langowski, J. Closing the Gap between Single Molecule and Bulk FRET Analysis of Nucleosomes. *PLoS One* **8**, (2013).

60. Chen, J. J. *et al.* Mechanistic studies of substrate-assisted inhibition of ubiquitin-activating enzyme by adenosine sulfamate analogues. *J. Biol. Chem.* **286**, 40867–40877 (2011).

61. Fujimuro, M., Sawada, H. & Yokosawa, H. Dynamics of ubiquitin conjugation during heat-shock response revealed by using a monoclonal antibody specific to multi-ubiquitin chains. *Eur. J. Biochem.* **249**, 427–433 (1997).

62. Fornace, A. J., Alamo, I., Hollander, M. C. & Lamoreaux, E. Ubiquftin mRNA is a major stress-induced transcript in mammalian cells. *Nucleic Acids Res.* **17**, 1215–1230 (1989).

63. Bond, U. & Schlesinger, M. J. The chicken ubiquitin gene contains a heat shock promoter and expresses an unstable mRNA in heat-shocked cells. *Mol. Cell. Biol.* **6**, 4602–4610 (1986).

64. Du, J. & Strieter, E. R. A fluorescence polarization-based competition assay for measuring interactions between unlabeled ubiquitin chains and UCH37•RPN13. *Anal. Biochem.* **550**, 84–89 (2018).

65. Groothuis, T. A. M., Dantuma, N. P., Neefjes, J. & Salomons, F. A. Ubiquitin

crosstalk connecting cellular processes. *Cell Div.* **1**, 21 (2006).

66.   Bett, J. S., Benn, C. L., Ryu, K. Y., Kopito, R. R. & Bates, G. P. The polyubiquitin
      Ubc gene modulates histone H2A monoubiquitylation in the R6/2 mouse model of
      Huntington's disease. *J. Cell. Mol. Med.* **13**, 2645–2657 (2009).

67.   Cao, R., Tsukada, Y. I. & Zhang, Y. Role of Bmi-1 and Ring1A in H2A
      ubiquitylation and hox gene silencing. *Mol. Cell* **20**, 845–854 (2005).

68.   de Napoles, M. *et al.* Polycomb group proteins Ring1A/B link ubiquitylation of
      histone H2A to heritable gene silencing and X inactivation. *Dev. Cell* **7**, 663–76
      (2004).

69.   Yao, T. & Cohen, R. E. A cryptic protease couples deubiquitination and
      degradation by the proteasome. *Nature* **419**, 403–407 (2002).

70.   Chen, P. C. *et al.* The proteasome-associated deubiquitinating enzyme Usp14 is
      essential for the maintenance of synaptic ubiquitin levels and the development of
      neuromuscular junctions. *J. Neurosci.* **29**, 10909–10919 (2009).

71.   Crimmins, S. *et al.* Transgenic rescue of ataxia mice with neuronal-specific
      expression of ubiquitin-specific protease 14. *J. Neurosci.* **26**, 11423–11431
      (2006).

72.   Wang, C. H. *et al.* USP5/leon deubiquitinase confines postsynaptic growth by
      maintaining ubiquitin homeostasis through ubiquilin. *Elife* **6**, 1–26 (2017).

73.   Majetschak, M. Extracellular ubiquitin: immune modulator and endogenous
      opponent of damage-associated molecular pattern molecules. *J. Leukoc. Biol.* **89**,
      205–219 (2011).

74.   Xu, P. *et al.* Quantitative Proteomics Reveals the Function of Unconventional

Ubiquitin Chains in Proteasomal Degradation. *Cell* **137**, 133–145 (2009).

75. Na, C. H. & Peng, J. Analysis of ubiquitinated proteome by quantitative mass spectrometry. *Methods Mol. Biol.* **893**, 417–29 (2012).

76. Shevchenko, A., Tomas, H., Havliš, J., Olsen, J. V. & Mann, M. In-gel digestion for mass spectrometric characterization of proteins and proteomes. *Nat. Protoc.* **1**, 2856–2860 (2007).

77. Klis, F. M., Boorsma, A. & De Groot, P. W. J. Cell wall construction in Saccharomyces cerevisiae. *Yeast* **23**, 185–202 (2006).

78. Borle, A. B. Kinetic Analyses of Calcium Movements in HeLa Cell Cultures: II. Calcium efflux. *J. Gen. Physiol.* **53**, 57–69 (1969).

79. MR, A., M, N., S, K., M, H. & T, F. The effects of cell sizes, environmental conditions, and growth phases on the strength of individual W303 yeast cells inside ESEM. *IEEE Trans Nanobioscience* **3**, 185–93 (2008).

80. Amerik, A. Y., Li, S. J. & Hochstrasser, M. Analysis of the deubiquitinating enzymes of the yeast Saccharomyces cerevisiae. *Biol. Chem.* **381**, 981–992 (2000).

81. Gerashchenko, M. V. & Gladyshev, V. N. Translation inhibitors cause abnormalities in ribosome profiling experiments. *Nucleic Acids Res.* **42**, (2014).

82. Niles, R. H. *et al.* Acid-catalyzed Oxygen-18 labeling of peptides. *Anal. Chem.* **81**, 2804–2809 (2009).

83. Yen, H. C. S., Xu, Q., Chou, D. M., Zhao, Z. & Elledge, S. J. Global protein stability profiling in mammalian cells. *Science (80-.).* **322**, 918–923 (2008).

84. Käll, L., Canterbury, J. D., Weston, J., Noble, W. S. & MacCoss, M. J. Semi-

supervised learning for peptide identification from shotgun proteomics datasets. *Nat. Methods* **4**, 923–925 (2007).

85.   Perkins, D. N., Pappin, D. J. C., Creasy, D. M. & Cottrell, J. S. Probability-based protein identification by searching sequence databases using mass spectrometry data. *Electrophoresis* **20**, 3551–3567 (1999).

86.   Yates, J. R., Eng, J. K., McCormack, A. L. & Schieltz, D. Method to Correlate Tandem Mass Spectra of Modified Peptides to Amino Acid Sequences in the Protein Database. *Anal. Chem.* **67**, 1426–1436 (1995).

87.   Ong, S. E. & Mann, M. A practical recipe for stable isotope labeling by amino acids in cell culture (SILAC). *Nat. Protoc.* **1**, 2650–2660 (2007).

88.   Na, C. H. *et al.* Synaptic protein ubiquitination in rat brain revealed by antibody-based ubiquitome analysis. *J. Proteome Res.* **11**, 4722–4732 (2012).

89.   Ronan, T., Qi, Z. & Naegle, K. M. Avoiding common pitfalls when clustering biological data. *Sci. Signal.* **9**, 1–13 (2016).

90.   Huang, D. W., Sherman, B. T. & Lempicki, R. A. Systematic and integrative analysis of large gene lists using DAVID bioinformatics resources. *Nat. Protoc.* **4**, 44–57 (2009).

91.   Huang, D. W., Sherman, B. T. & Lempicki, R. A. Bioinformatics enrichment tools: Paths toward the comprehensive functional analysis of large gene lists. *Nucleic Acids Res.* **37**, 1–13 (2009).

92.   Feldenberg, L. R., Thevananther, S., Del Rio, M., De Leon, M. & Devarajan, P. Partial ATP depletion induces Fas- and caspase-mediated apoptosis in MDCK cells. *Am. J. Physiol. - Ren. Physiol.* **276**, 837–846 (1999).

93. Nieminen, A. L., Saylor, A. K., Herman, B. & Lemasters, J. J. ATP depletion rather than mitochondrial depolarization mediates hepatocyte killing after metabolic inhibition. *Am. J. Physiol. - Cell Physiol.* **267**, (1994).

94. Wiener, R. *et al.* E2 ubiquitin conjugating enzymes regulate the deubiquitinating activity of OTUB1. *Nat. Struct. Mol. Biol.* **20**, 1033–1039 (2013).

95. Harshman, S. W., Young, N. L., Parthun, M. R. & Freitas, M. A. H1 histones: Current perspectives and challenges. *Nucleic Acids Res.* **41**, 9593–9609 (2013).

96. Elderkin, S. *et al.* A Phosphorylated Form of Mel-18 Targets the Ring1B Histone H2A Ubiquitin Ligase to Chromatin. *Mol. Cell* **28**, 107–120 (2007).

97. Krum, S. A., Dalugdugan, E. D. L. R., Miranda-Carboni, G. A. & Lane, T. F. BRCA1 forms a functional complex with γ-H2AX as a late response to genotoxic stress. *J. Nucleic Acids* **2010**, (2010).

98. Sarcinella, E., Zuzarte, P. C., Lau, P. N. I., Draker, R. & Cheung, P. Monoubiquitylation of H2A.Z Distinguishes Its Association with Euchromatin or Facultative Heterochromatin. *Mol. Cell. Biol.* **27**, 6457–6468 (2007).

99. Xu, P. *et al.* Quantitative Proteomics Reveals the Function of Unconventional Ubiquitin Chains in Proteasomal Degradation. *Cell* **137**, 133–145 (2009).

100. Jacobson, A. D. Ubiquitin Signaling at the Mammalian Proteasome Thesis. (2013).

101. Amanchy, R., Kalume, D. E. & Pandey, A. Stable isotope labeling with amino acids in cell culture (SILAC) for studying dynamics of protein abundance and posttranslational modifications. *Sci. STKE* **2005**, pl2 (2005).

102. Castañeda, C. A. *et al.* Linkage via K27 Bestows Ubiquitin Chains with Unique

Properties among Polyubiquitins. *Structure* **24**, 423–436 (2016).

103. Manasanch, E. E. & Orlowski, R. Z. Proteasome Inhibitors in Cancer Therapy HHS Public Access. *Nat Rev Clin Oncol* **14**, 417–433 (2017).

104. Han, S.-W., Jung, B.-K., Park, S.-H. & Ryu, K.-Y. Reversible Regulation of Polyubiquitin Gene UBC via Modified Inducible CRISPR/Cas9 System. *Int. J. Mol. Sci.* **20**, 3168 (2019).

105. Fang, N. N., Ng, A. H. M., Measday, V. & Mayor, T. Hul5 HECT ubiquitin ligase plays a major role in the ubiquitylation and turnover of cytosolic misfolded proteins. *Nat. Cell Biol.* **13**, 1344–1352 (2011).

106. Fang, N. N. *et al.* Rsp5 / Nedd4 is the major ubiquitin ligase that targets cytosolic misfolded proteins upon heat-stress. **16**, 1227–1237 (2017).

107. Kee, Y., Lyon, N. & Huibregtse, J. M. The Rsp5 ubiquitin ligase is coupled to and antagonized by the Ubp2 deubiquitinating enzyme. *EMBO J.* **24**, 2414–2424 (2005).

108. Fang, N. N., Zhu, M., Rose, A., Wu, K. P. & Mayor, T. Deubiquitinase activity is required for the proteasomal degradation of misfolded cytosolic proteins upon heat-stress. *Nat. Commun.* **7**, 1–16 (2016).

109. De Jong, H. Modeling and simulation of genetic regulatory systems: A literature review. *J. Comput. Biol.* **9**, 67–103 (2002).

110. Mann, M. & Jensen, O. N. Proteomic analysis of post-translational modifications. *Nat. Biotechnol.* **21**, 255–261 (2003).

111. Olsen, J. V. *et al.* Global, In Vivo, and Site-Specific Phosphorylation Dynamics in Signaling Networks. *Cell* **127**, 635–648 (2006).

112. van der Veen, A. G. & Ploegh, H. L. Ubiquitin-Like Proteins. *Annu. Rev. Biochem.* **81**, 323–57 (2012).

113. Giannakopoulos, N. V. *et al.* Proteomic identification of proteins conjugated to ISG15 in mouse and human cells. *Biochem. Biophys. Res. Commun.* **336**, 496–506 (2005).